

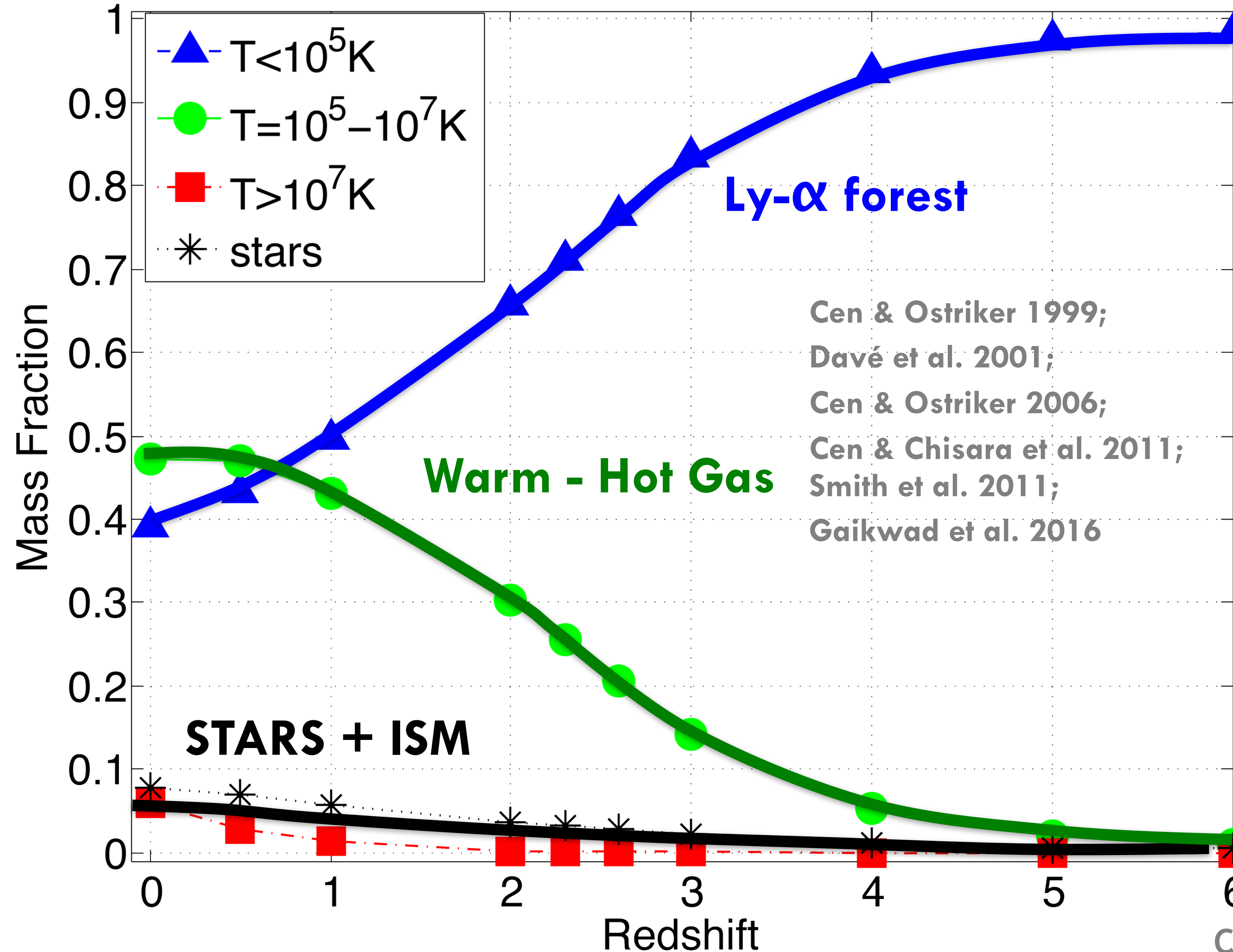


EXPLORING CGM / IGM moving away from large surveys

anand narayanan

Purvi Udhwani, Aditya Manuwal, Jayadev Pradeep, Sriram Sankar,
Pratyush Anshul, Mathin Yadav, Sachin PC, Dheeraj Kumar Khonde

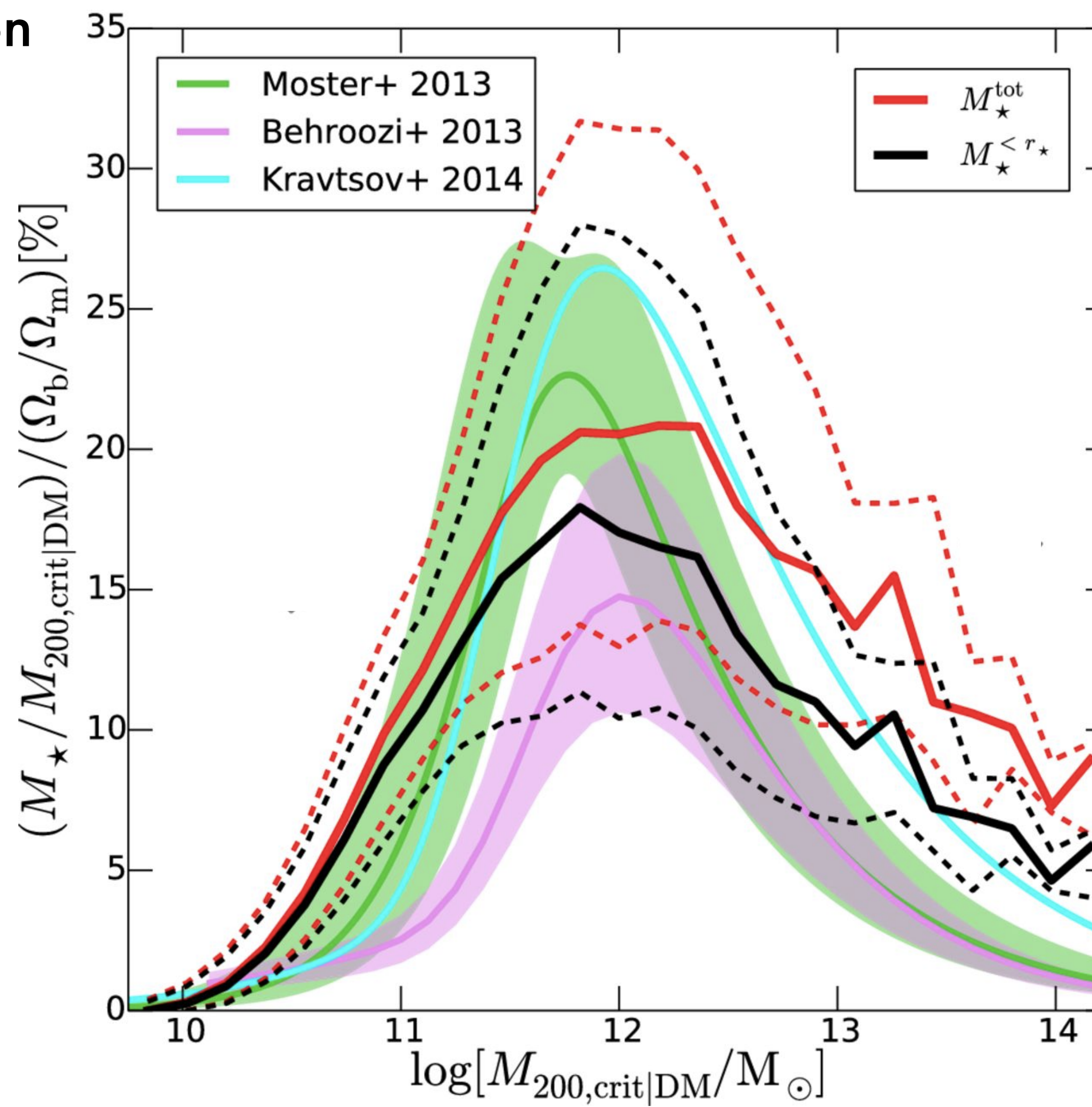
Raghunathan Srianand (IUCAA), Sowgat Muzahid (IUCAA), Vikram Khaire (IIST), Hum Chand (ARIES),
Jane Charlton (Penn State), Blair Savage (U of Wisconsin), Bart Wakker (U of Wisconsin)



Courtesy: Todd Tripp

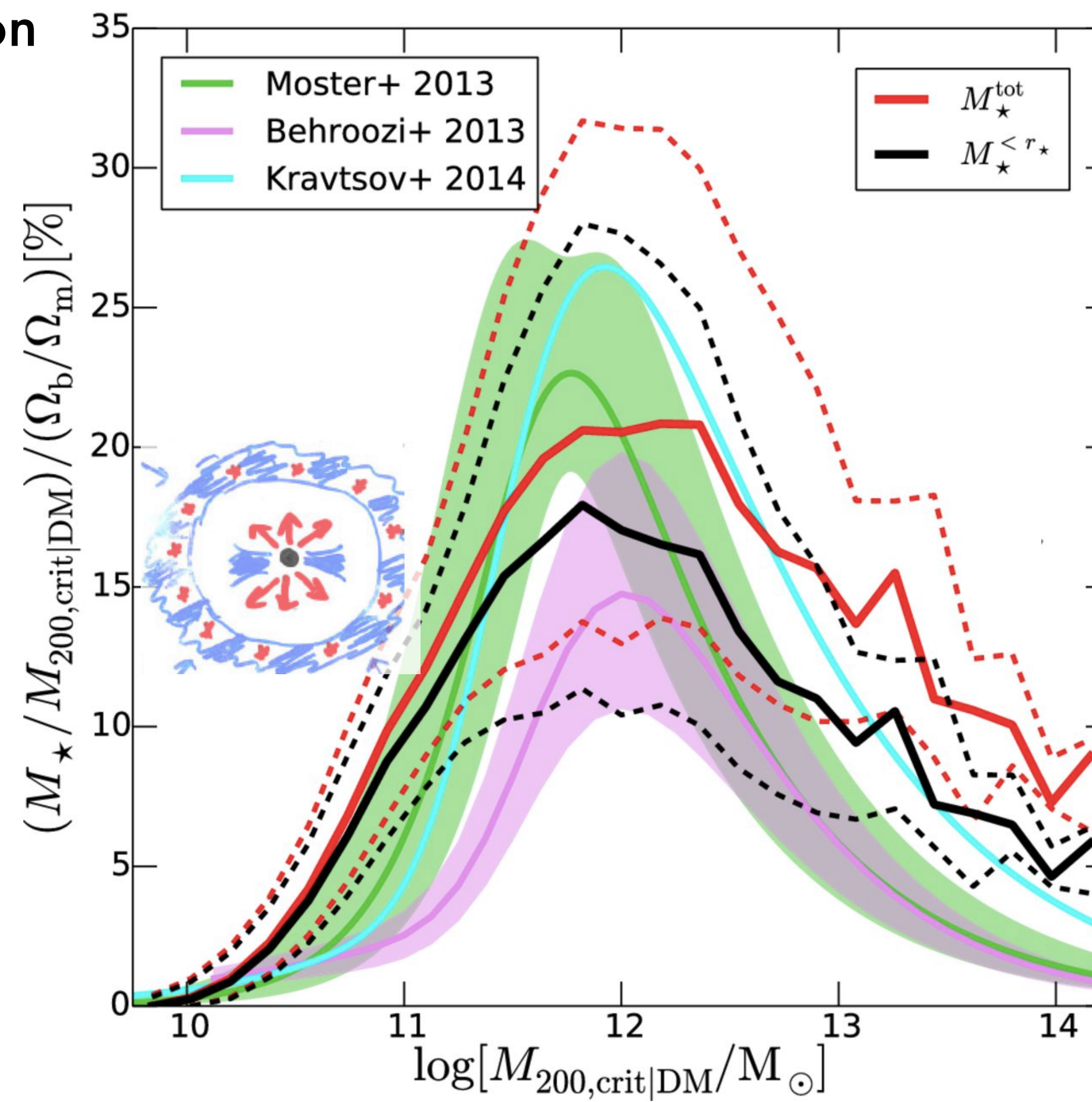
Feedback processes and accretion
rearrange baryons

cosmic baryon fraction (19% from CMB)
if baryons accreted onto the halos all become stars



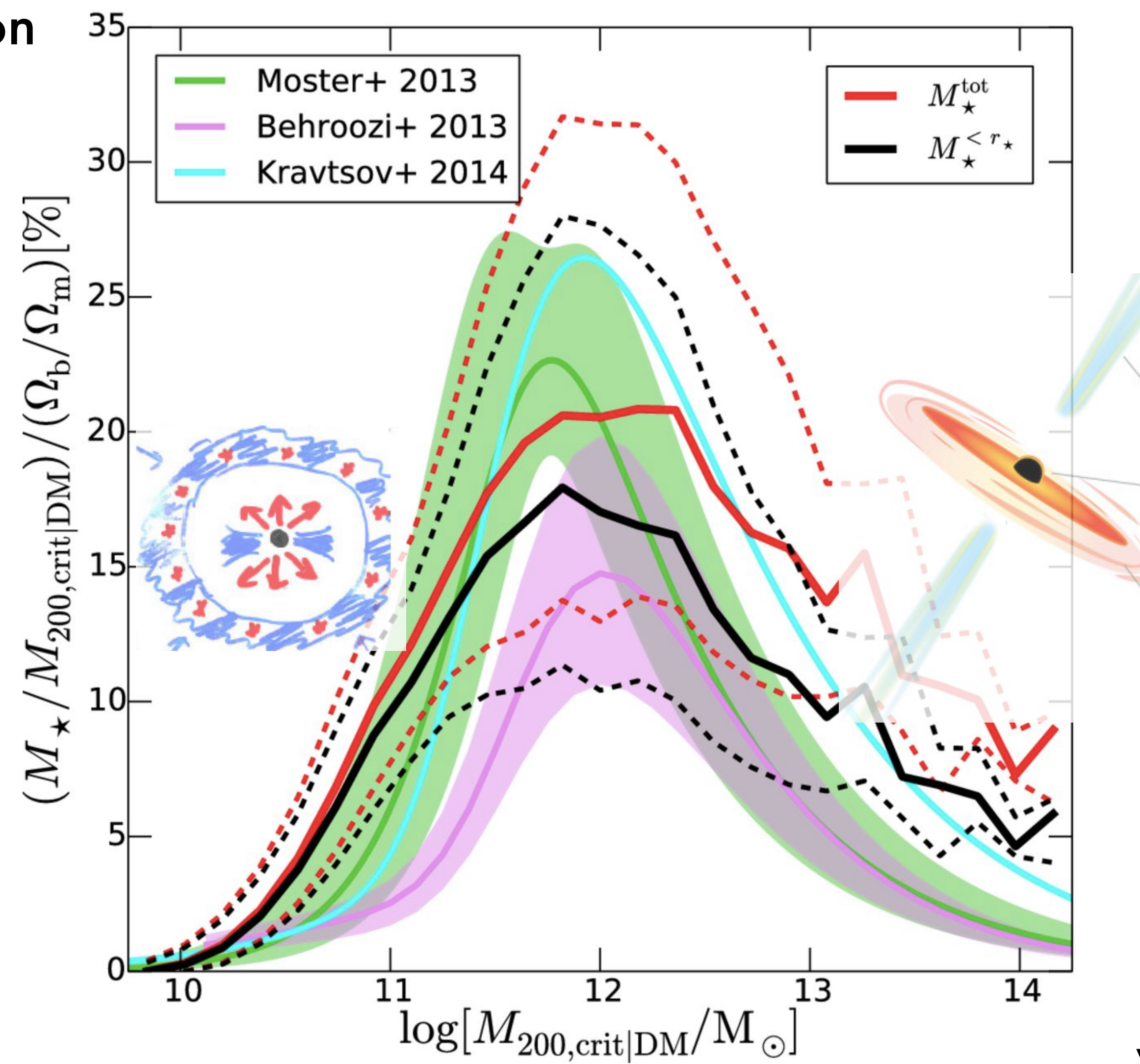
Feedback processes and accretion
rearrange baryons

cosmic baryon fraction (19% from CMB)
if baryons accreted onto the halos all become stars



Feedback processes and accretion
rearrange baryons

cosmic baryon fraction (19% from CMB)
if baryons accreted onto the halos all become stars



M81 Galaxy group

Chynoweth et al., NRAO/

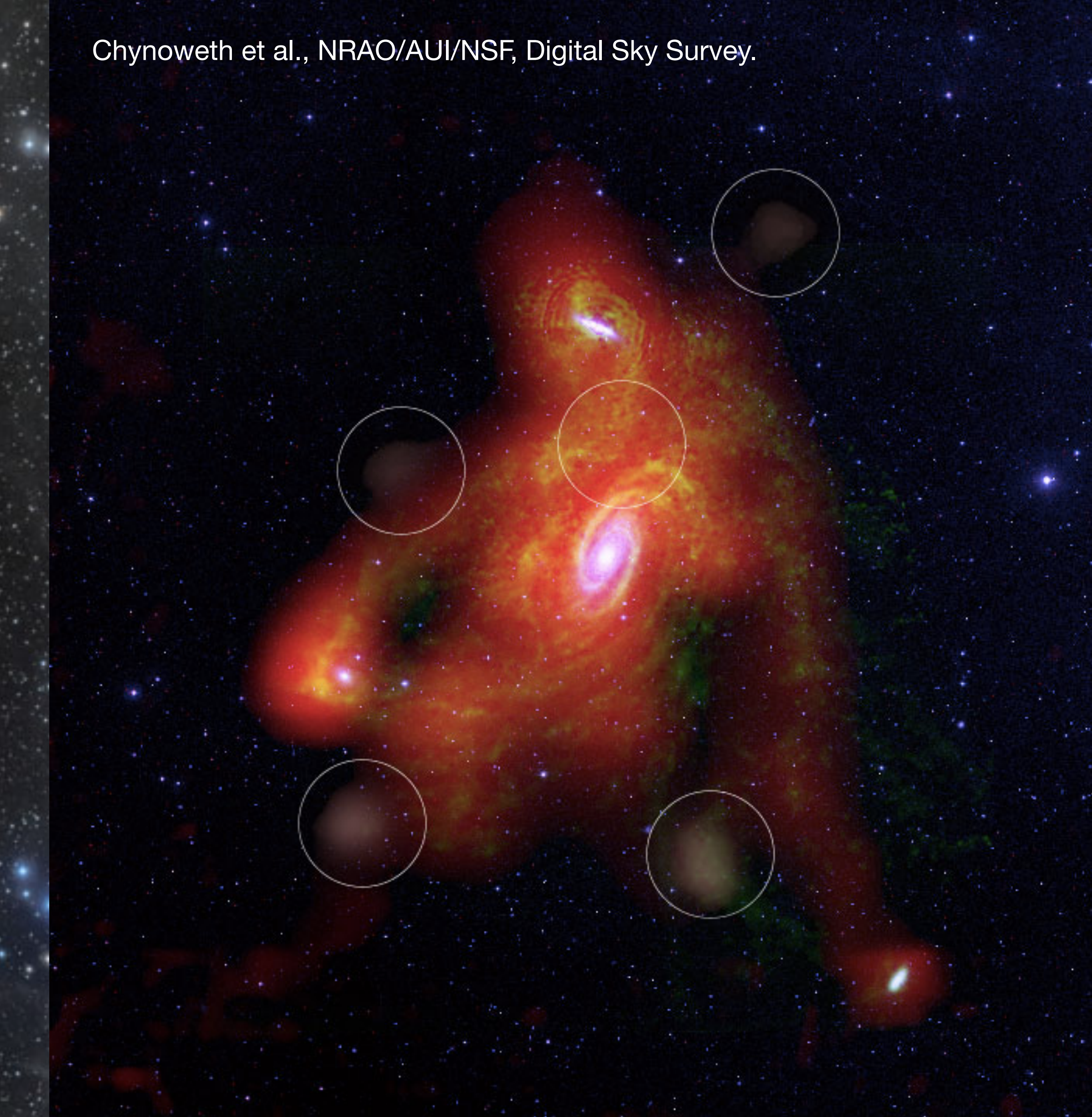
(c) APOD / Jordi Gallego



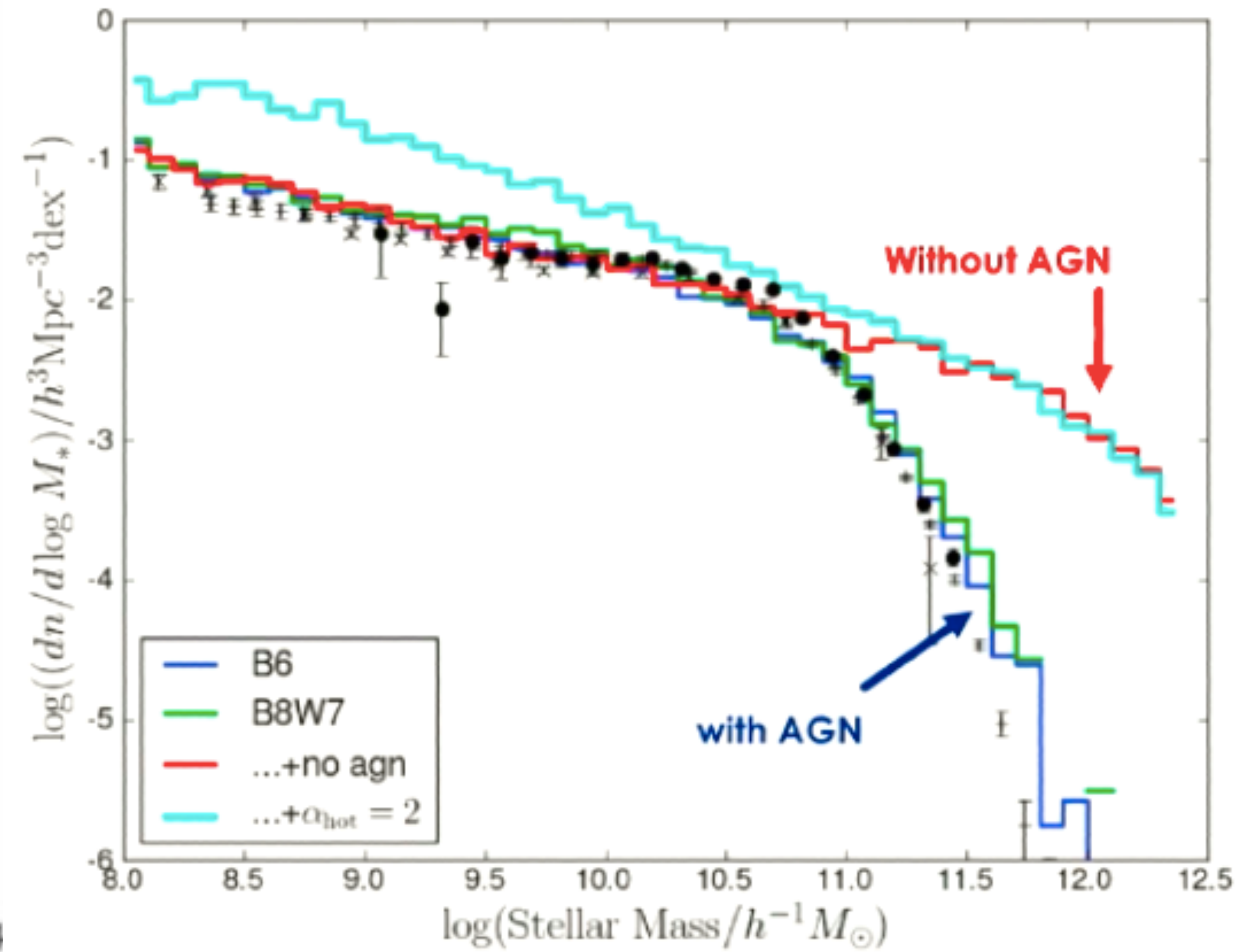
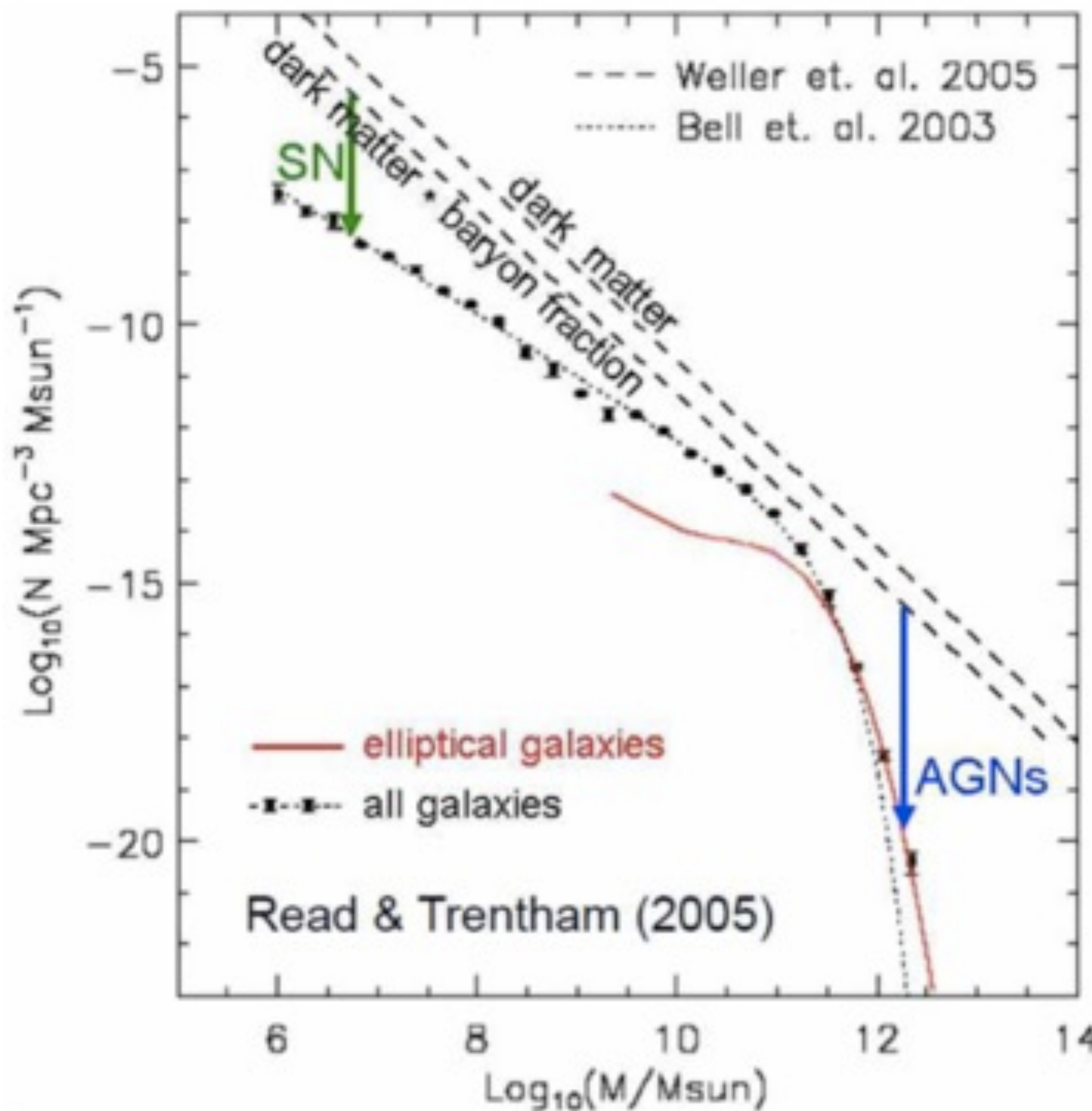
M81 Galaxy group

Chynoweth et al., NRAO/AUI/NSF, Digital Sky Survey.

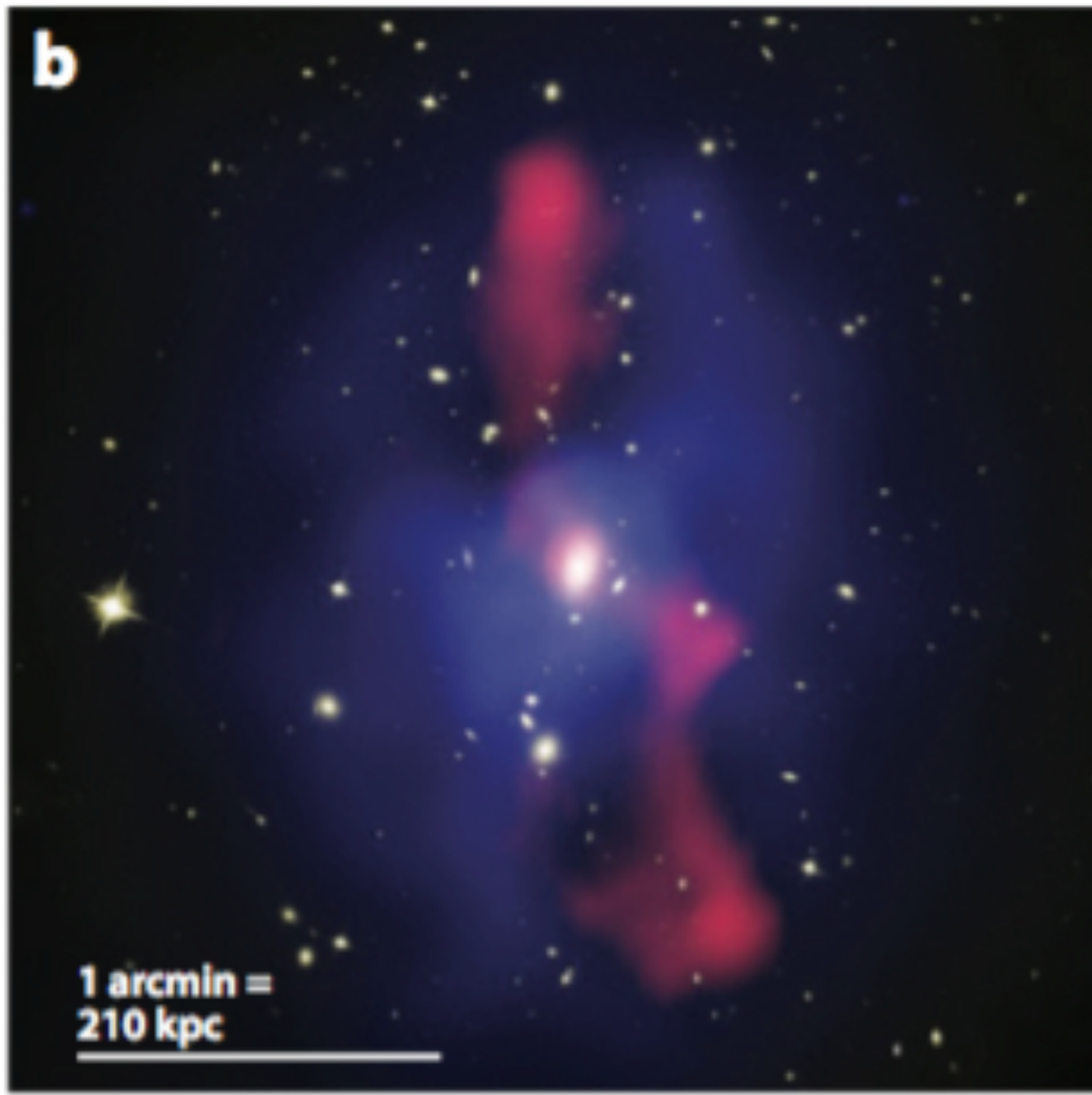
(c) APOD / Jordi Gallego



The Role of AGN Feedback

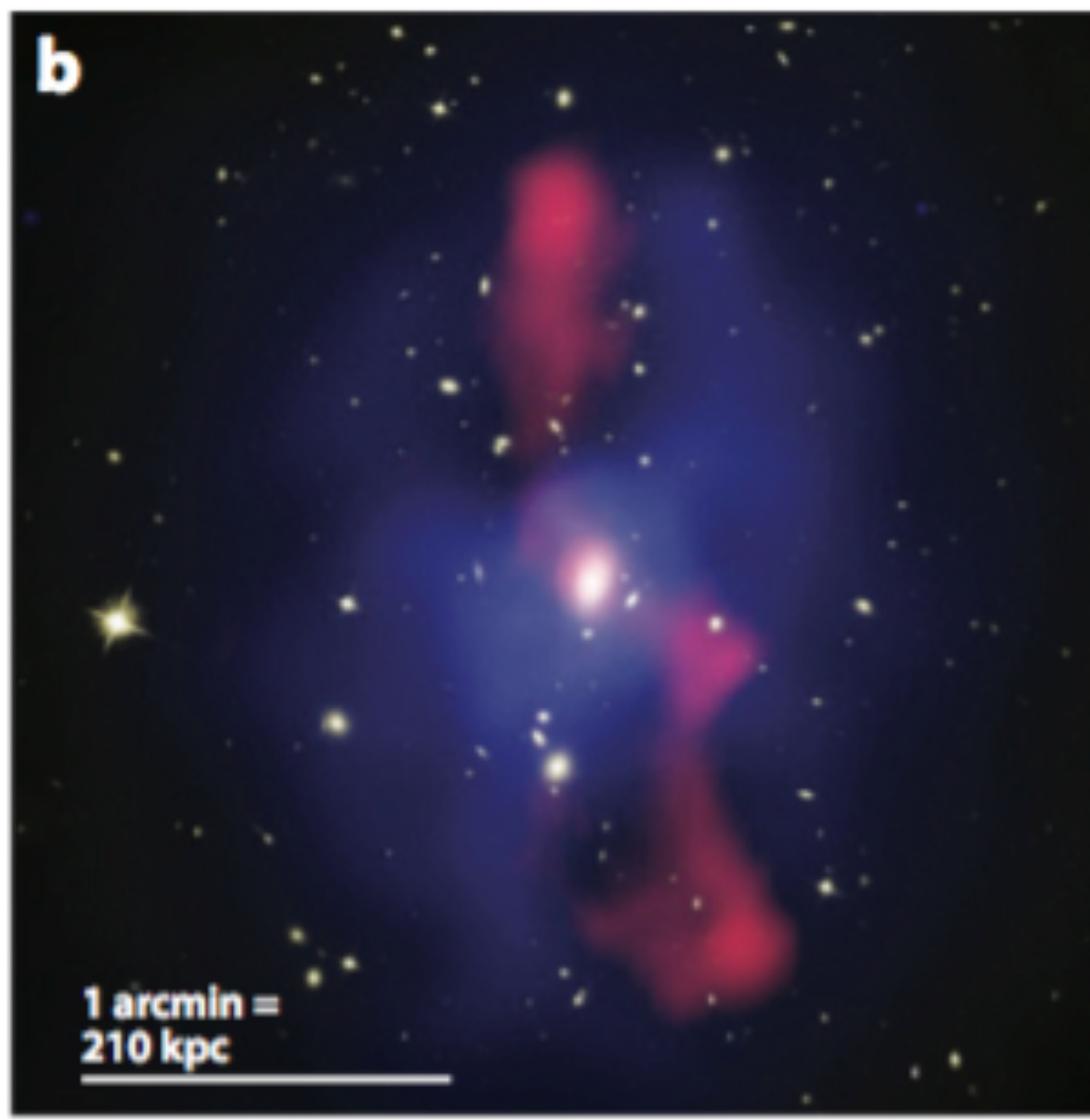


The Role of AGN Feedback

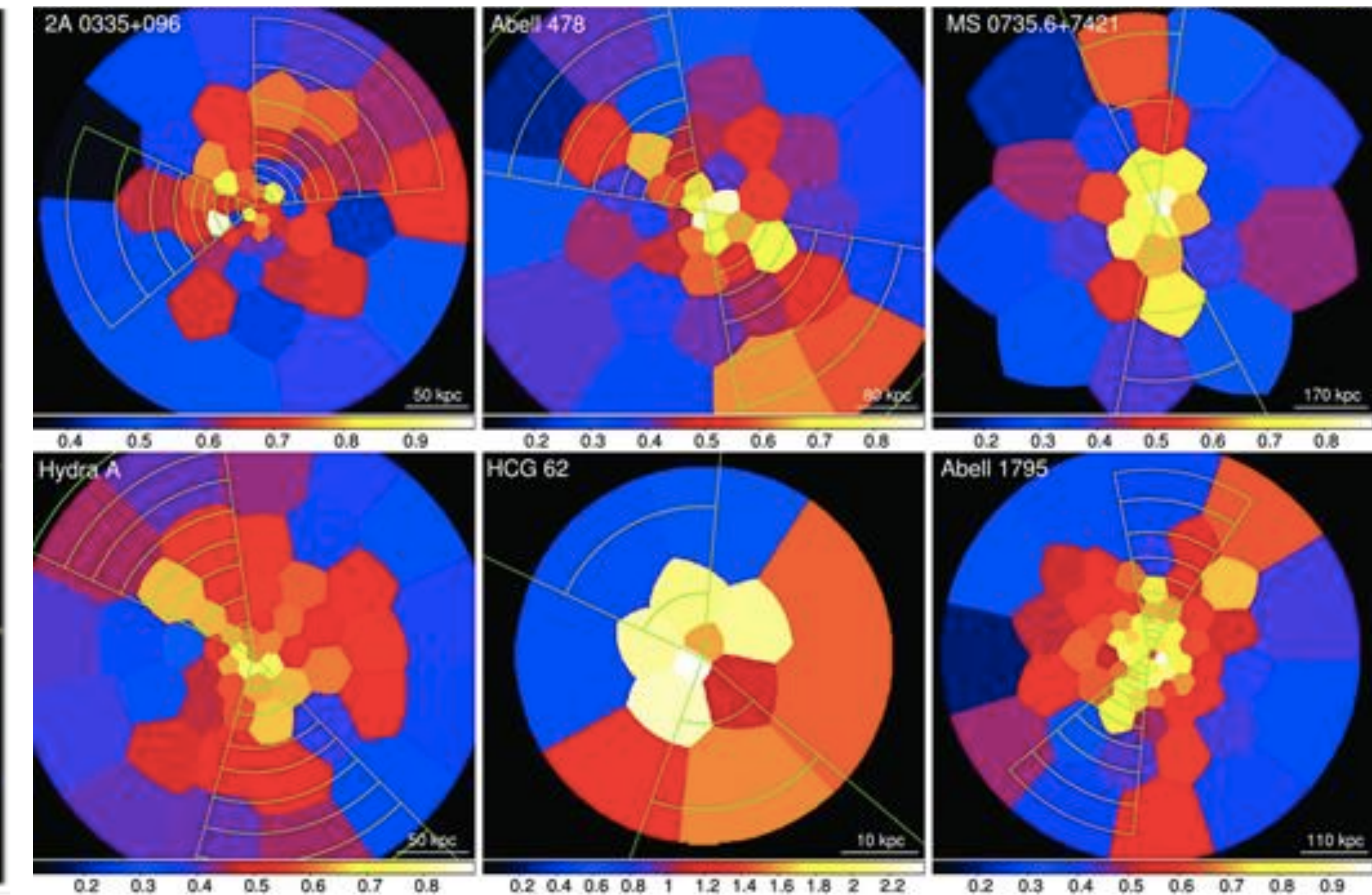


M87 diffuse X-ray (blue) +
radio continuum (red)

The Role of AGN Feedback



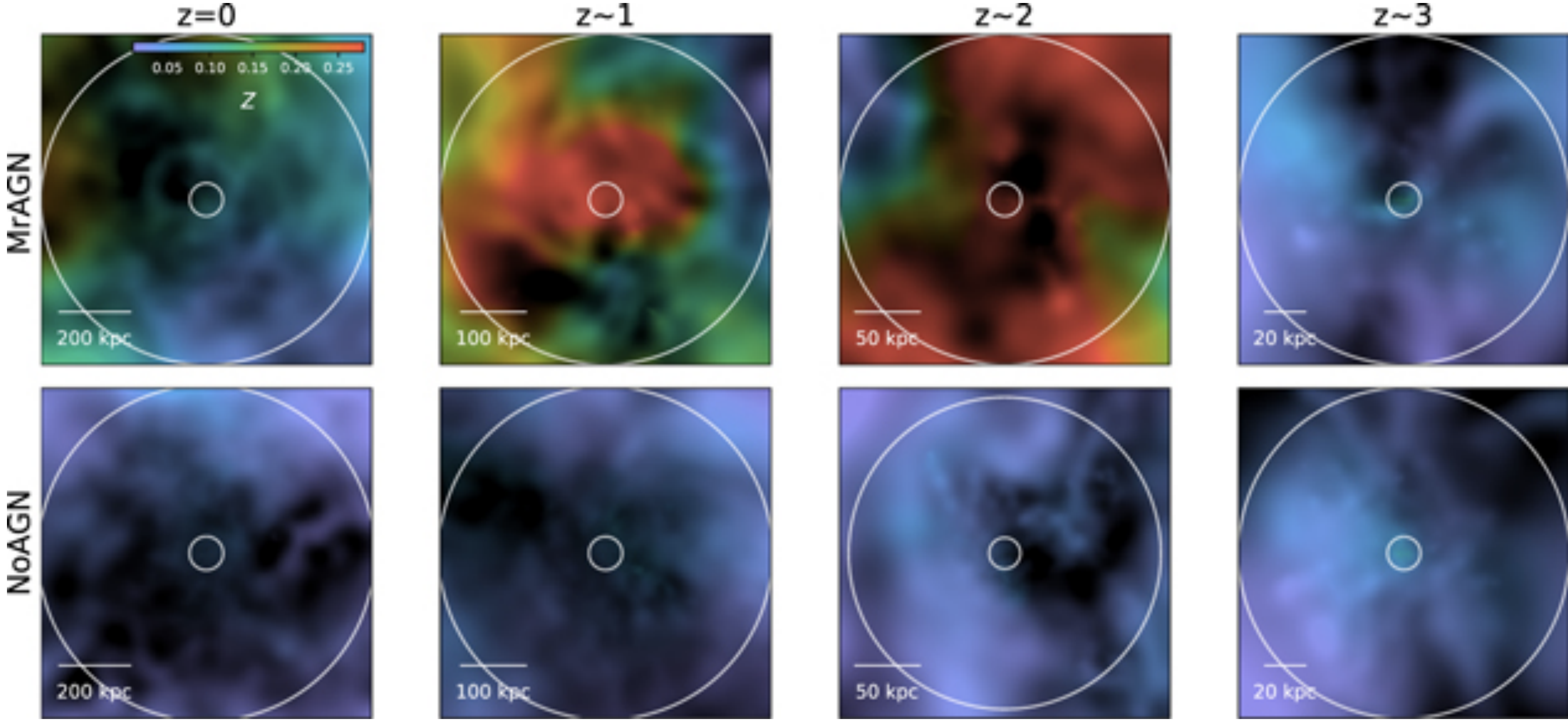
M87 diffuse X-ray (blue) +
radio continuum (red)



C. C. Kirkpatrick, B. R. McNamara, 2015, MNRAS

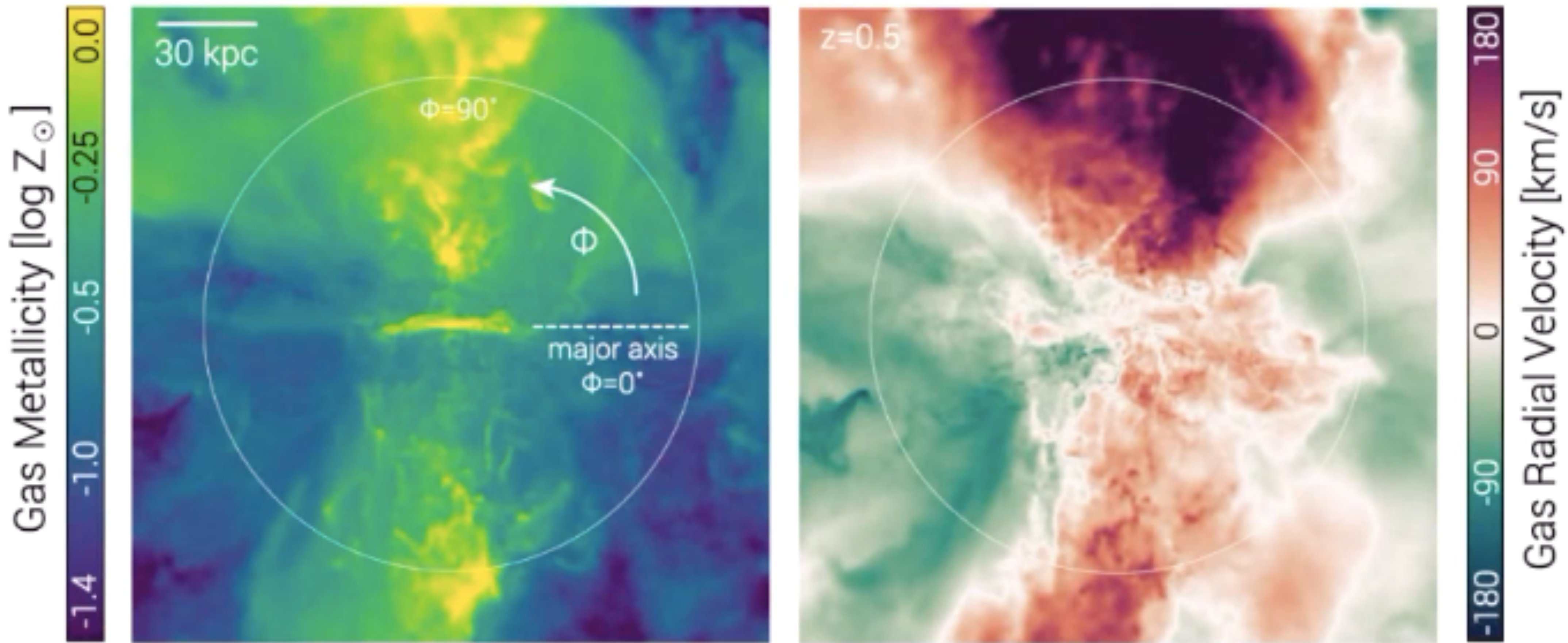
The Role of AGN Feedback

Choi, Ena et al. 2020, ApJ



Two matched sets of simulations of massive halos ($10^{10} < M^*/M_{\text{solar}} < 10^{12}$) with and without AGN feedback

Feedback from Star Formation



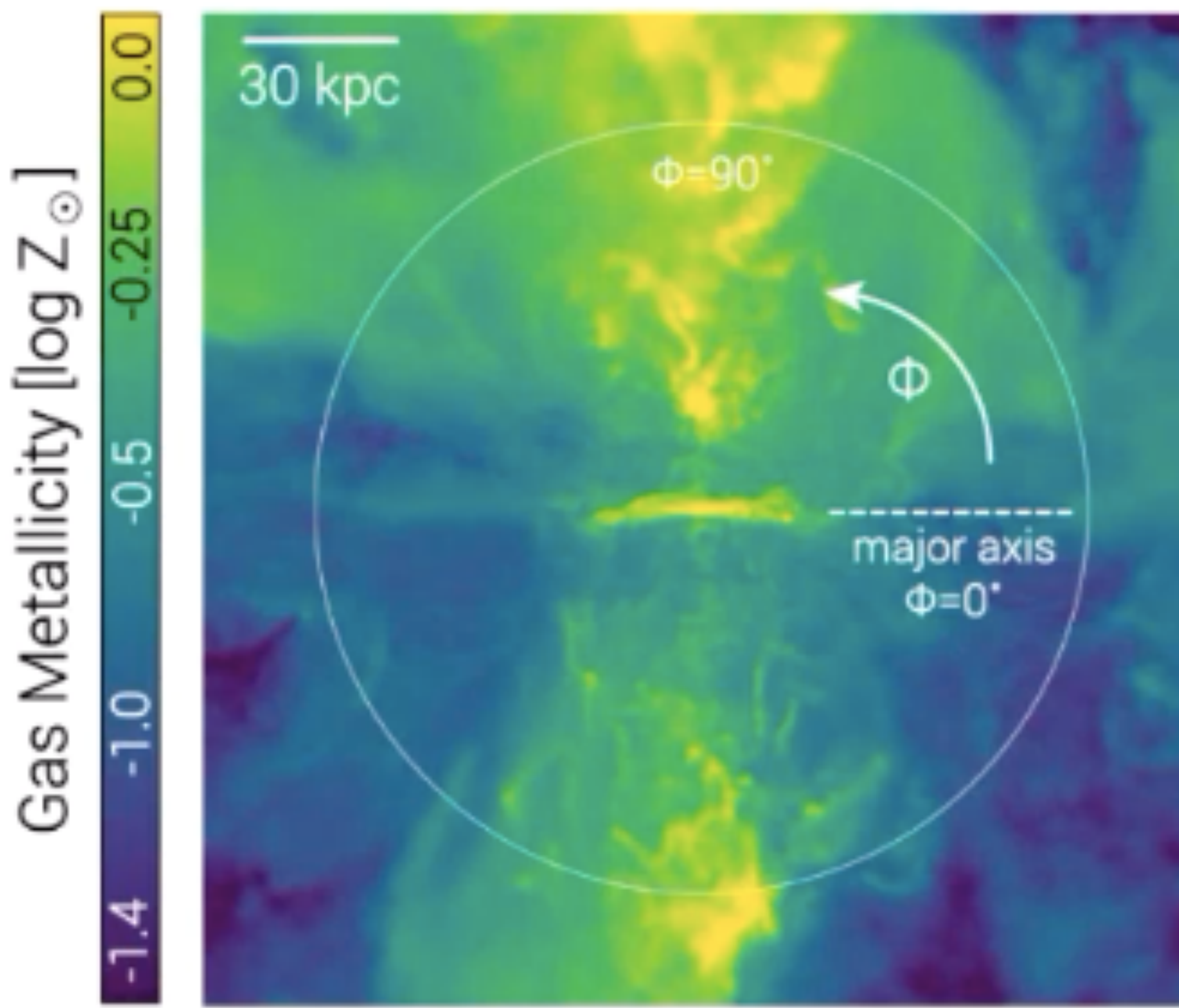
<https://www.tng-project.org/media/>

IllustrisTNG50

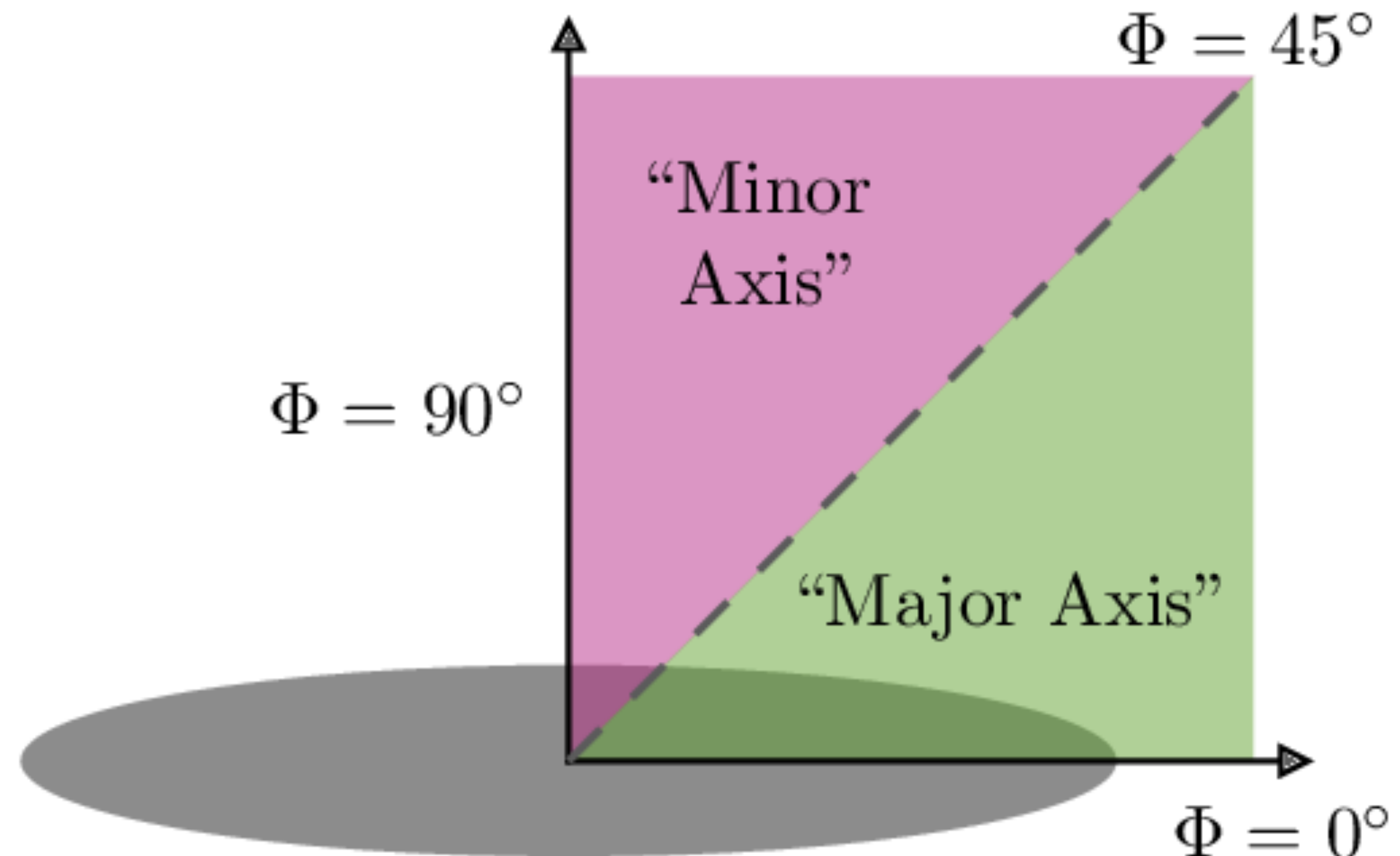
Tumlinson et al. 2011

Feedback from Star Formation & Accretion

Azimuthal Angle Dependence

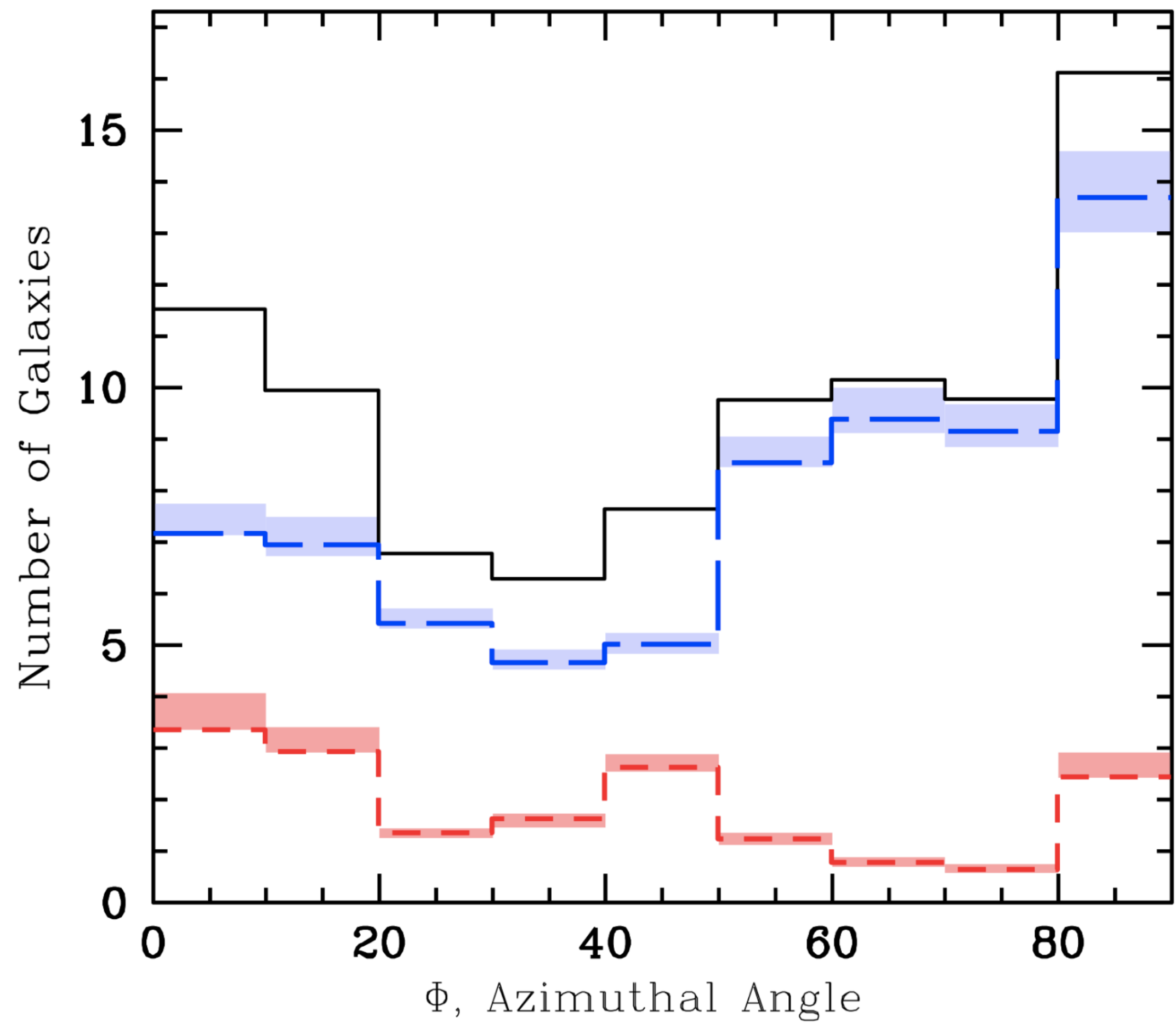


Azimuthal Angle
(sky view)



Outflows & Accretion

Azimuthal Angle Dependance

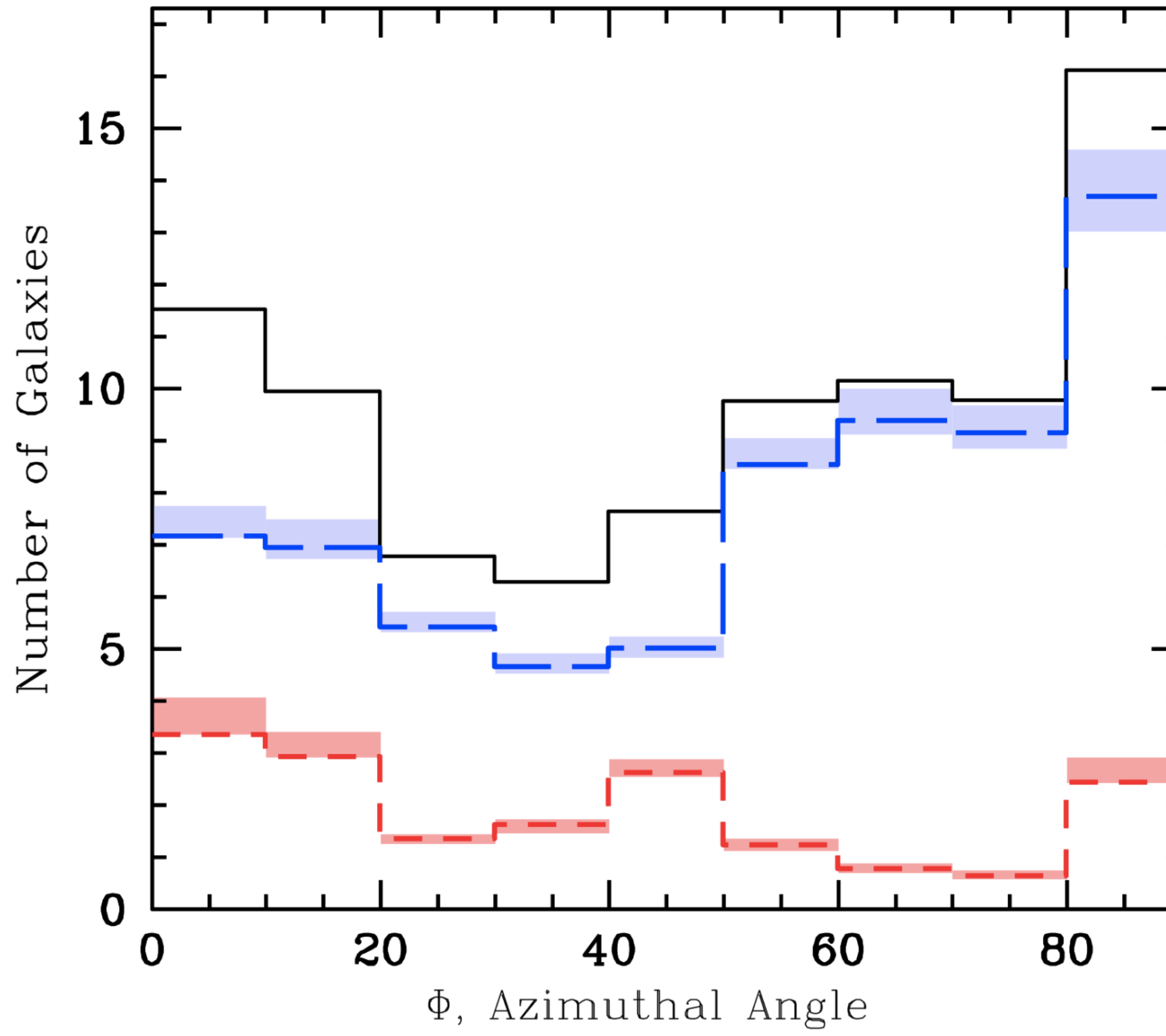


Azimuthal angle dependence of Mg II

Kacprzak et al. 2012

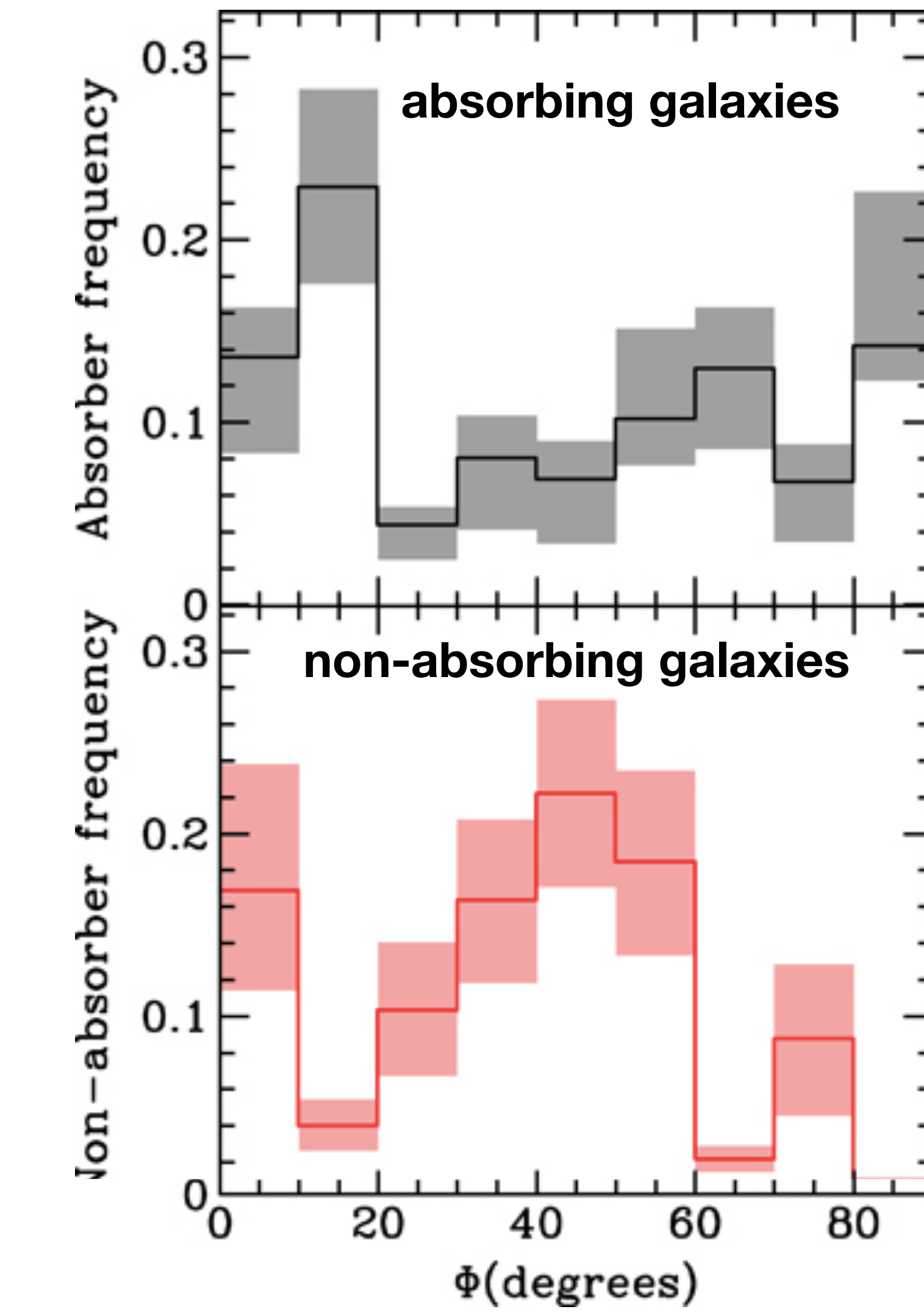
Outflows & Accretion

Azimuthal Angle Dependance



Azimuthal angle dependence of Mg II

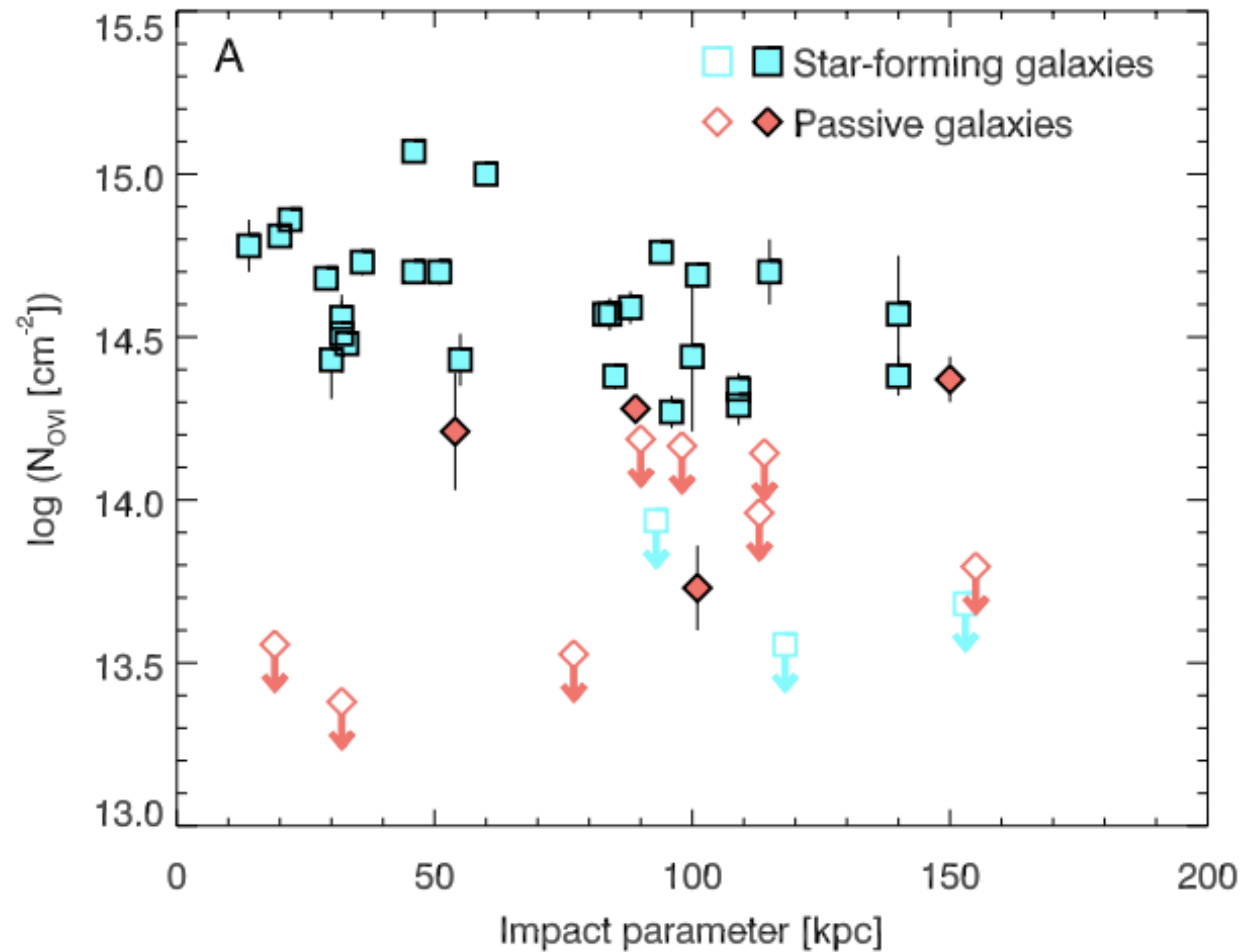
Kacprzak et al. 2012



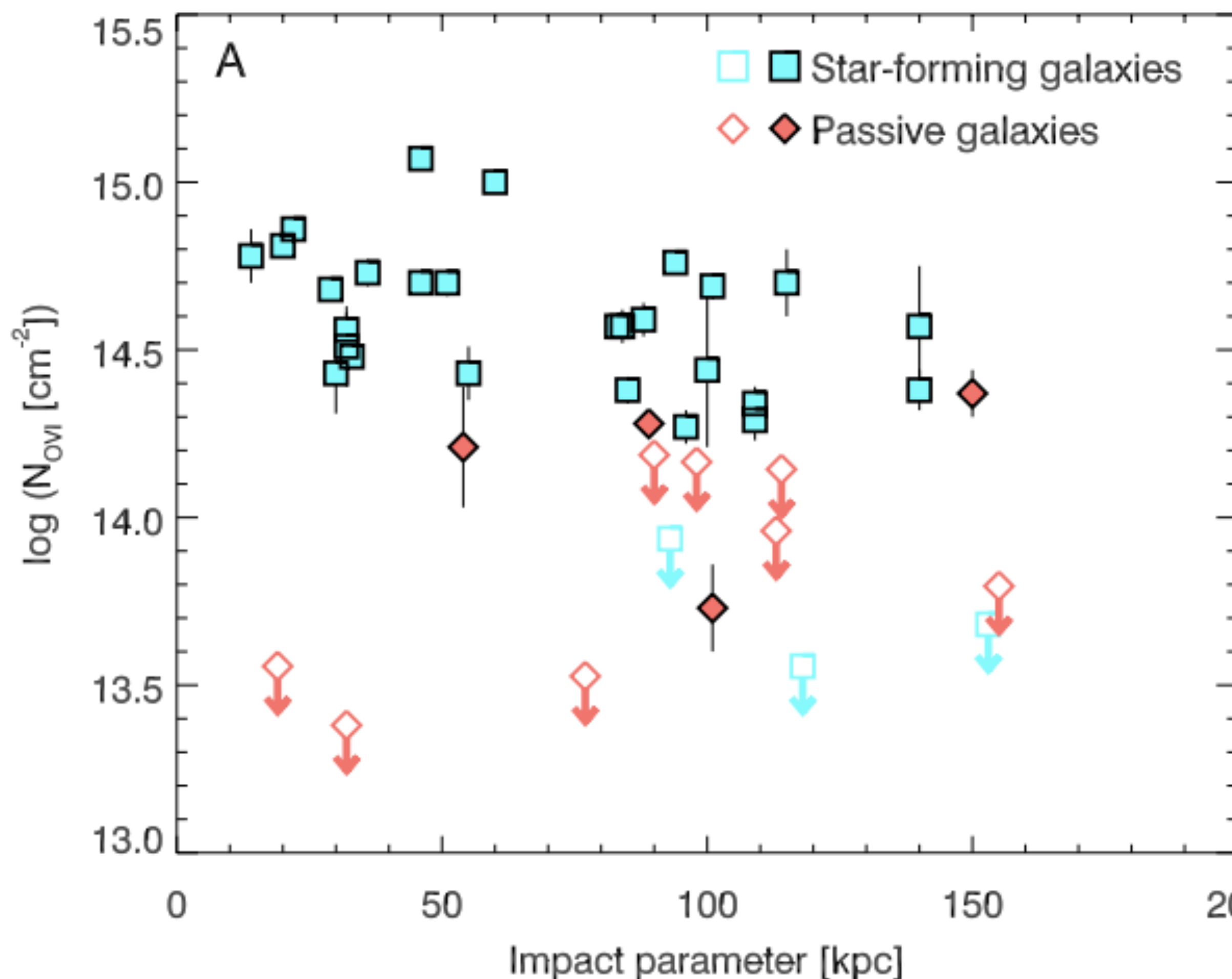
Azimuthal angle dependence of O VI

Kacprzak et al. 2015

High SFR → enriched winds → large covering fraction of warm absorbers

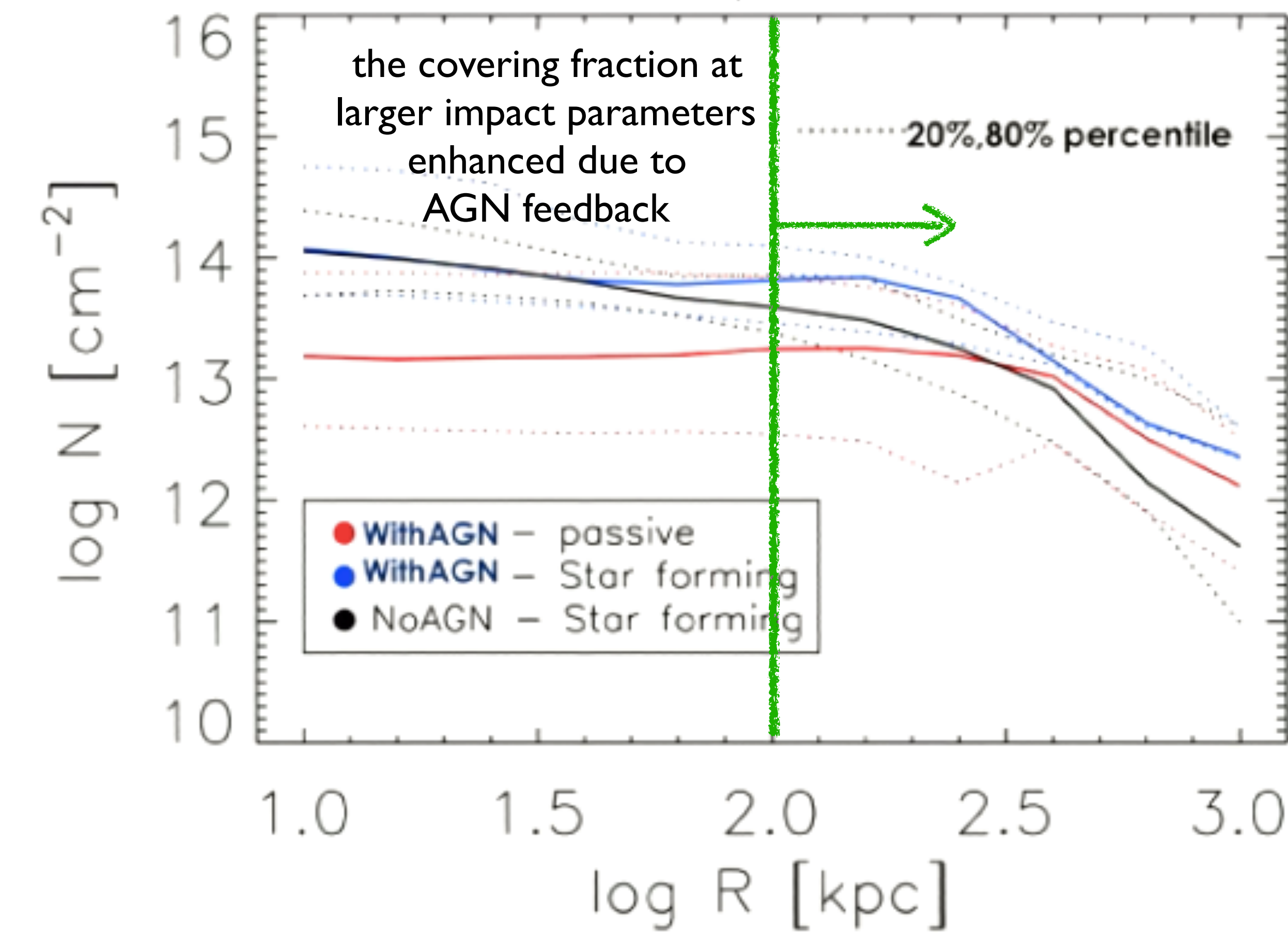


High SFR → enriched winds → large covering fraction of warm absorbers



Tumlinson et al. 2011

OVI profile



Choi, Ena et al. 2020, ApJ

AGN radiation impacts the CGM anisotropically → asymmetry in metal ion absorption ?
Spatial sampling at high spectral resolutions as it has been done for some normal galaxy CGMs

AGN radiation impacts the CGM anisotropically → asymmetry in metal ion absorption ?
Spatial sampling at high spectral resolutions as it has been done for some normal galaxy CGMs

For galaxies of similar mass, to what extent does AGN lower the fraction of halo gas that is cooling?
(covering fraction of HI, cool metals - in CGM of galaxies with and without AGN)

AGN radiation impacts the CGM anisotropically → asymmetry in metal ion absorption ?
Spatial sampling at high spectral resolutions as it has been done for some normal galaxy CGMs

For galaxies of similar mass, to what extent does AGN lower the fraction of halo gas that is cooling?
(covering fraction of HI, cool metals - in CGM of galaxies with and without AGN)

Do all AGN host galaxy CGM have enhanced metal abundances and higher covering fraction of O VI?

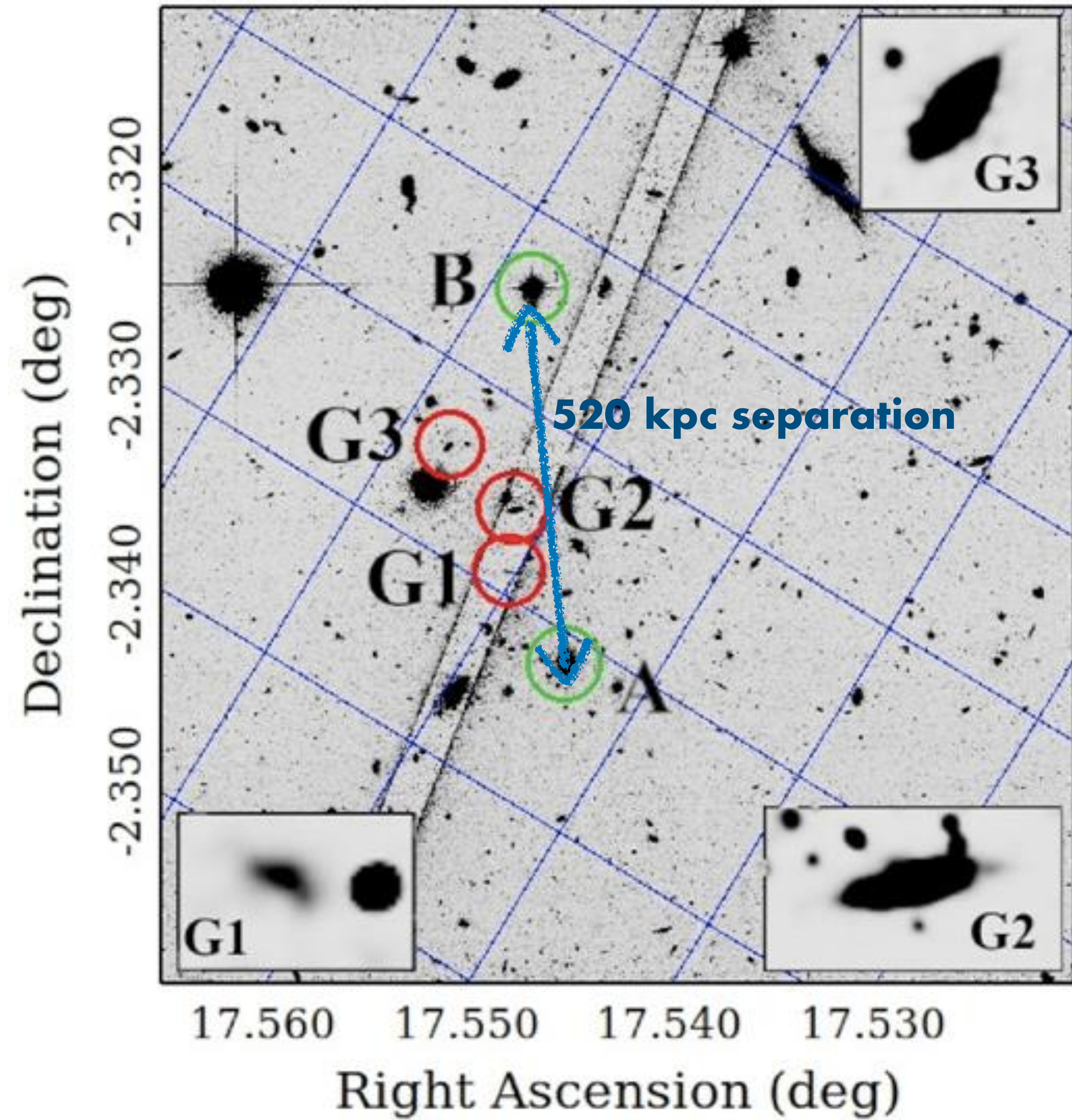
AGN activity picks up → outflows and jets push CGM gas away → strong AGN feedback quenches SF → lowers the covering fraction of OVI in the CGM.

enhanced covering fraction of metals around AGNs a temporary phenomenon? (simulations and observations)

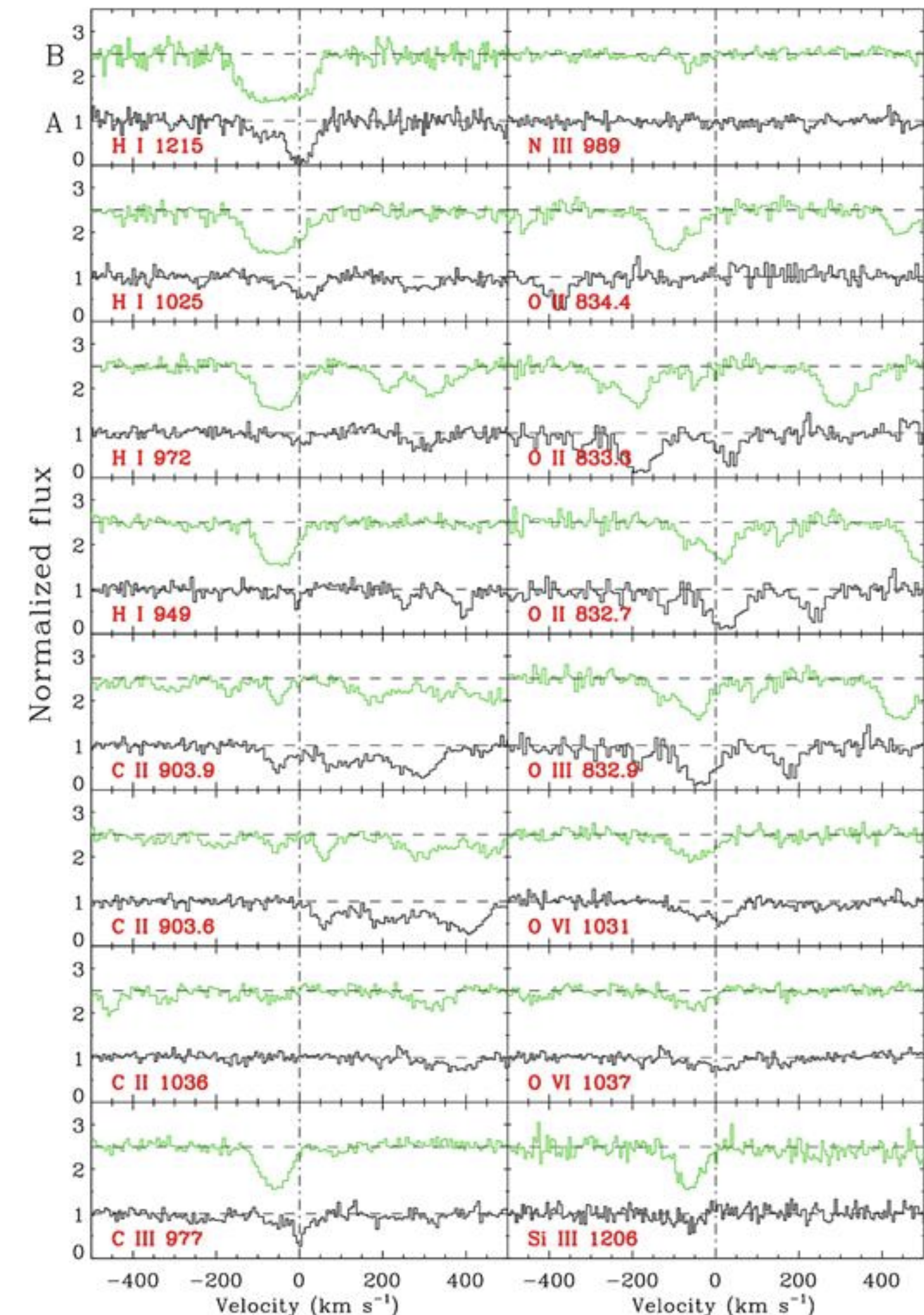
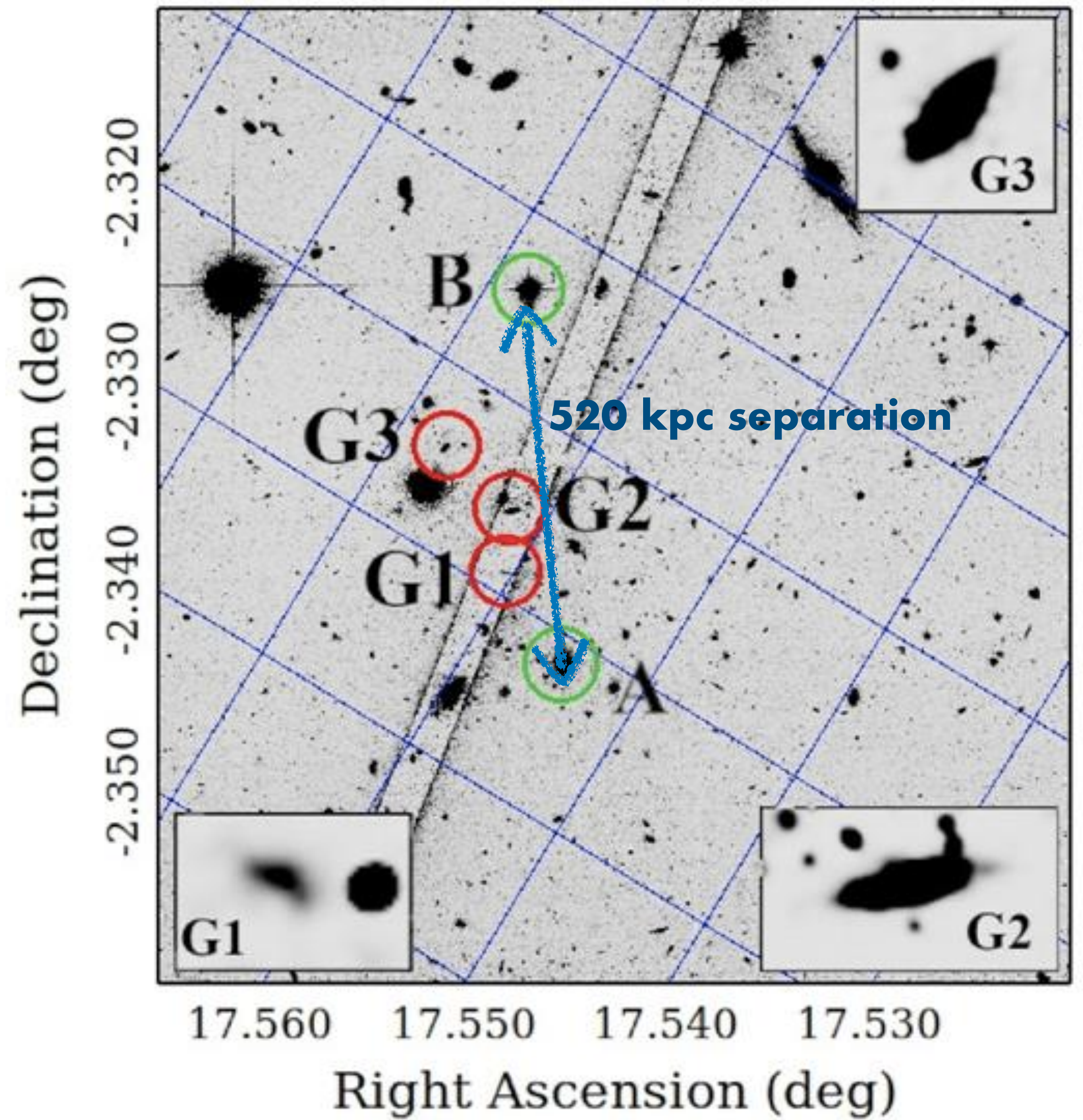
**PAIR QUASAR SIGHTLINES PROBING
MULTIPHASE GAS ASSOCIATED WITH CGM AND GALAXY GROUP ENVIRONMENT**

Q0107-025A & B : pair quasar sightline

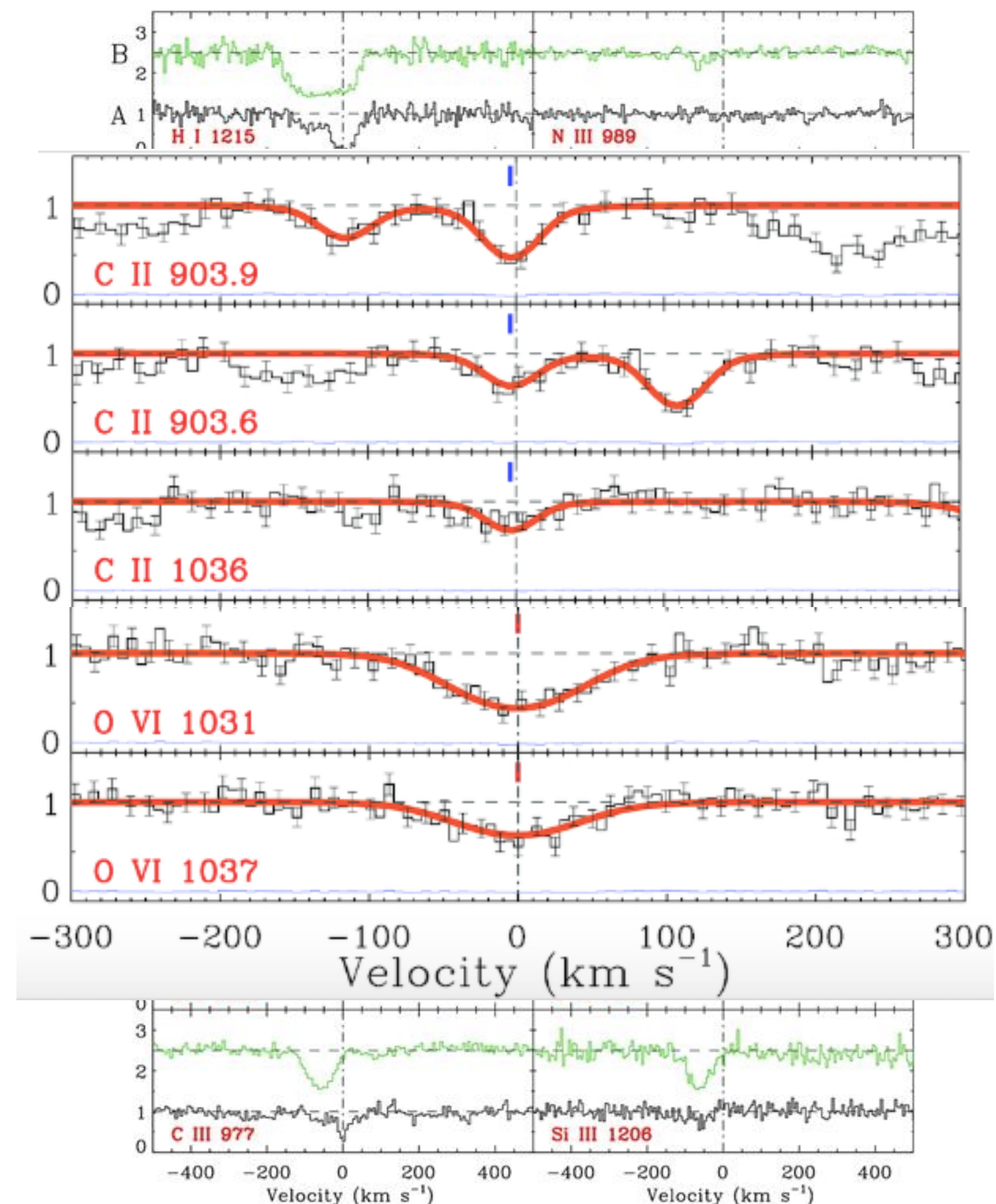
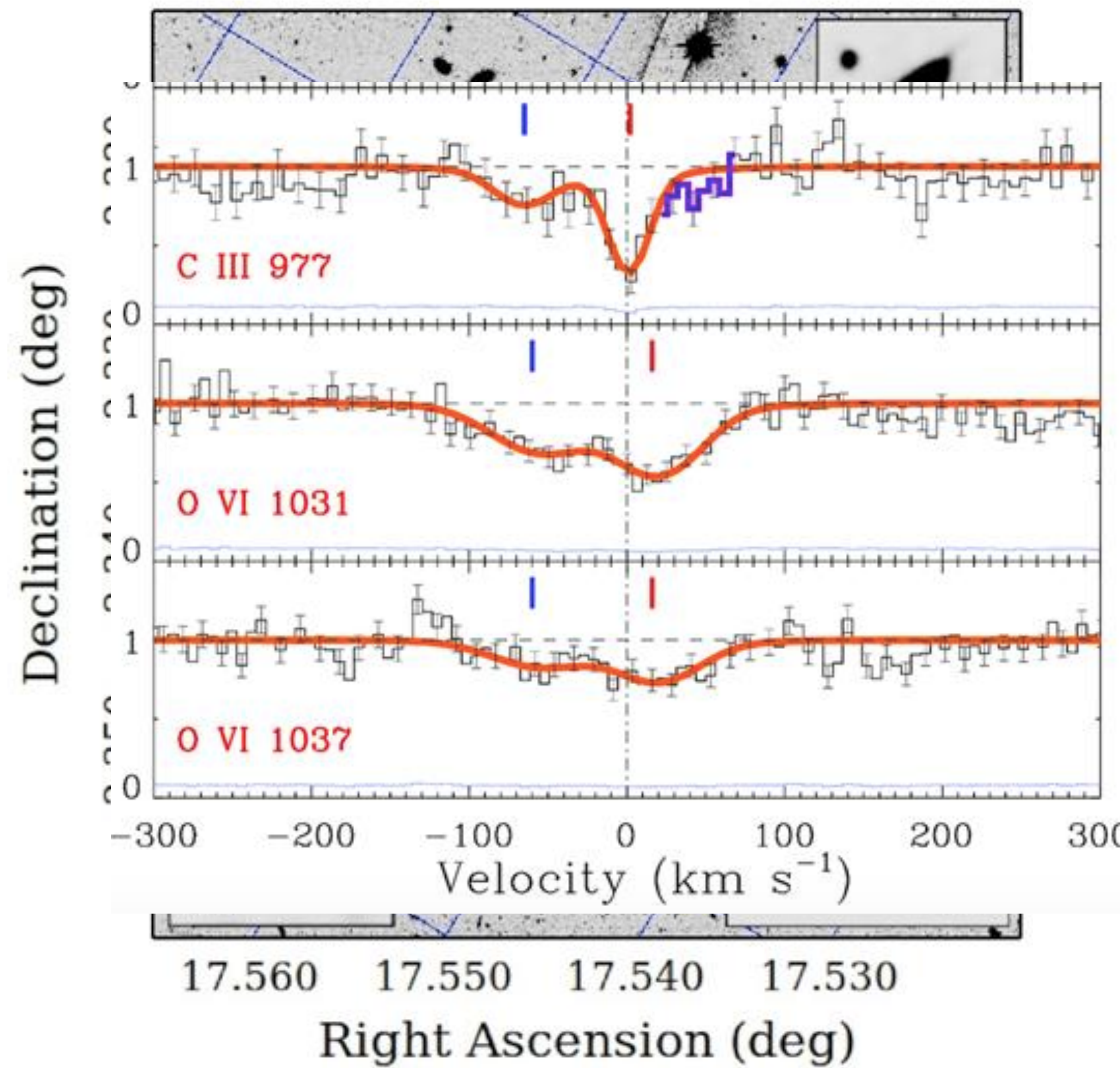
absorber z ~ 0.4



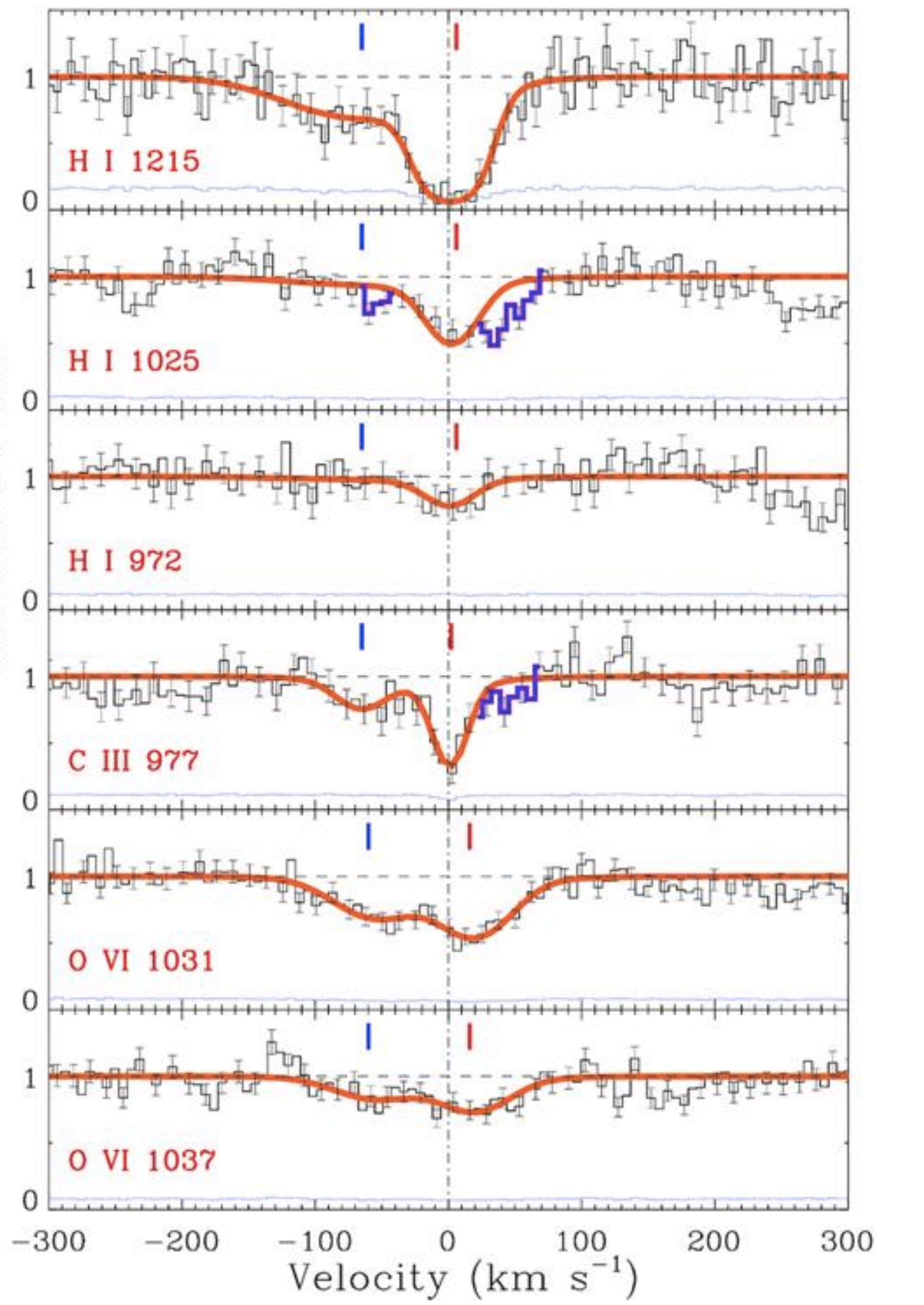
Q0107-025A & B : pair quasar sightline
absorber z ~ 0.4

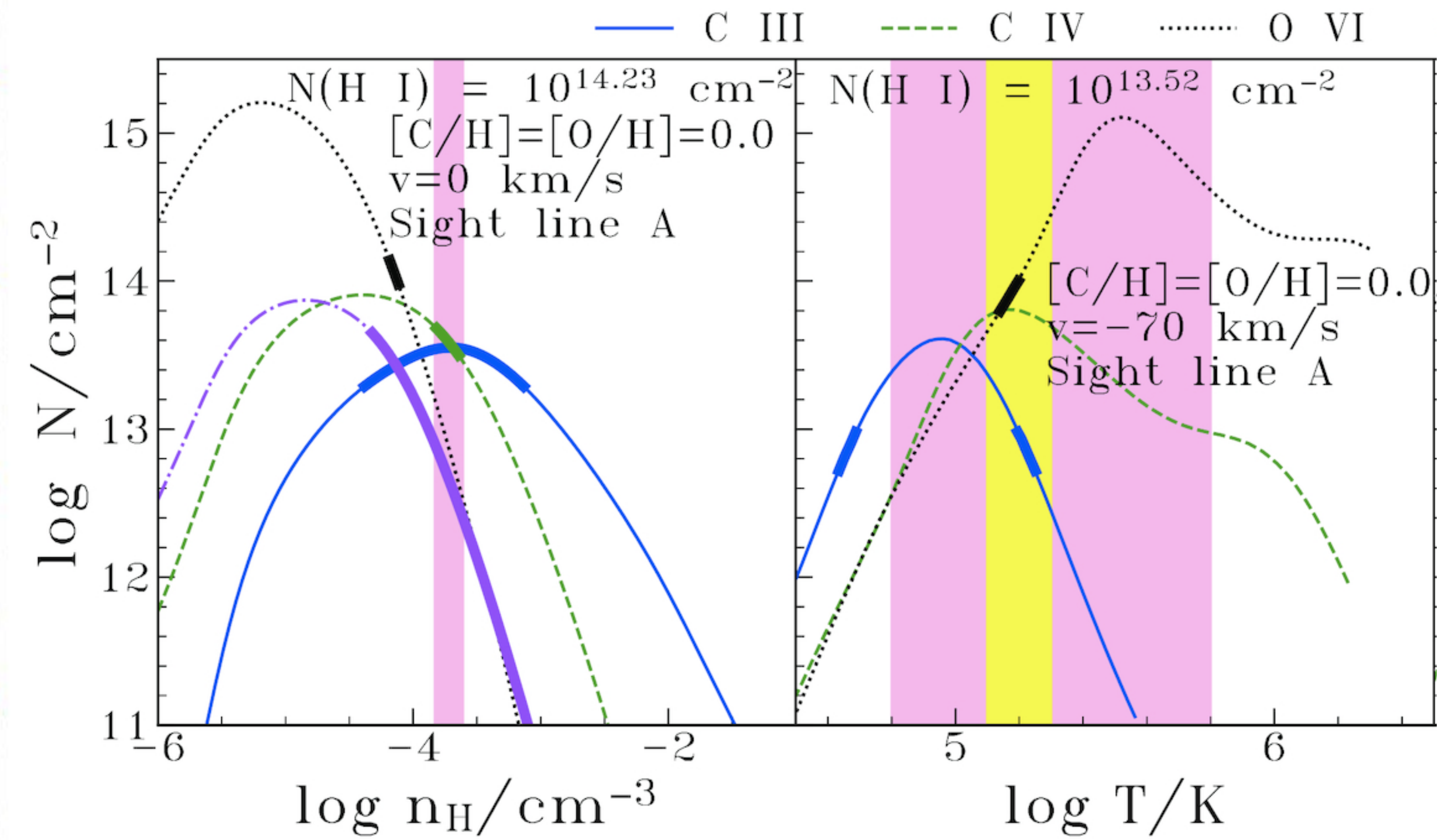
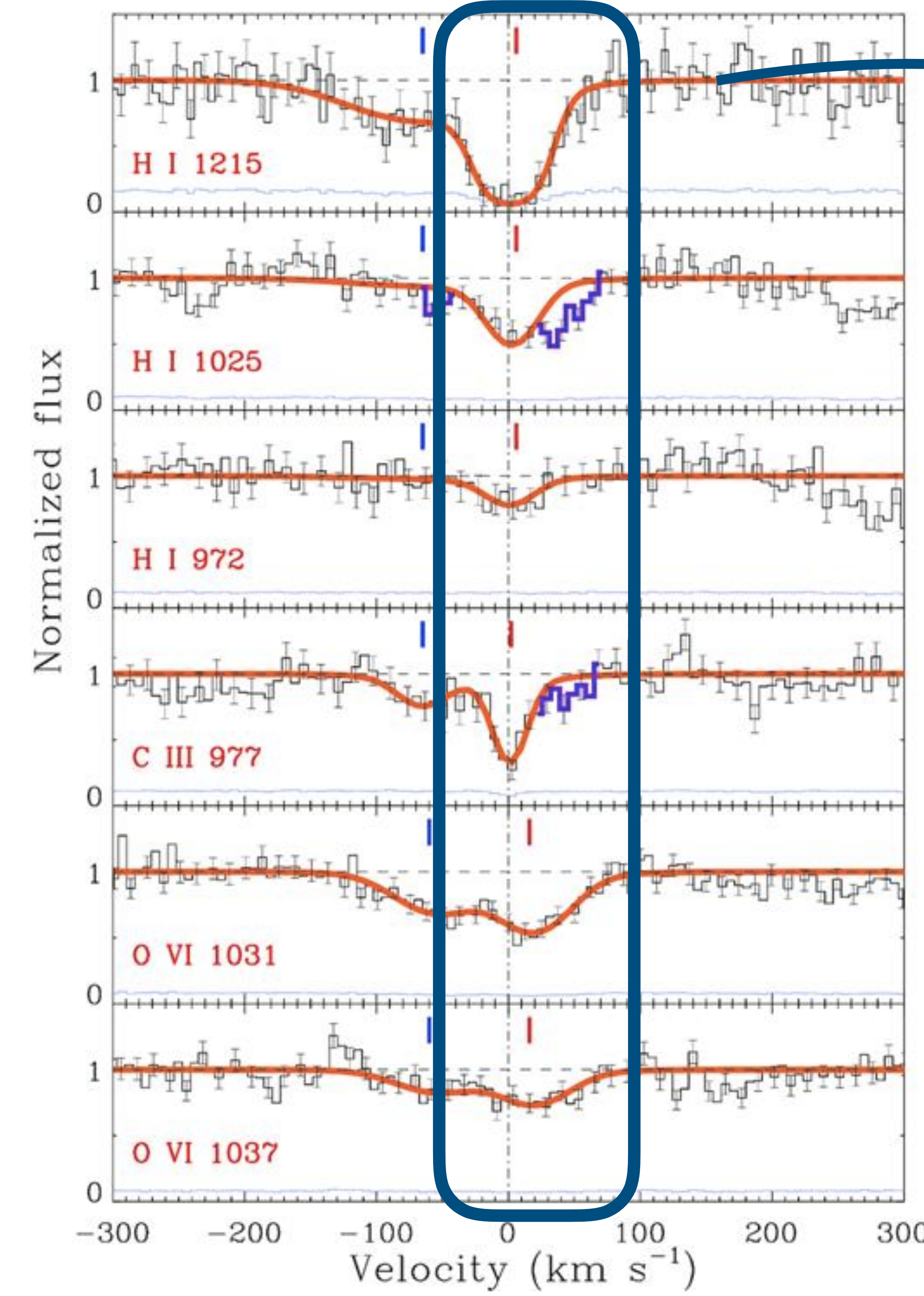


Q0107-025A & B : pair quasar sightline

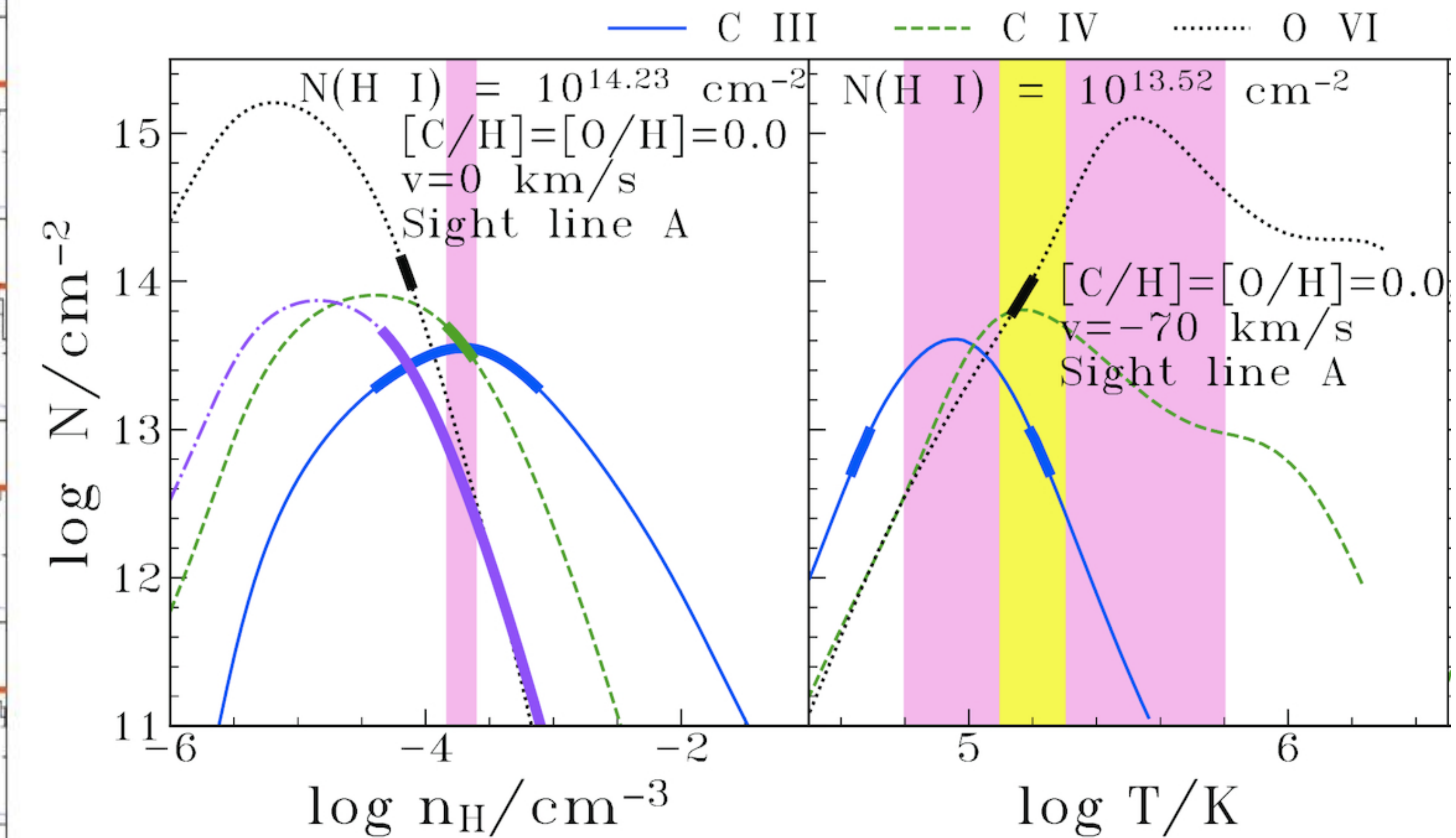
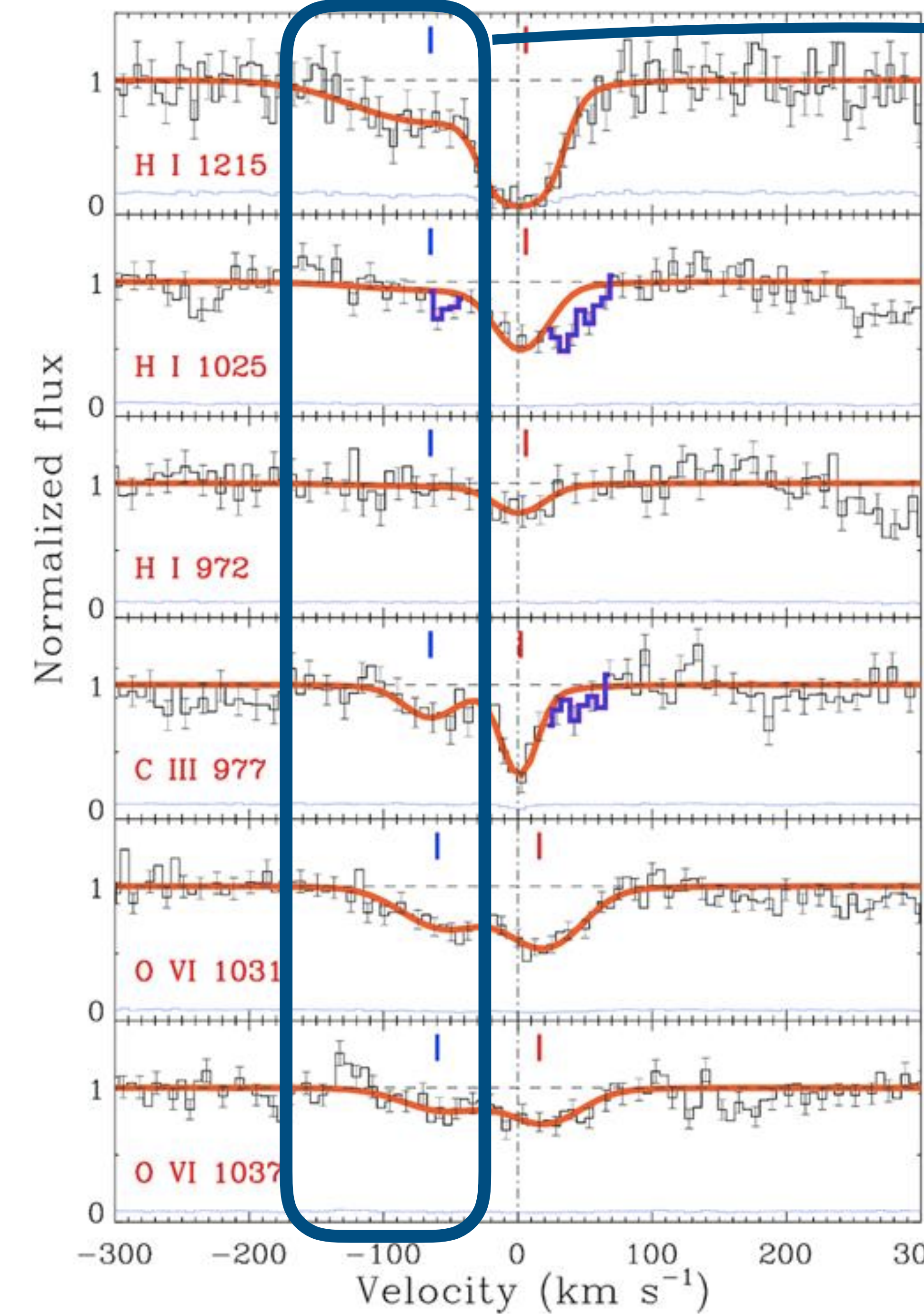
absorber $z \sim 0.4$ 

Normalized flux



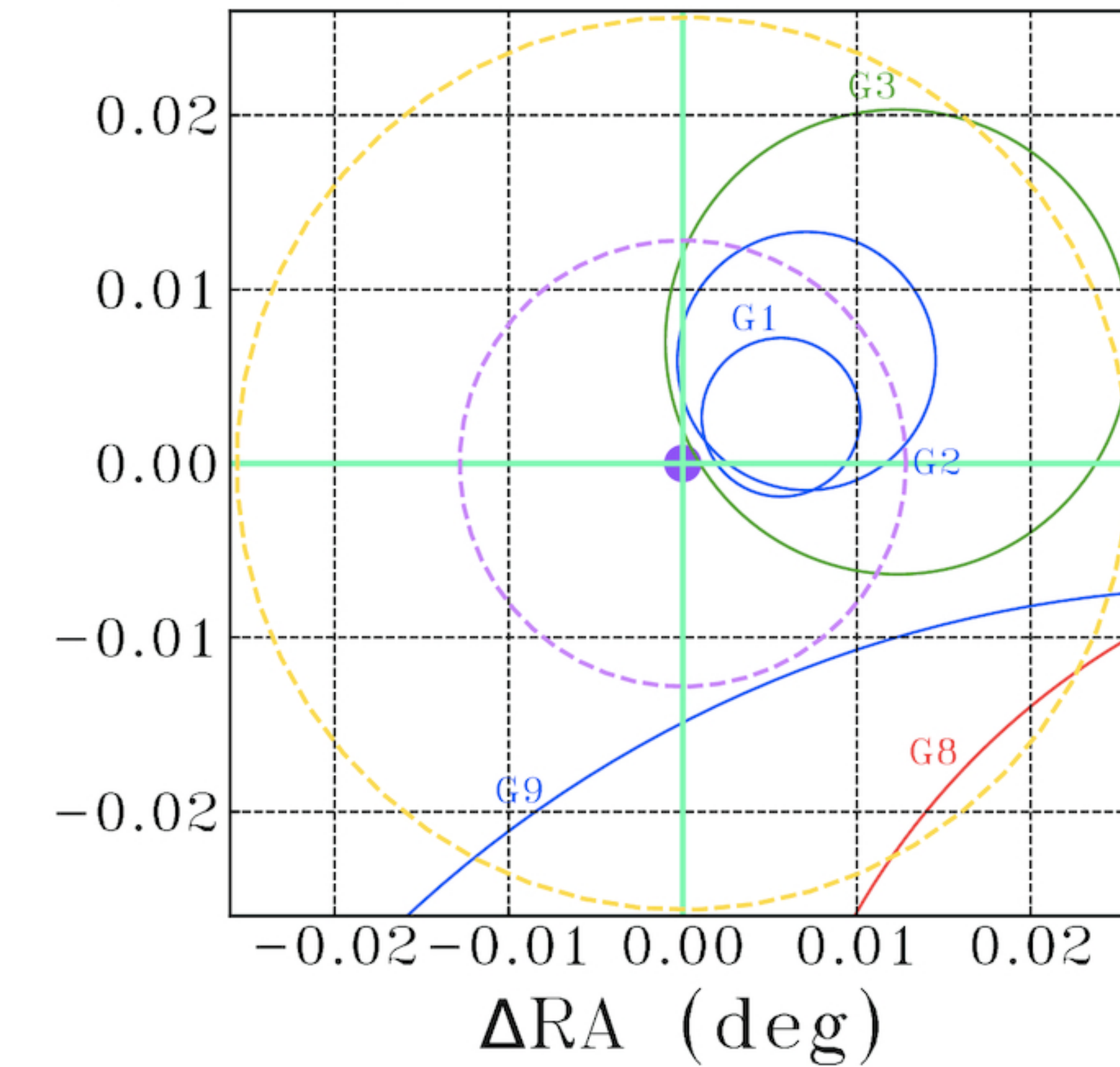
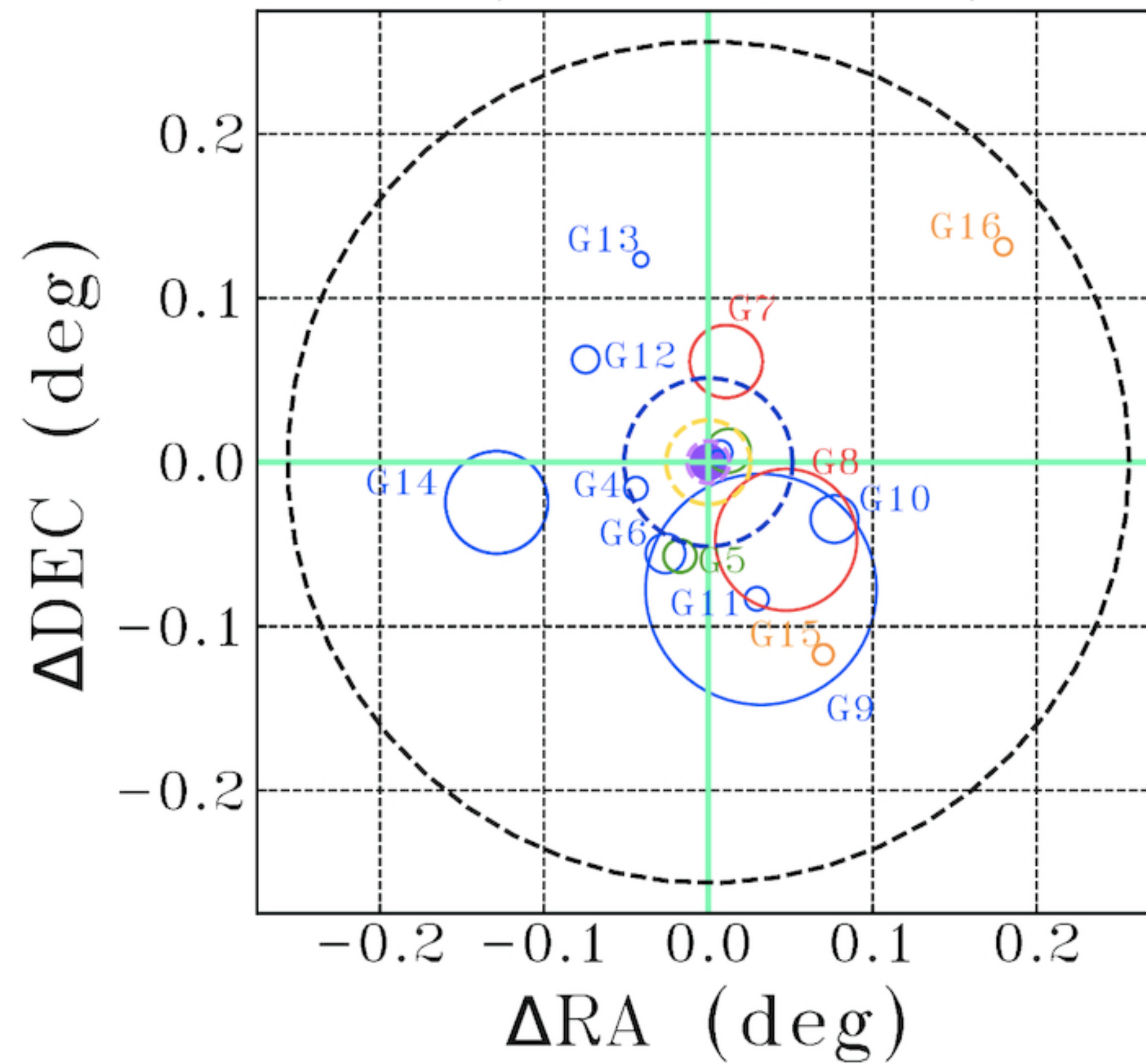


Along sightline A



Along sightline A

○ 0–100 km/s ○ 200–300 km/s — 250 kpc
○ 100–200 km/s ○ 300–500 km/s — 500 kpc
— 1 Mpc ● Line of sight A ($z=0.39949$)



12 galaxies within ± 250 km/s and 2 Mpc of projected distance from the sightlines of which five are within 500 kpc. Stellar masses range from $M_* \sim 10^{8.7} - 10^{11.5} \text{ M}_{\odot}$

Galaxies in the Group Environment

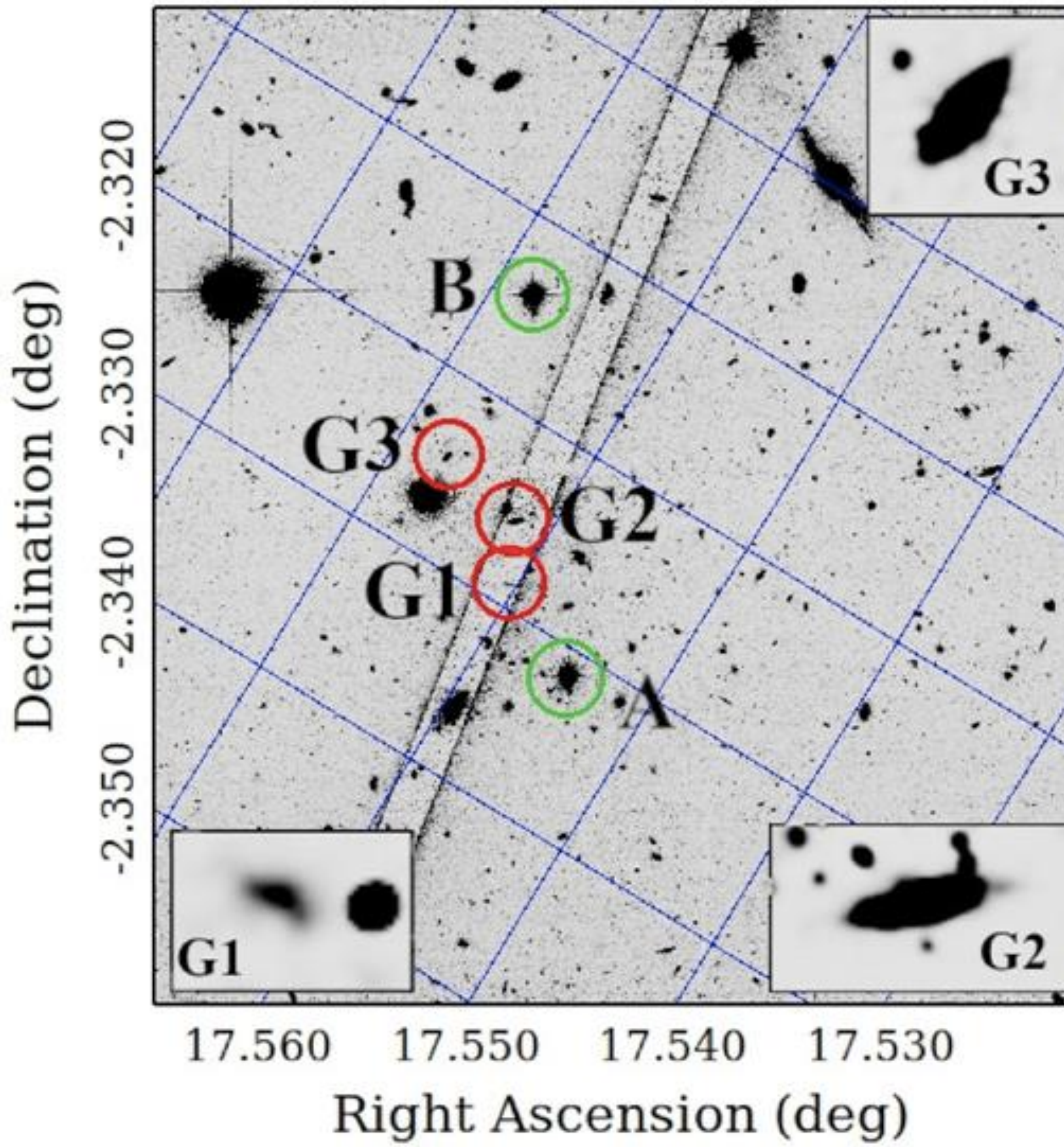
Label	RA (deg)	Dec. (deg)	m_R	z_{gal}	ρ (Mpc)		Δv (km s $^{-1}$)		M_R	$\log(L/L^*)$	$\log(M_*/M_\odot)$	R_{vir} (kpc)	ρ_A/R_{vir}		$\log(M_h/M_\odot)$	
					(6)	(7)	(8)	(9)					(13)	(14)	(15)	(16)
(1)	(2)	(3)	(4)	(5)	(6)	(7)	(8)	(9)	(10)	(11)	(12)	(13)	(14)	(15)	(16)	
G1	17.56048	-2.32871	25.1	0.39954	0.121	0.318	-12	-83	-16.5	-2.6	8.7	87.9	1.3	3.5	11.0	
G2	17.56194	-2.32547	22.0	0.39935	0.179	0.249	28	-42	-19.6	-1.4	10.0	143.2	1.2	1.7	11.6	
G3	17.56718	-2.32438	21.3	0.39882	0.276	0.200	142	71	-20.3	-1.1	10.6	257.2	1.0	0.7	12.4	
G4	17.51073	-2.34742	21.3	0.39992	0.915	1.288	-92	-163	-20.3	-1.1	9.9	136.3	6.6	9.3	11.6	
G5	17.53755	-2.38853	21.3	0.39882	1.164	1.566	143	73	-20.3	-1.1	10.4	193.2	5.9	8.0	12.0	
G6	17.52869	-2.38692	20.8	0.39930	1.197	1.611	40	-31	-20.8	-0.9	10.6	232.2	5.0	6.8	12.3	
G7	17.56568	-2.27001	20.1	0.40054	1.214	0.861	-226	-296	-21.5	-0.6	11.0	428.5	2.8	1.9	13.1	
G8	17.60223	-2.37862	19.8	0.40053	1.305	1.425	-223	-294	-21.9	-0.4	11.2	834.3	1.5	1.6	13.9	
G9	17.58691	-2.40884	19.7	0.39912	1.635	1.884	79	8	-21.9	-0.4	11.4	1357.3	1.1	1.3	14.6	
G10	17.63162	-2.36604	21.6	0.39922	1.643	1.604	57	-13	-20.0	-1.2	10.7	279.9	5.8	5.6	12.5	
G11	17.58439	-2.41457	21.4	0.39993	1.722	1.985	-96	-167	-20.2	-1.1	9.9	138.1	12.3	14.2	11.6	
G12	17.48010	-2.26885	23.9	0.39950	1.900	1.924	-4	-74	-17.7	-2.1	10.1	160.2	11.7	11.8	11.8	
G13	17.51376	-2.20793	22.3	0.39978	2.536	2.323	-63	-134	-19.3	-1.5	8.6	86.5	29.0	26.5	11.0	
G14	17.42589	-2.35586	20.3	0.39945	2.559	2.884	7	-64	-21.3	-0.7	11.1	602.1	4.2	4.7	13.5	
G15	17.62484	-2.44852	22.1	0.40178	2.661	2.847	-491	-562	-19.5	-1.4	9.6	120.1	21.9	23.4	11.4	
G16	17.73452	-2.20009	21.7	0.40180	4.339	3.939	-496	-567	-20.0	-1.2	9.2	102.5	41.8	38.0	11.2	

Data from VLT/VIMOS, Keck/DEIMOS, and Gemini/GMOS and Tejos et al. (2014)

stellar masses from M^*/L ratio as a function of color tables

halo masses estimated using the stellar-to-halo-mass relation

SFR using H-alpha or [O II]



gas detected at $z \sim 0.4$ along sightline B

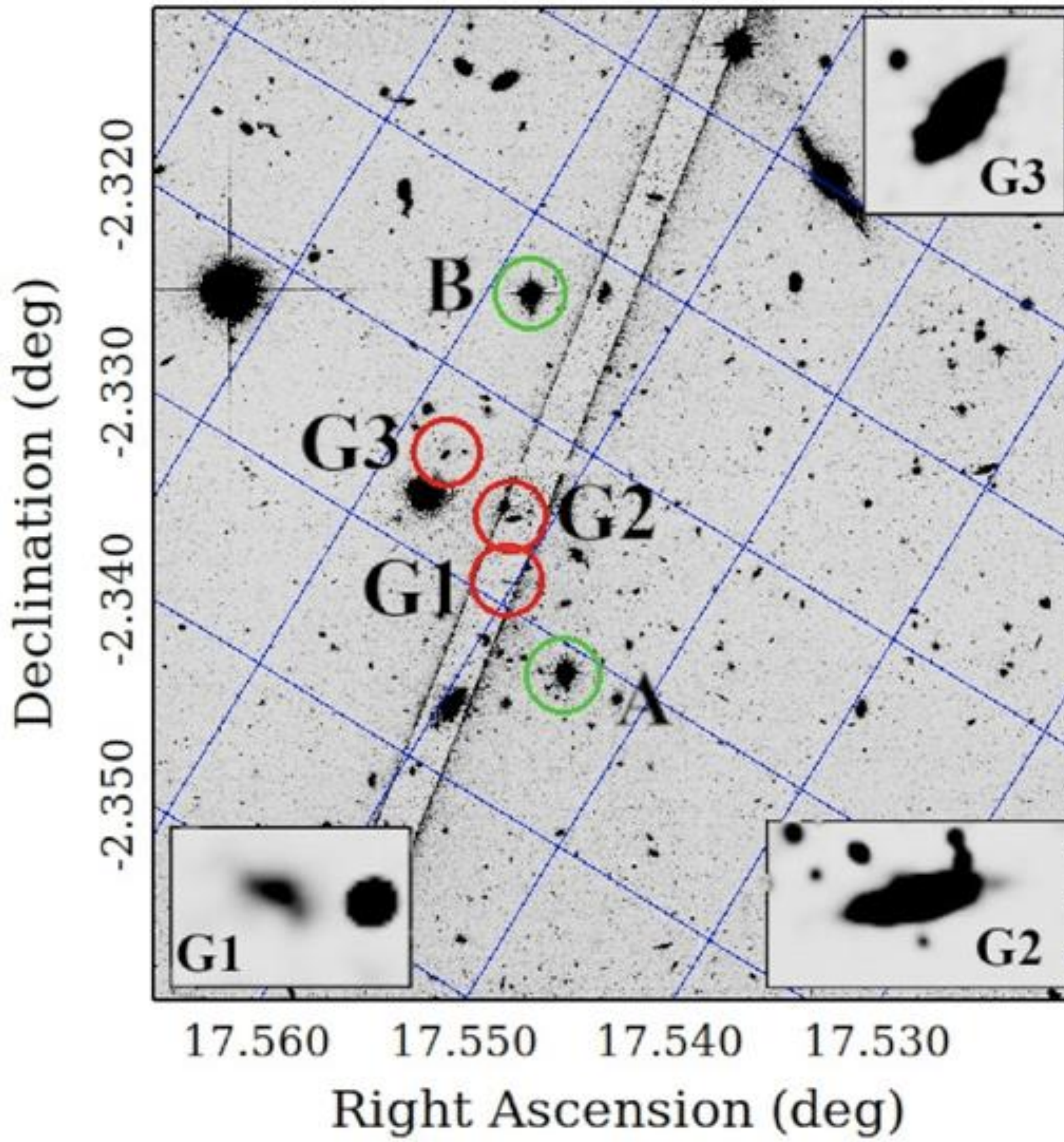
is a partial Lyman limit system

multiple photoionised gas phases with metallicities of 1/10 solar

O VI tracing collisionally ionized gas of higher temperature

absorber along the projected major axis of the nearest galaxy (G3)

$$\Phi \approx 3^0, d/R_{vir} \approx 0.7, \text{SFR} < 0.1 M_\odot \text{ yr}^{-1}$$



gas detected at $z \sim 0.4$ along sightline B

is a partial Lyman limit system

multiple photoionised gas phases with metallicities of 1/10 solar

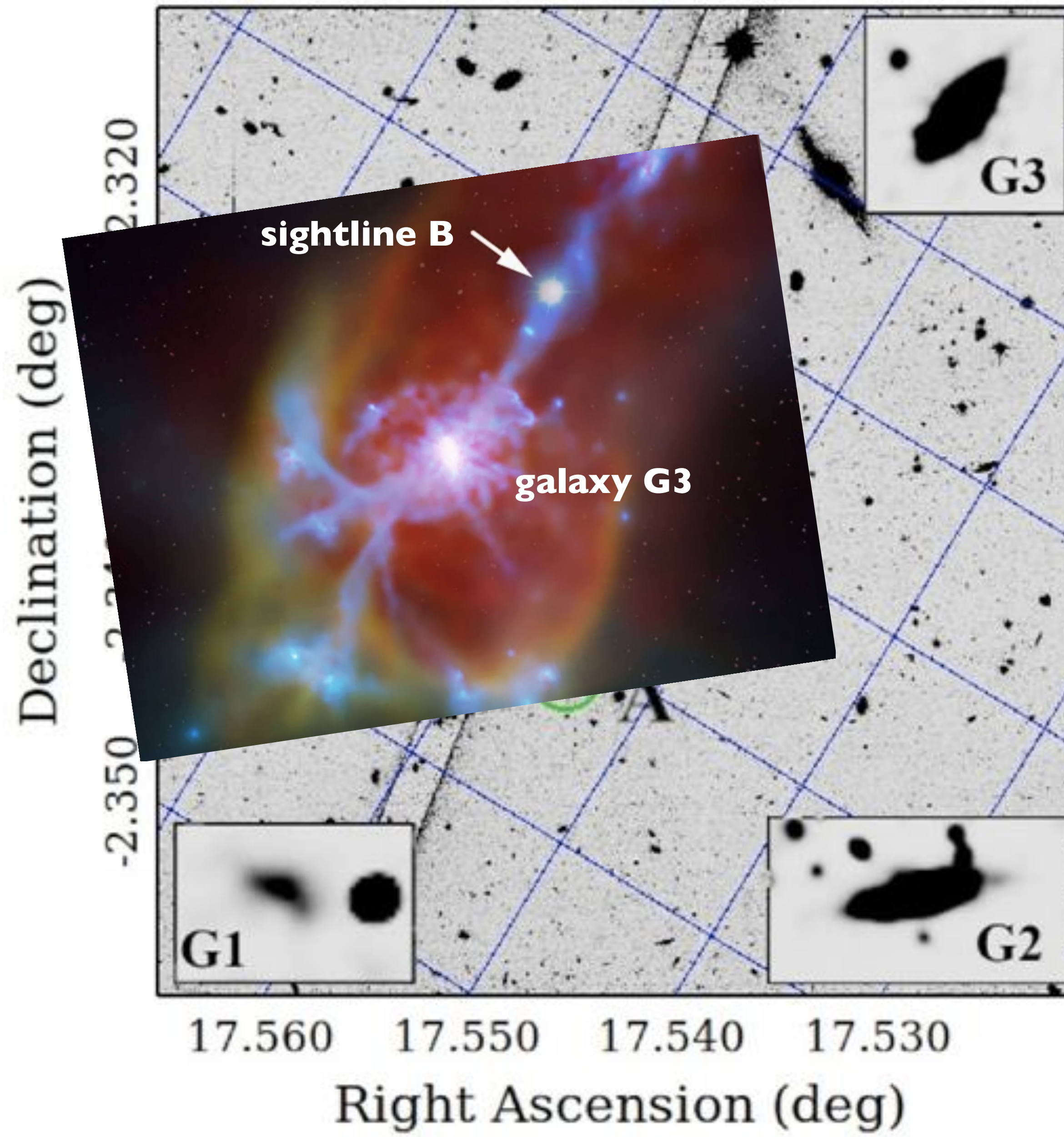
O VI tracing collisionally ionized gas of higher temperature

absorber along the projected major axis of the nearest galaxy (G3)

$\Phi \approx 3^0$, $d/R_{vir} \approx 0.7$, $SFR < 0.1 M_\odot \text{ yr}^{-1}$

cold accretion stream from the group environment ?

Group environments have plenty of cool gas away from galaxies mixed with metals from past outflows and tidal streams. Accreting gas need not be pristine.



gas detected at $z \sim 0.4$ along sightline B

is a partial Lyman limit system

multiple photoionised gas phases with metallicities of 1/10 solar

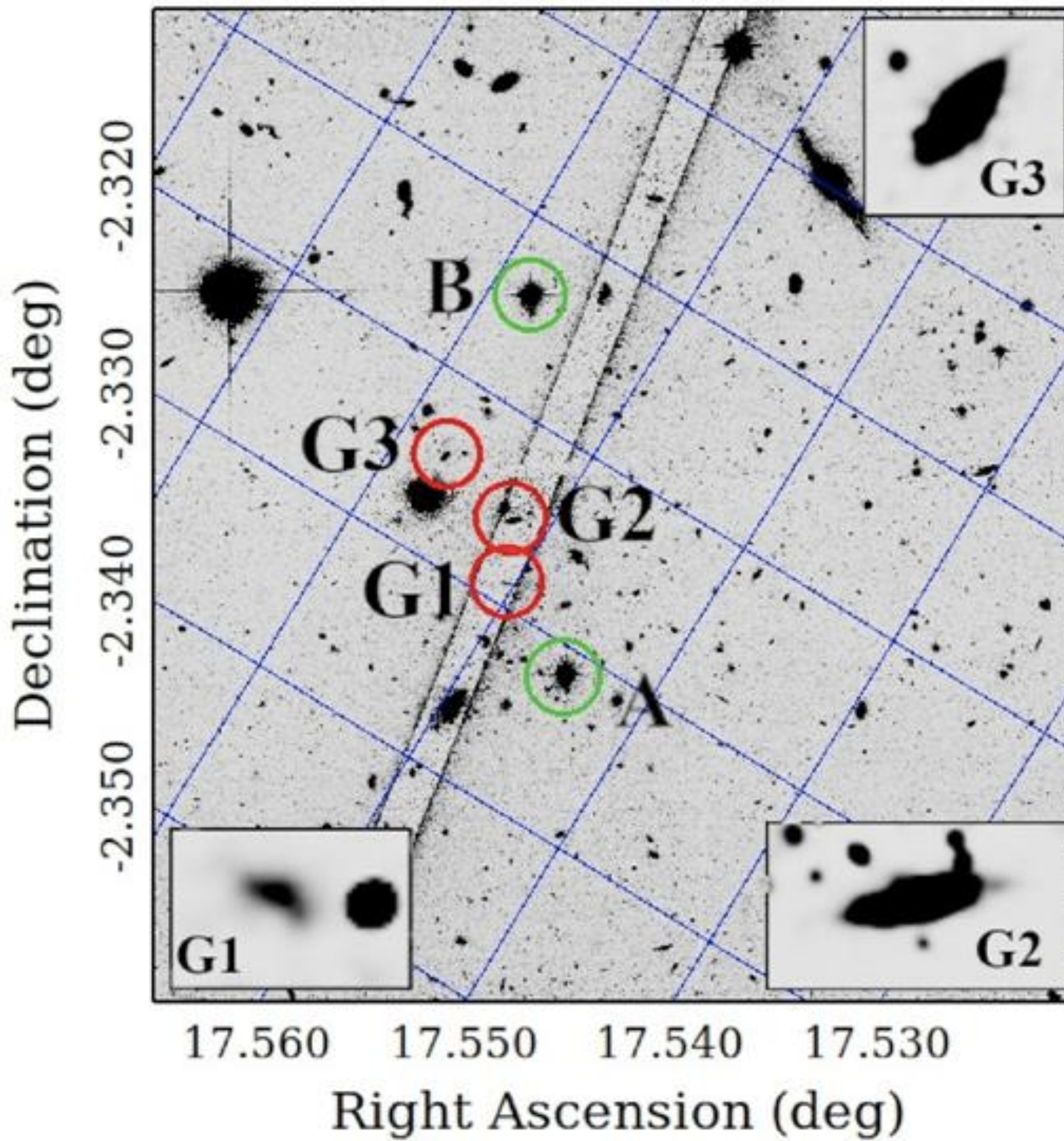
O VI tracing collisionally ionized gas of higher temperature

absorber along the projected major axis of the nearest galaxy (G3)

$\Phi \approx 3^0$, $d/R_{vir} \approx 0.7$, $SFR < 0.1 M_\odot \text{ yr}^{-1}$

cold accretion stream from the group environment ?

Group environments have plenty of cool gas away from galaxies mixed with metals from past outflows and tidal streams. Accreting gas need not be pristine.



gas detected at $z \sim 0.4$ along sightline A

has a lower column density in cold gas

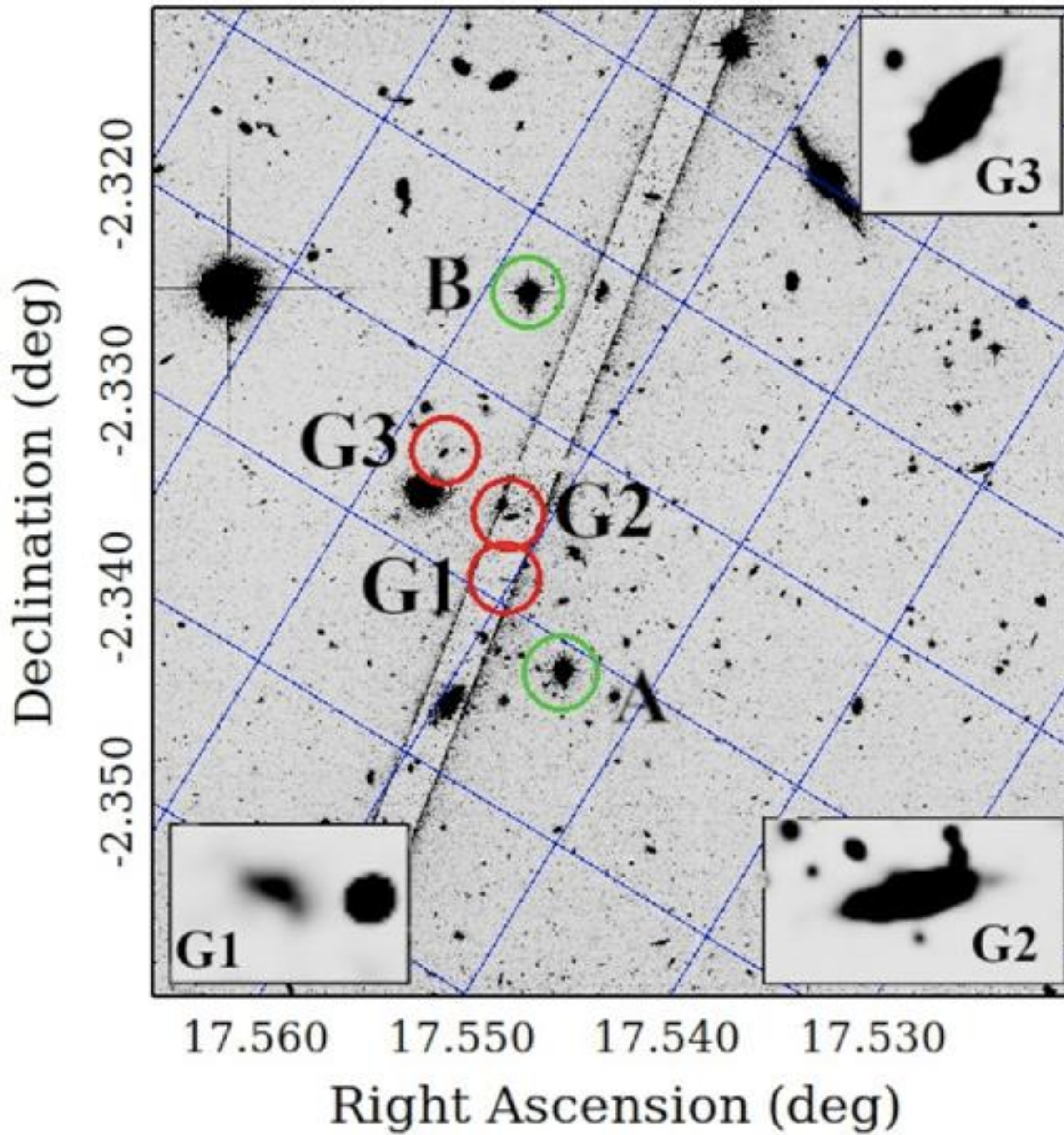
O VI and HI line broadening suggests $T \gtrsim 10^5$ K

absorption from both photoionised and collisionally ionised phases of gas

metal abundances of solar

absorber along the projected minor axis of G2

$\Phi \approx 86^\circ$, $d/R_{vir} \approx 1.1$, $SFR \approx 3 M_\odot \text{ yr}^{-1}$



gas detected at $z \sim 0.4$ along sightline A

has a lower column density in cold gas

O VI and HI line broadening suggests $T \gtrsim 10^5$ K

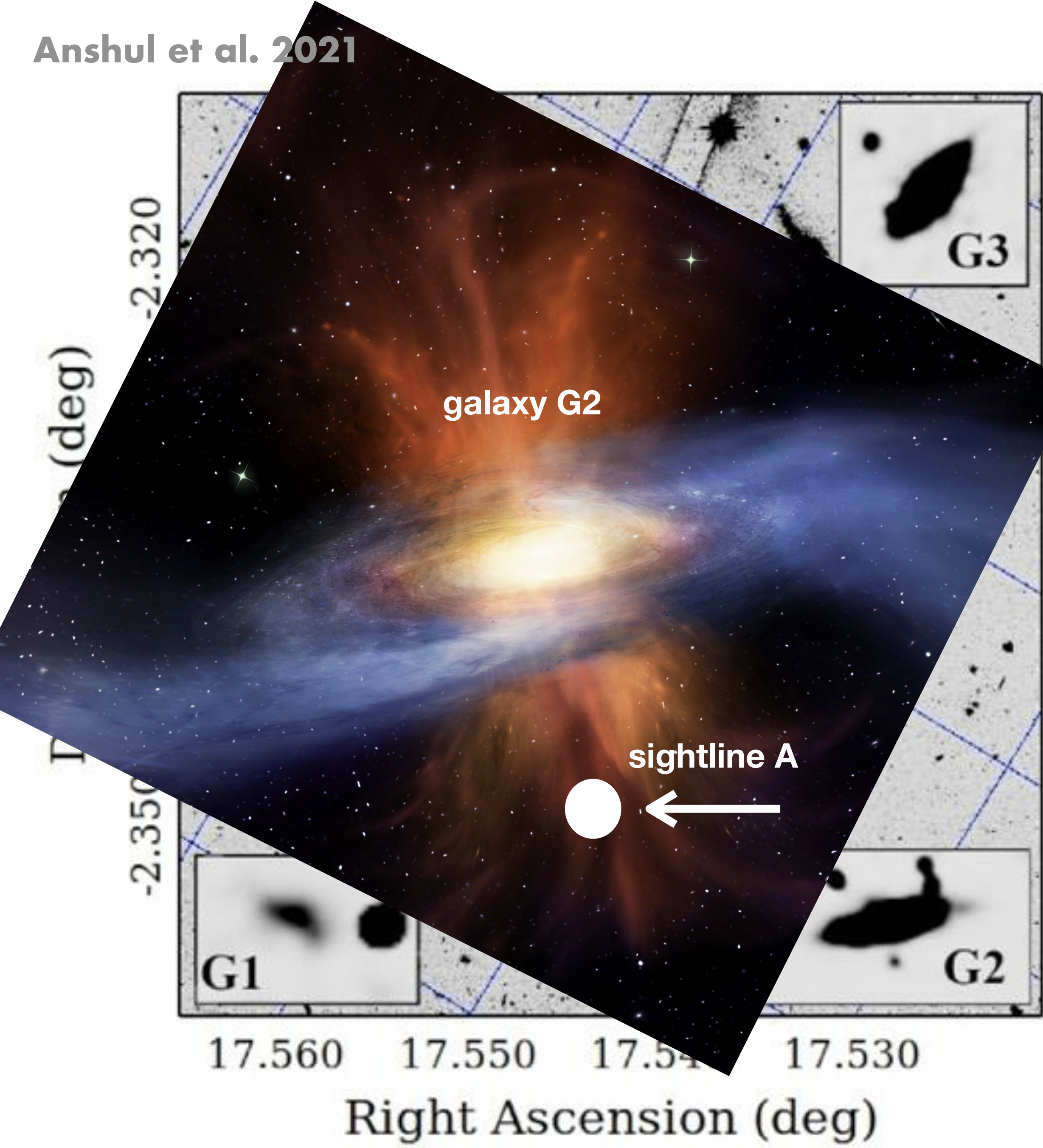
absorption from both photoionised and collisionally ionised phases of gas

metal abundances of solar

absorber along the projected minor axis of G2

$\Phi \approx 86^\circ$, $d/R_{vir} \approx 1.1$, $SFR \approx 3 M_\odot \text{ yr}^{-1}$

tracing earlier metal-rich outflows from G2?



gas detected at $z \sim 0.4$ along sightline A

has a lower column density in cold gas

O VI and HI line broadening suggests $T \gtrsim 10^5$ K

absorption from both photoionised and collisionally ionised phases of gas

metal abundances of solar

absorber along the projected minor axis of G2

$\Phi \approx 86^\circ$, $d/R_{vir} \approx 1.1$, $SFR \approx 3 M_\odot \text{ yr}^{-1}$

tracing earlier metal-rich outflows from G2?

Declination (deg)

-2.350 -2.340 -2.330 -2.320



G3

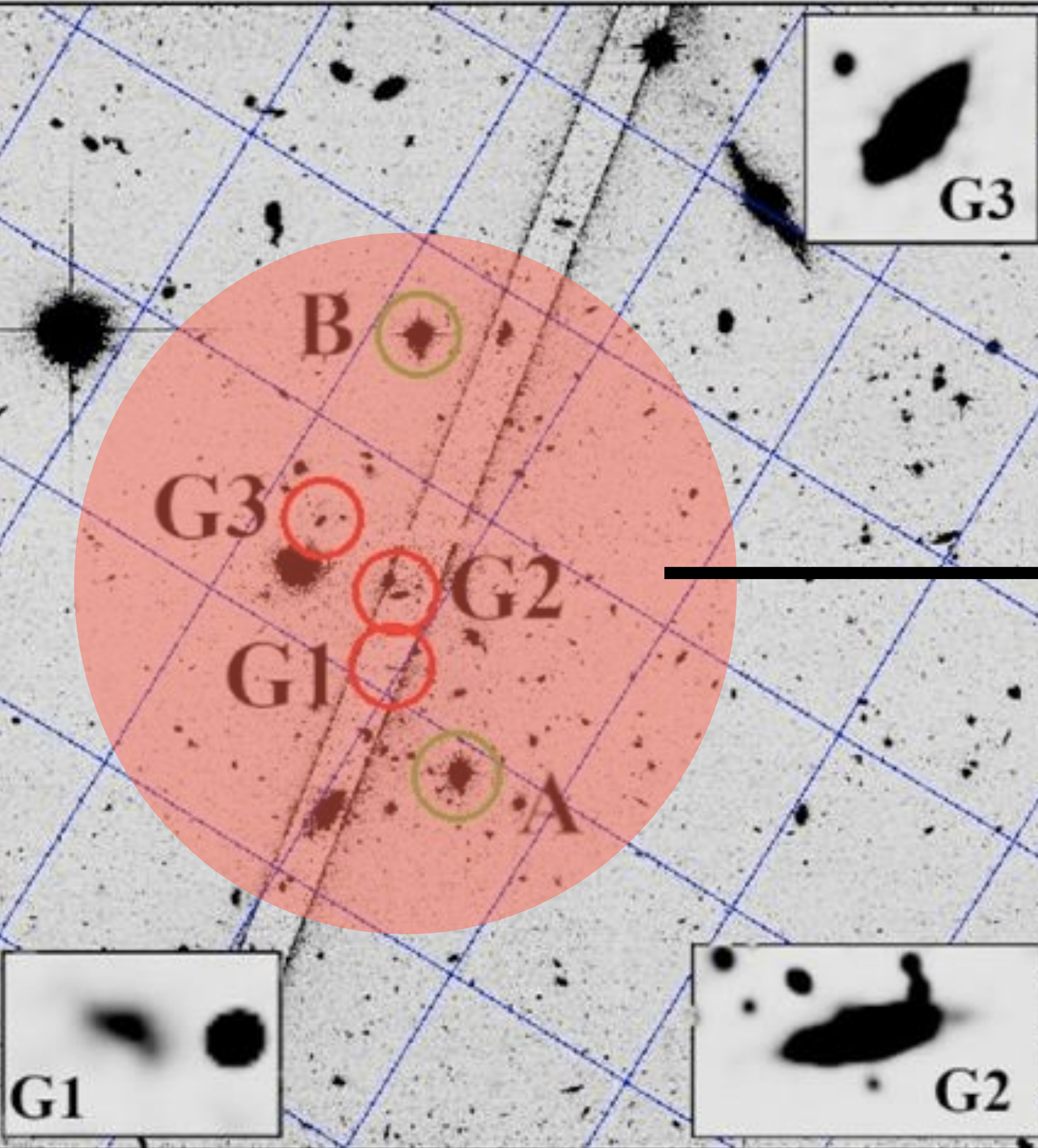
G1

G2

B

G3

G2



17.560 17.550 17.540 17.530

Right Ascension (deg)

O VI similar absorption along both lines of sight
broader than other metals

Galaxy groups contain warm gas
O VI part of the warm phase of the intragroup medium

Stocke et al. 2014

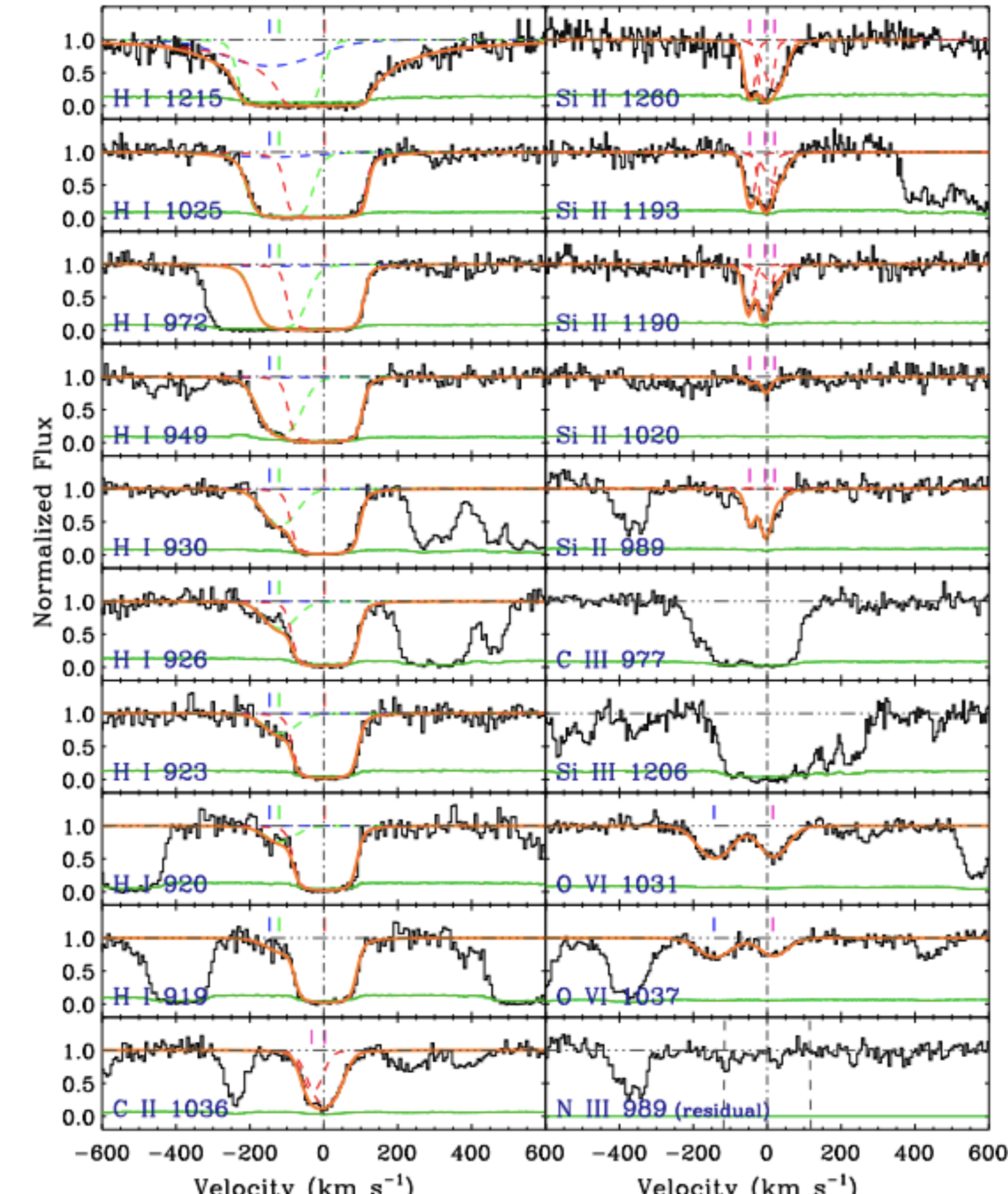
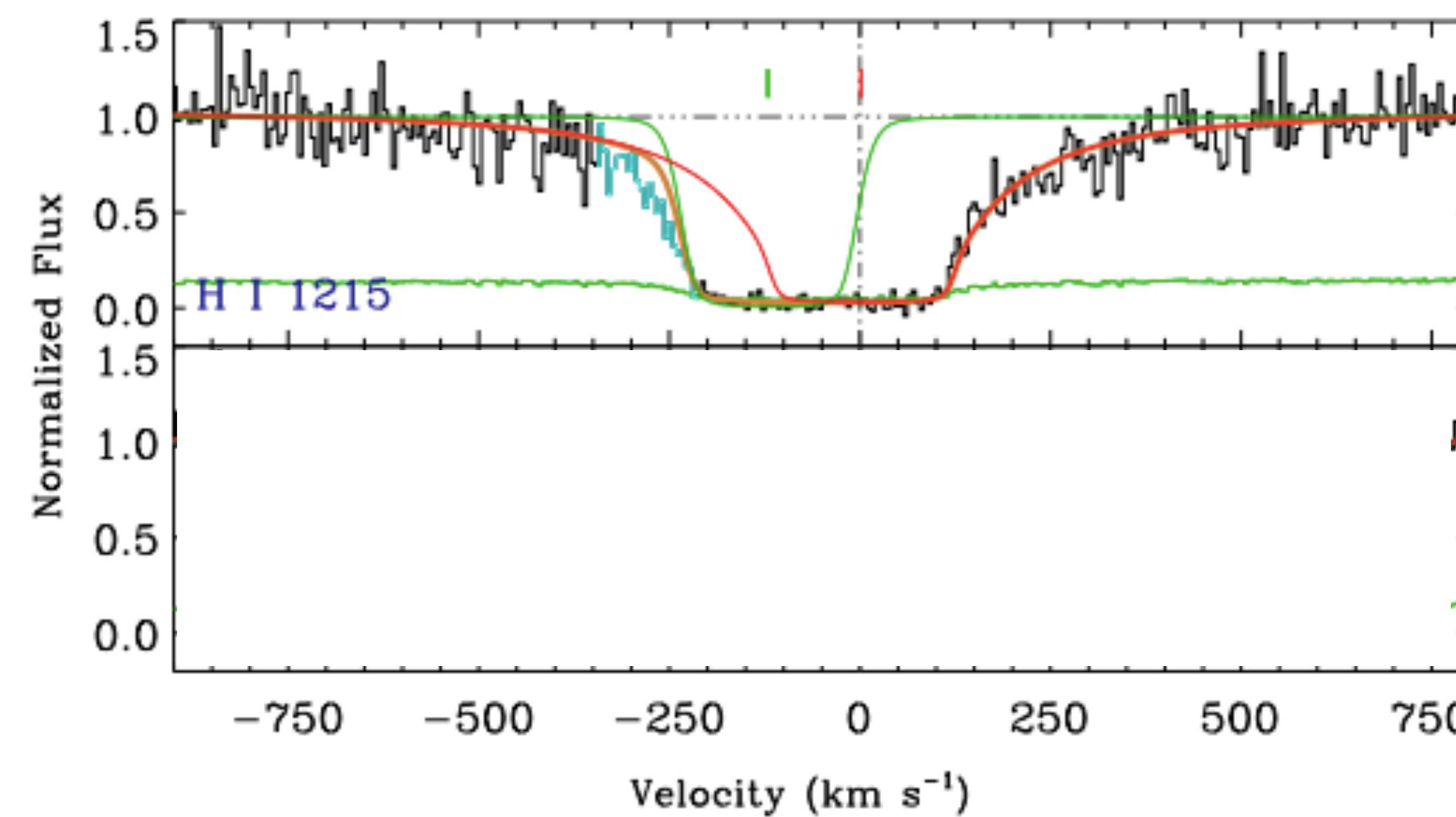
Anshul et al. 2021

Lyman Limit System - BLA - OVI Tracing (Possible) Gas Accretion onto CGM

Khonde et al. 2024, submitted

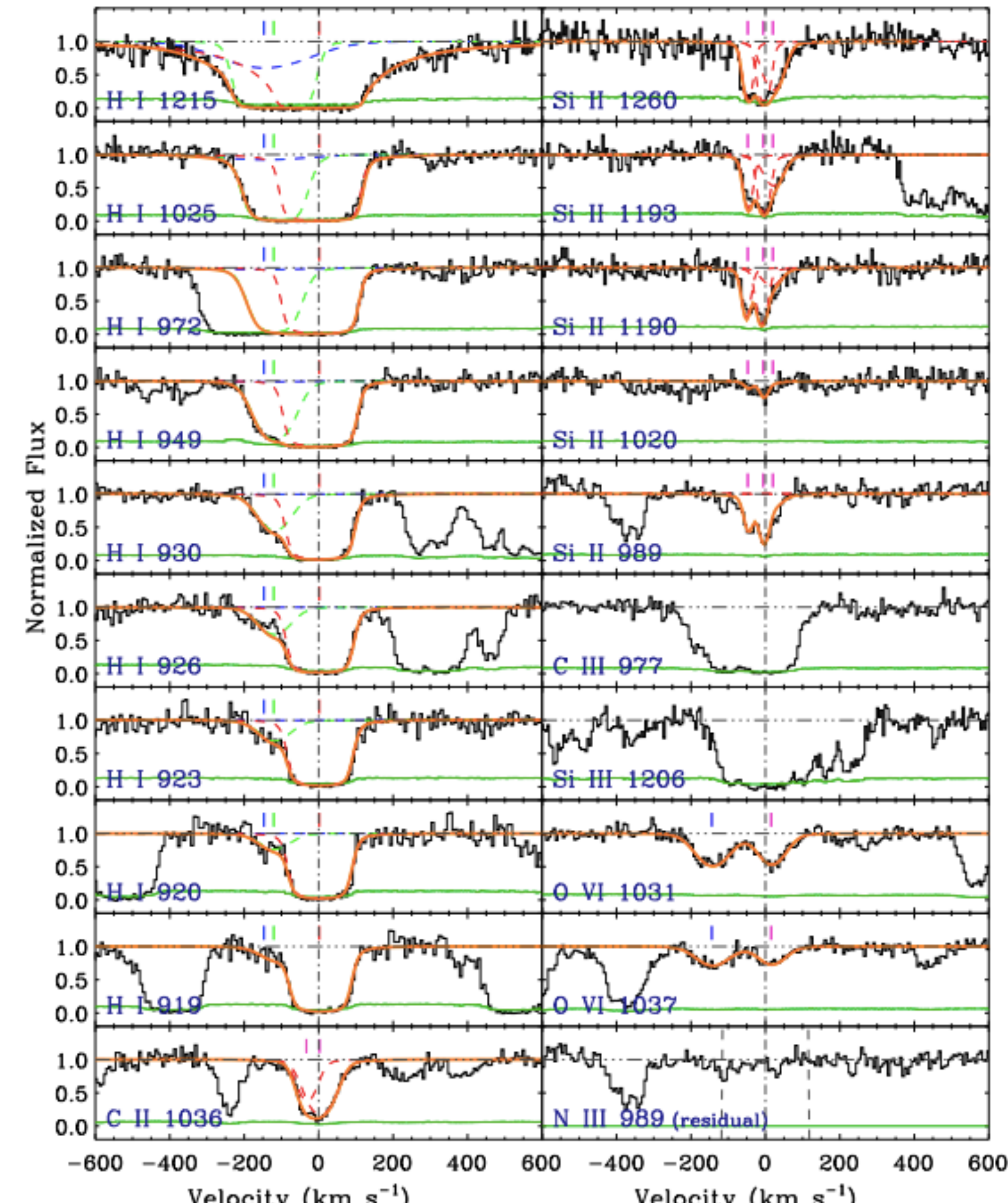
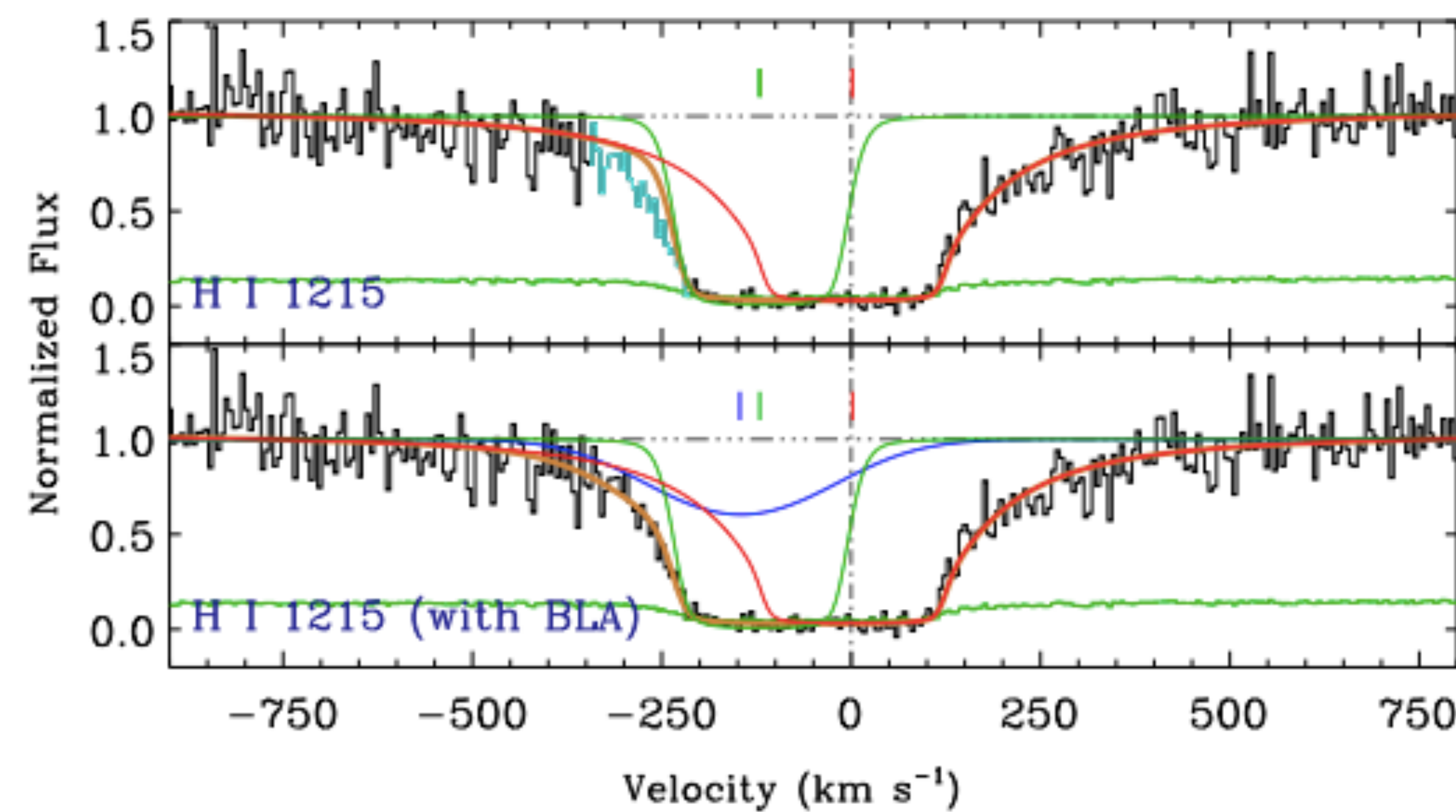
HST/COS + VLT/MUSE Observations of a LLS with BLA - O VI at $z \sim 0.4$

Khonde et al. 2024, submitted



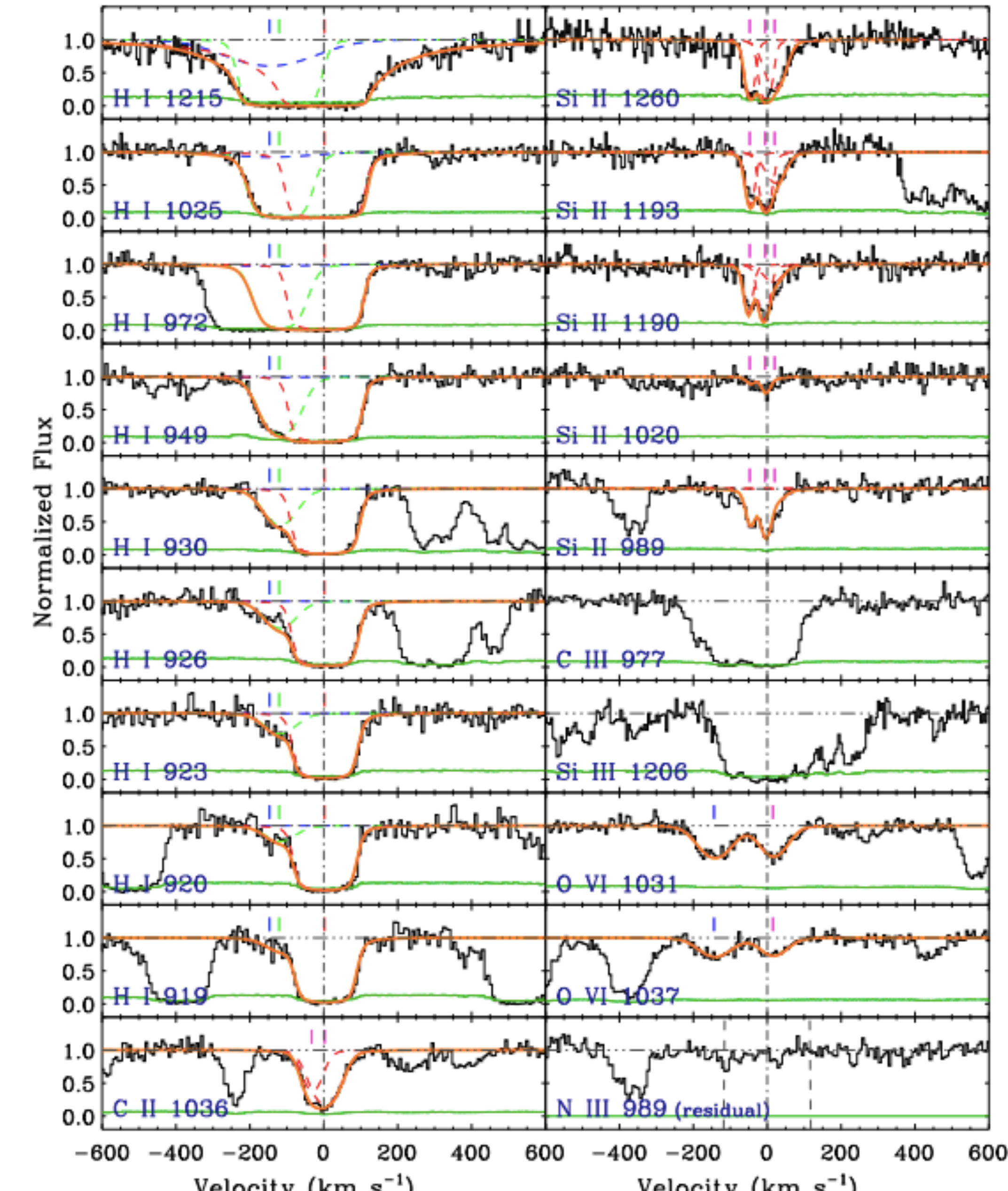
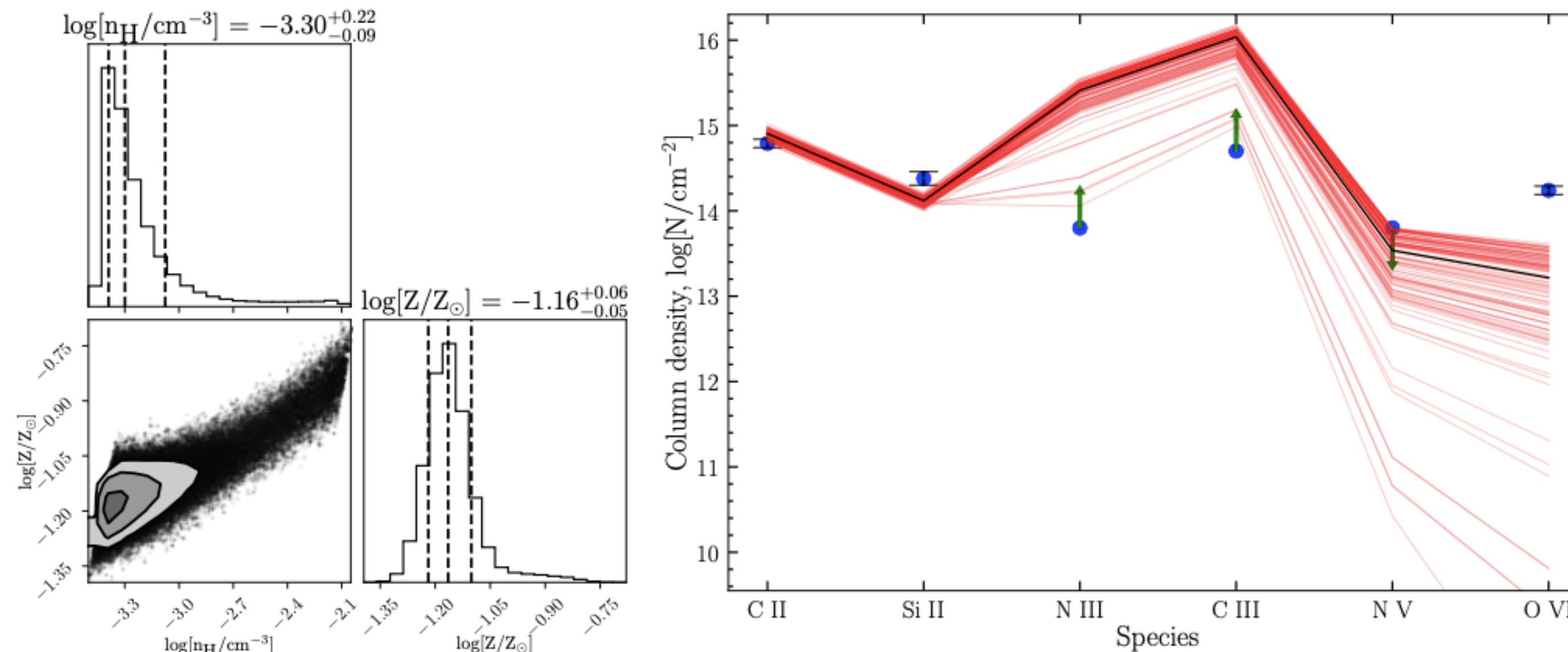
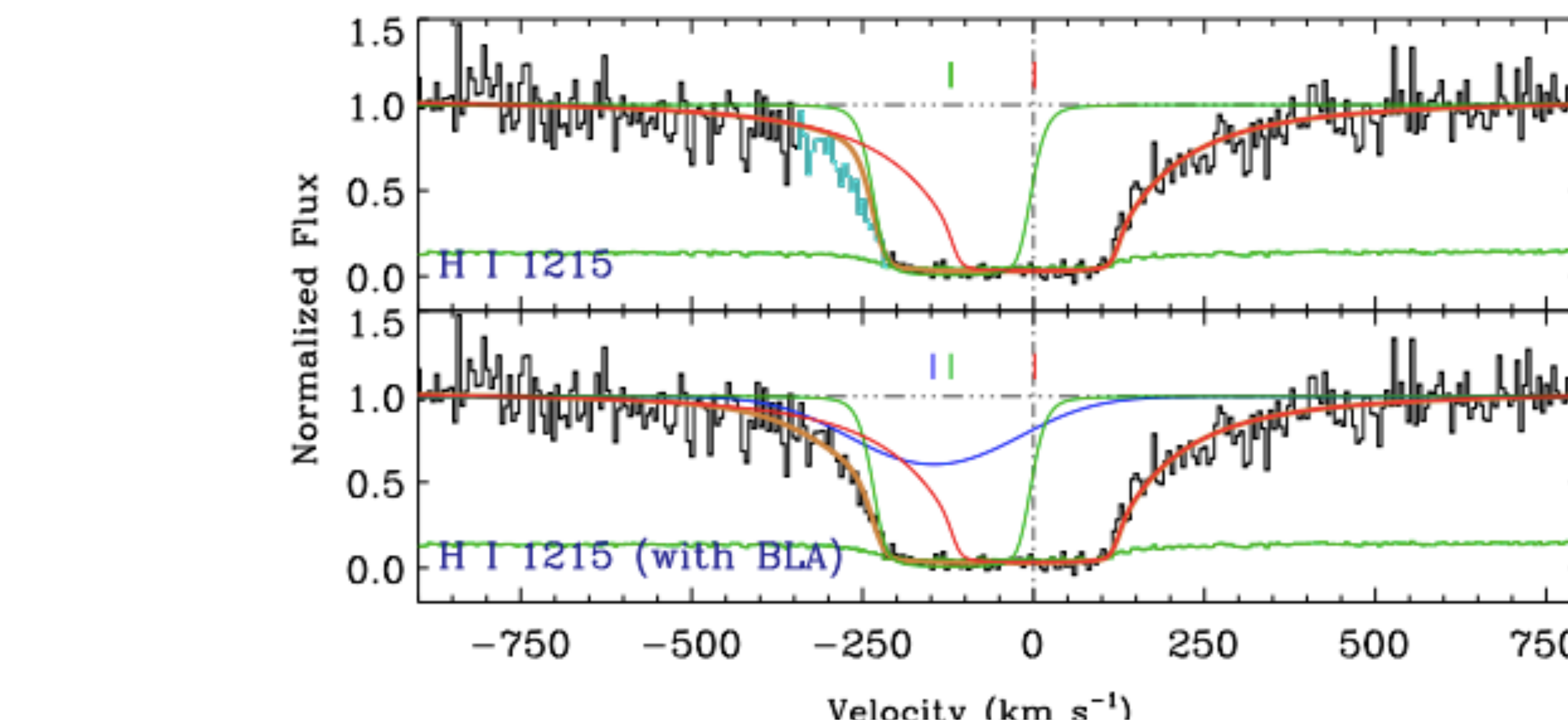
HST/COS + VLT/MUSE Observations of a LLS with BLA - O VI at $z \sim 0.4$

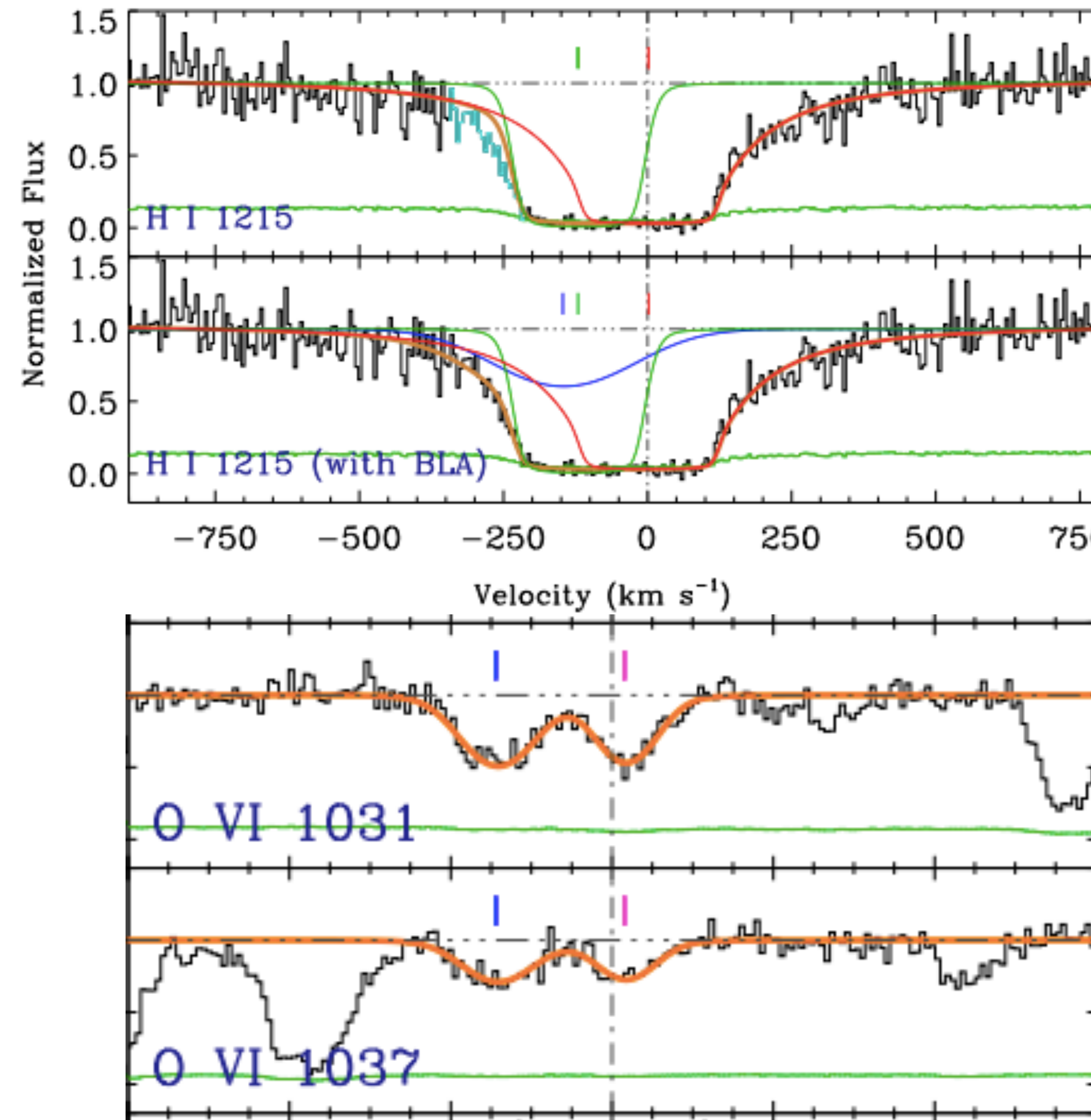
Khonde et al. 2024, submitted



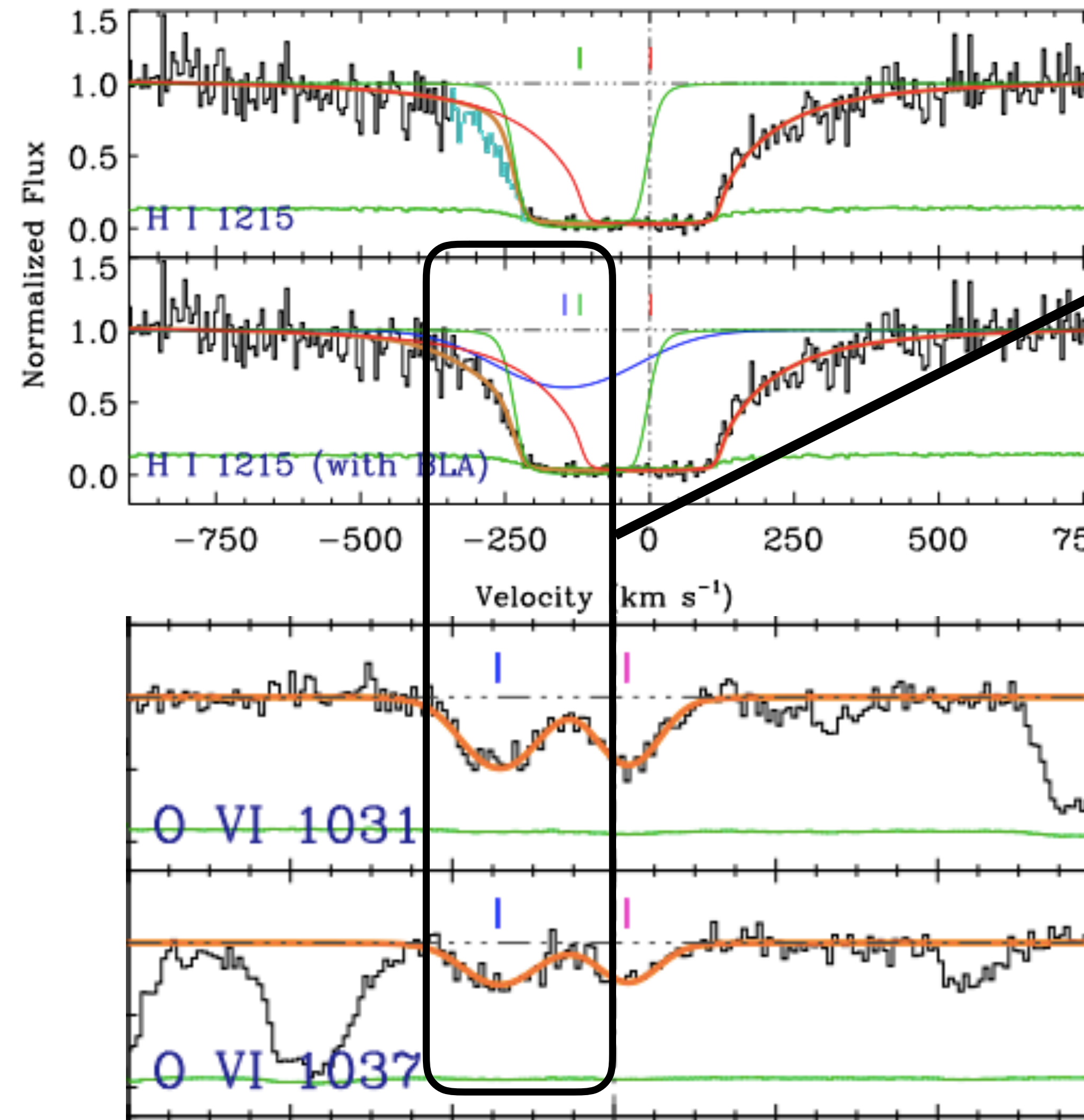
HST/COS + VLT/MUSE Observations of a LLS with BLA - O VI at $z \sim 0.4$

Khonde et al. 2024, submitted





Lyman limit component + low ionization metals trace gas with $T \sim 10^4 \text{ K}$



Lyman limit component + low ionization metals trace gas with $T \sim 10^4 \text{ K}$

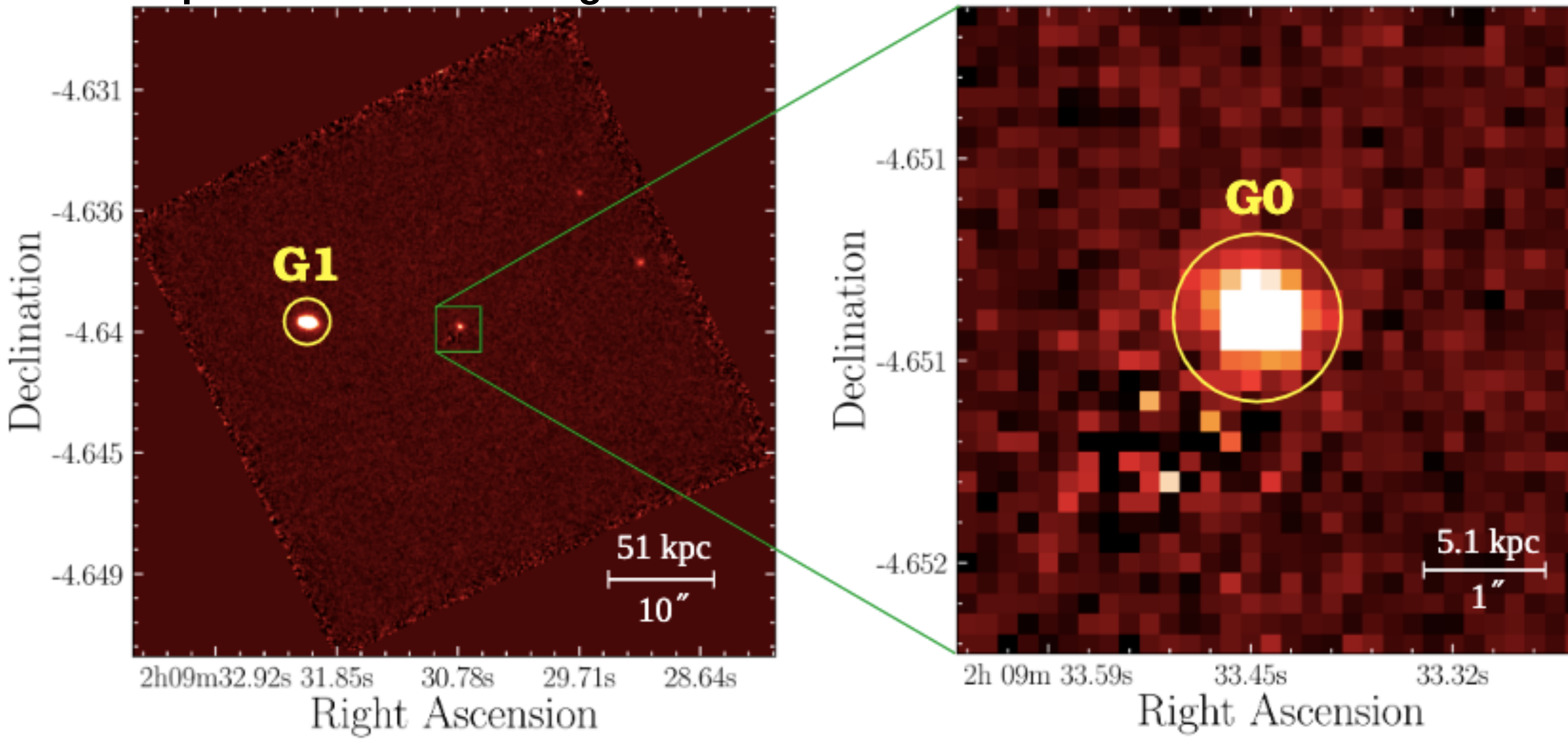
$\text{O VI} + \text{BLA}$ traces gas with $T \sim 10^6 \text{ K}$

The baryonic column density in the cold and hot phases are comparable
 $N(\text{H}) = N(\text{H I}) + N(\text{H II}) \sim 10^{20} \text{ cm}^{-2}$

HST/COS + VLT/MUSE Observations of a LLS with BLA - O VI at $z \sim 0.4$

Khonde et al. 2024, submitted

H-alpha narrow band image at $z \sim 0.4$



$G0 : \rho = 12 \text{ kpc}, |\Delta v| = 54 \text{ km/s}$

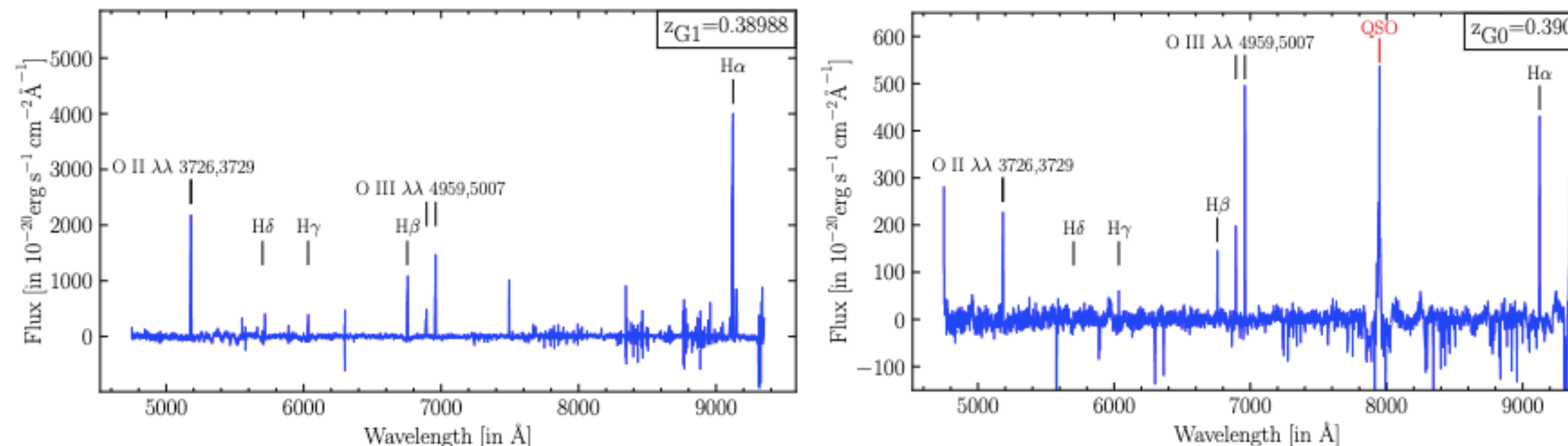
$G1 : \rho = 104 \text{ kpc}, |\Delta v| = 127 \text{ km/s}$

Parameter	G0	G1
z	0.39022	0.38988
$M_*(M_\odot)$	$\approx 10^6$	$\approx 10^{10}$
SFR ($M_\odot \text{ yr}^{-1}$)	0.01	1.78
R_{vir} (kpc)	31.53	138.93
[O/H]	-0.058	0.218

$G0$ is probably a dwarf satellite of $G1$

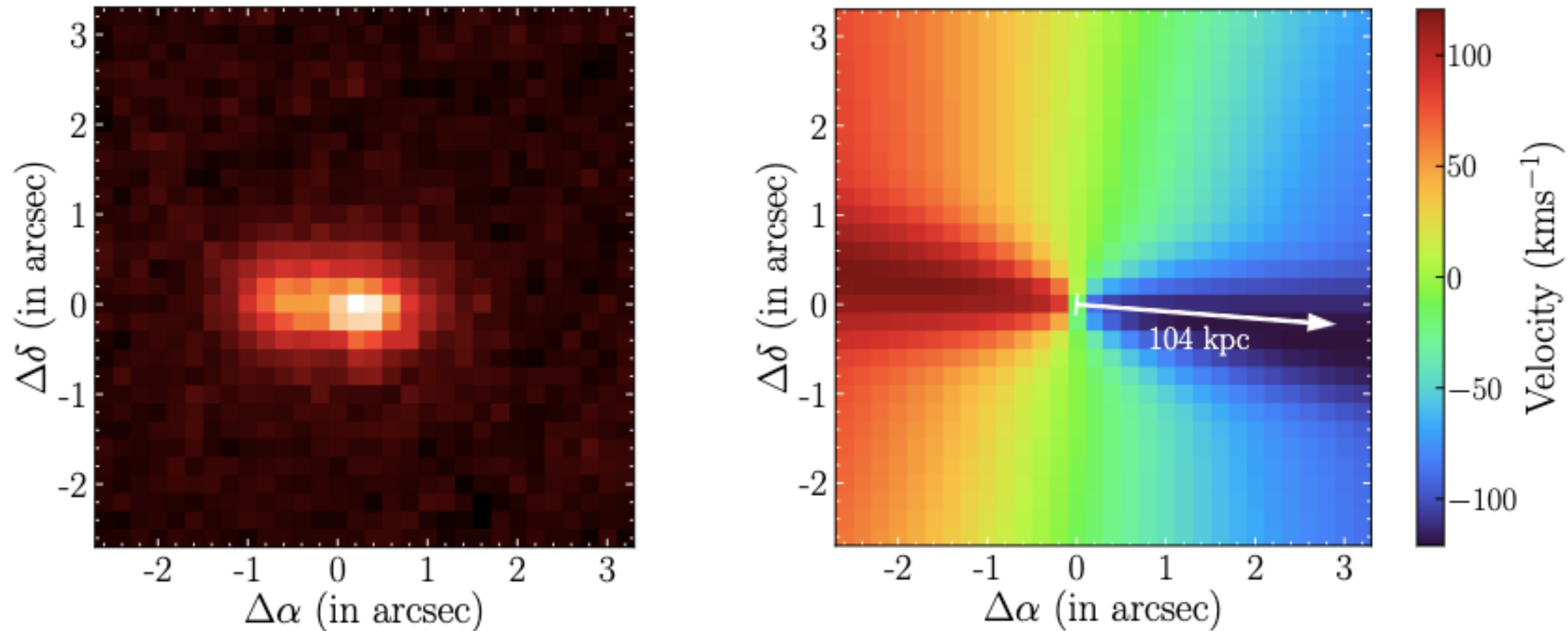
$$\rho/R_{\text{vir}} \approx 0.7$$

The [O/H] for the galaxies is much higher than the metallicity inferred from ionization models for the cold and warm gas phases



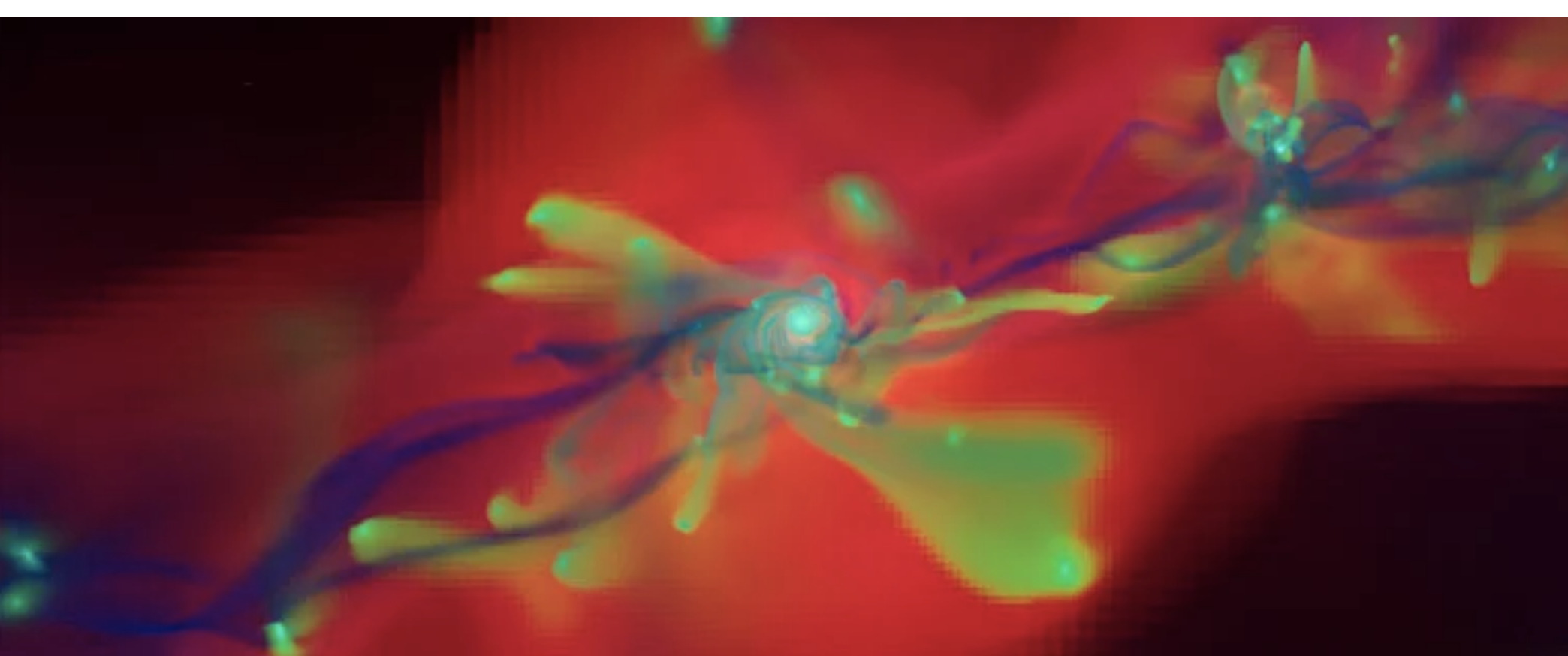
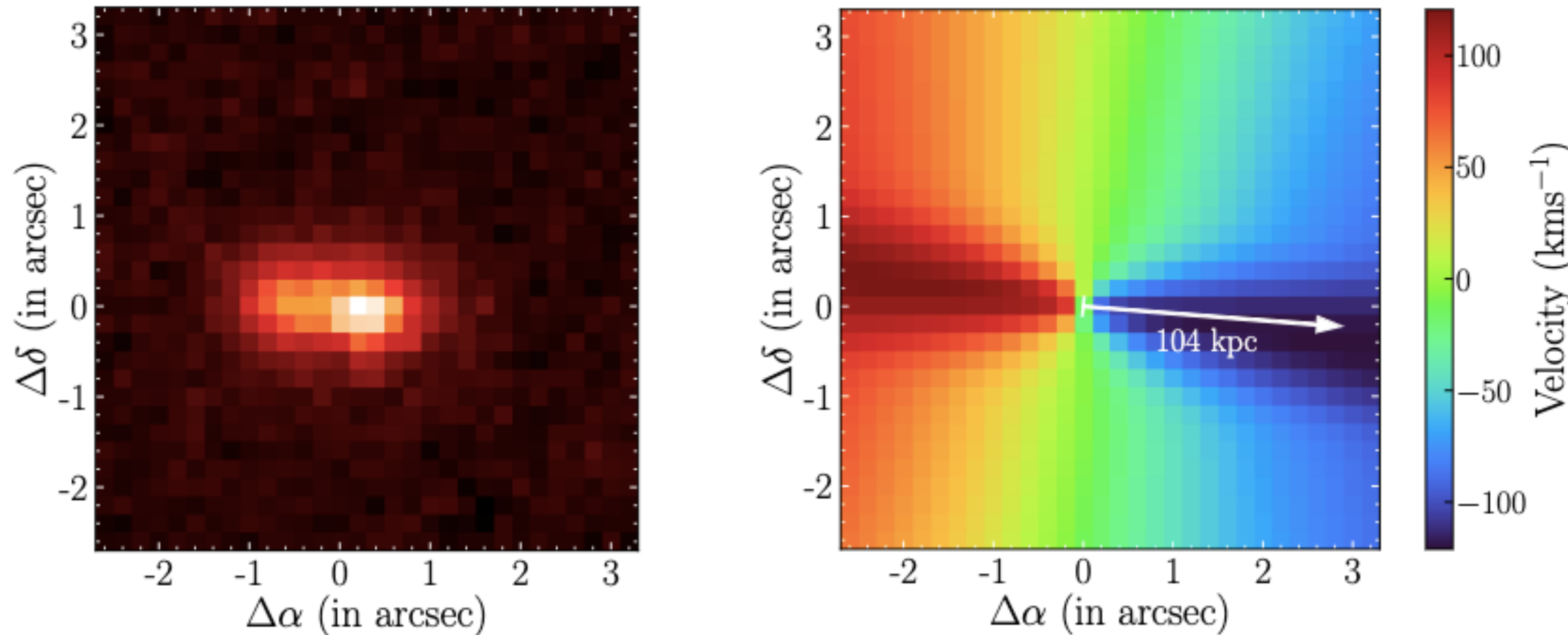
HST/COS + VLT/MUSE Observations of a LLS with BLA - O VI at $z \sim 0.4$

Khonde et al. 2024, submitted

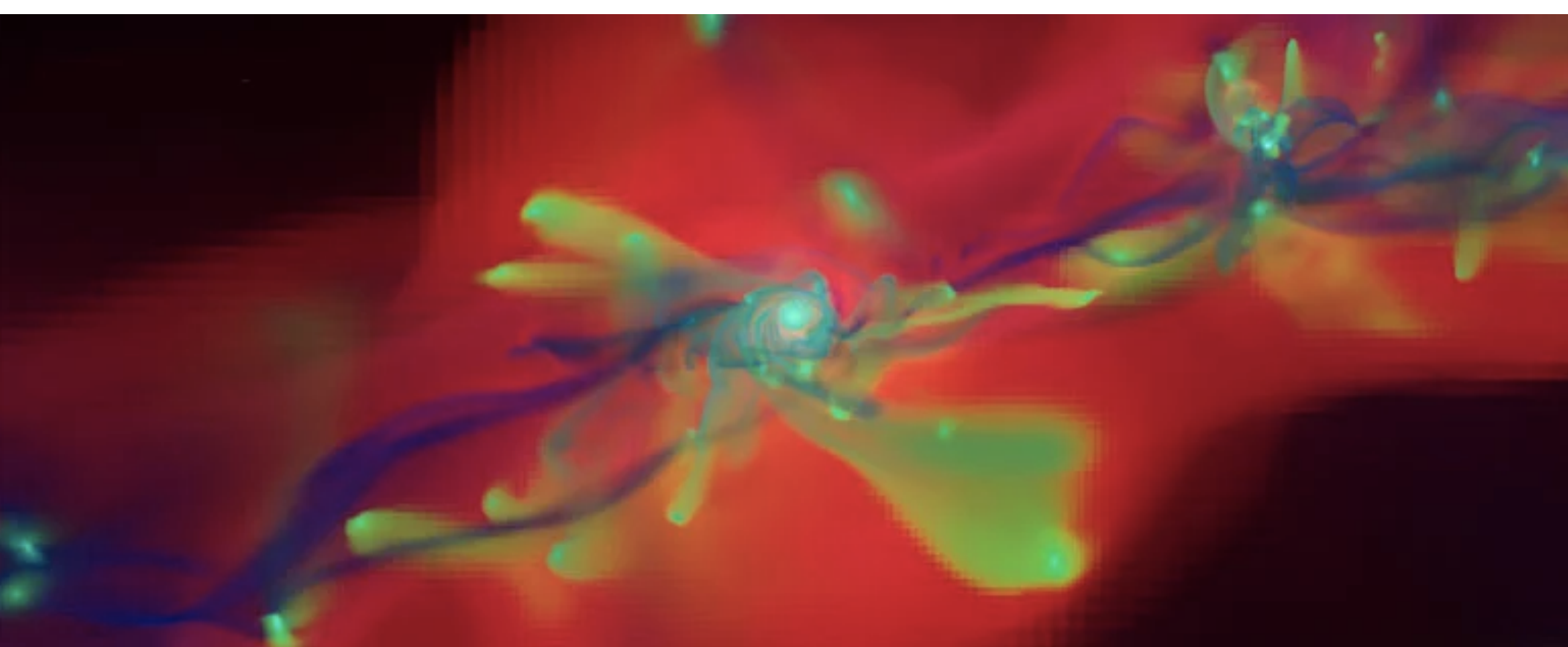
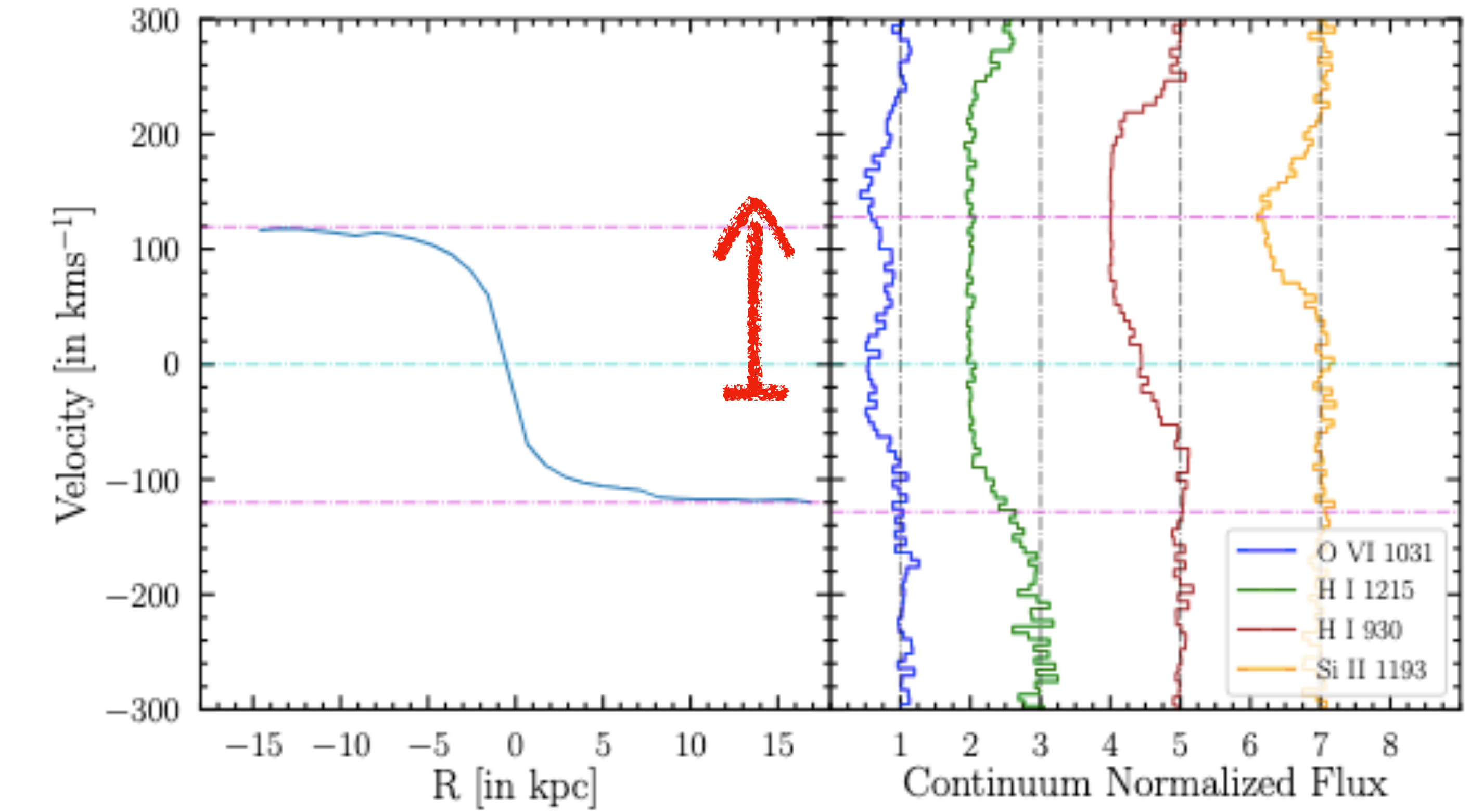
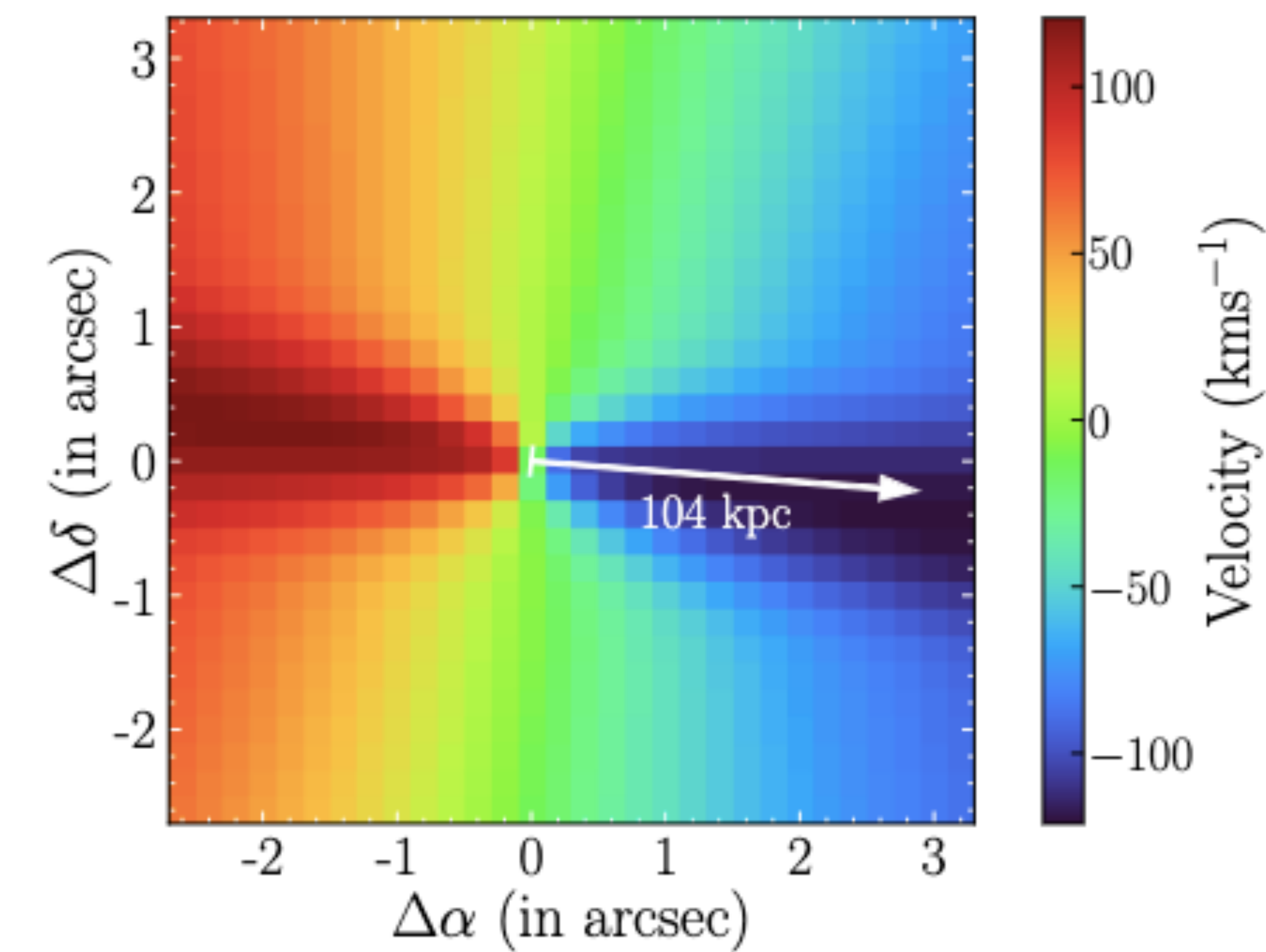


HST/COS + VLT/MUSE Observations of a LLS with BLA - O VI at $z \sim 0.4$

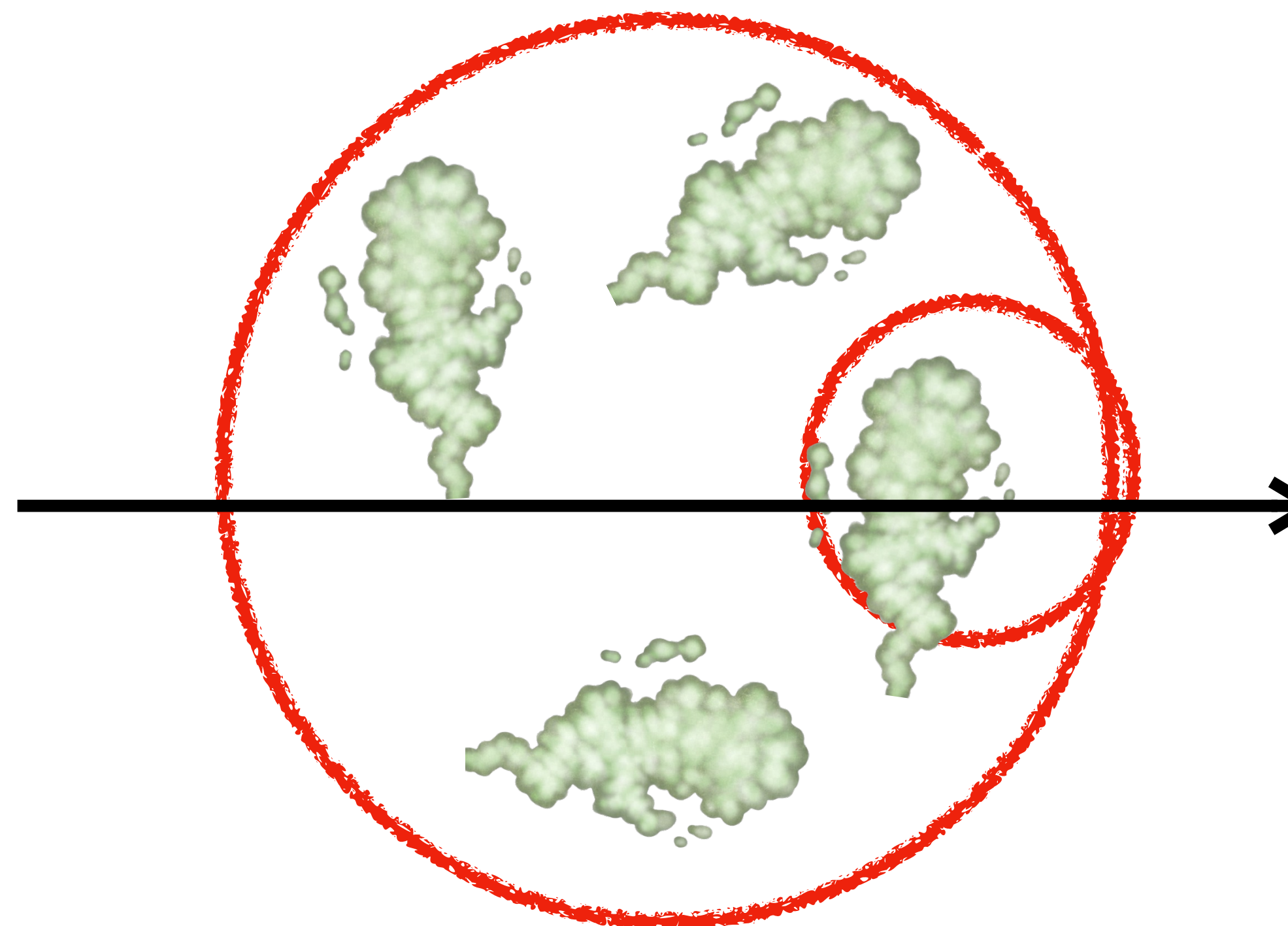
Khonde et al. 2024, submitted



Accreting streams from the cosmic web (blue) typically starts corotating with the disk in the final stages of its accretion.



Accreting streams from the cosmic web (blue) typically starts corotating with the disk in the final stages of its accretion. Here it is counter rotating

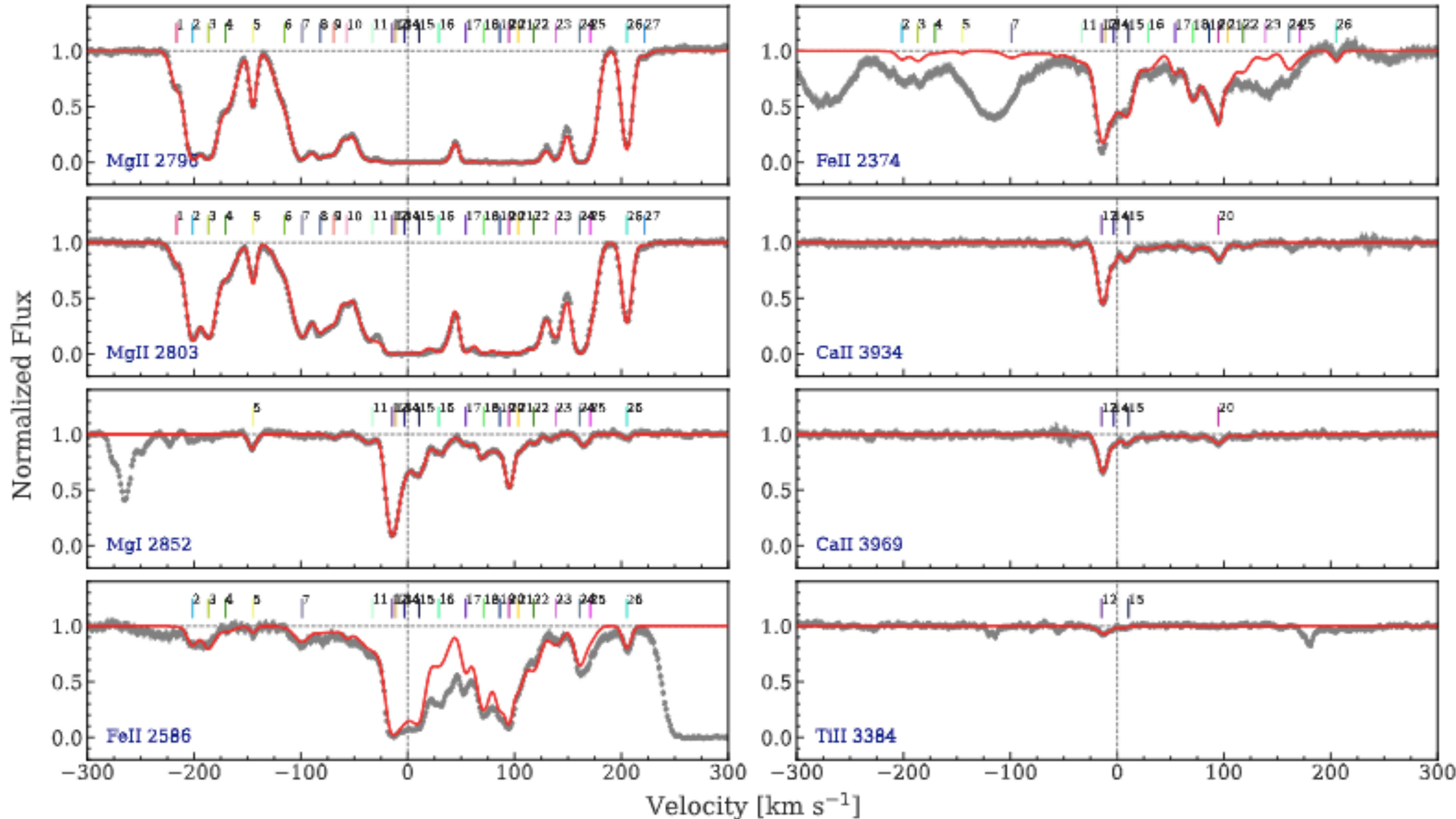


The metallicity 1/10th solar for the LLS compares well with median metallicity of such absorbers in simulations where they trace past outflows or tidally stripped material

LLS tracing high velocity gas
O VI transition temperature gas

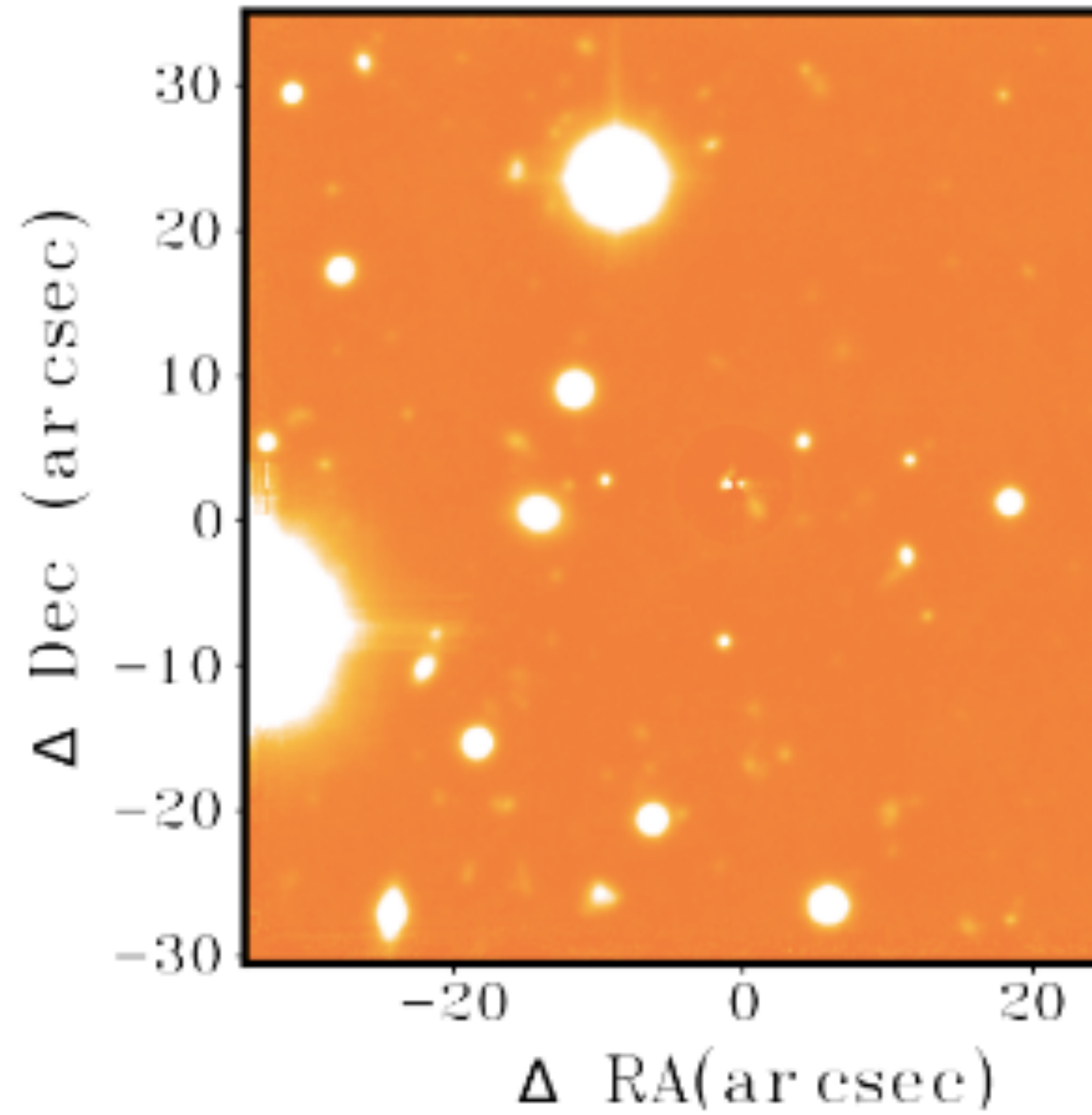
Ultra-Strong Mg II at $z \sim 1.13$ tracing gas accretion from the CGM?

Udhwani et al. in prep



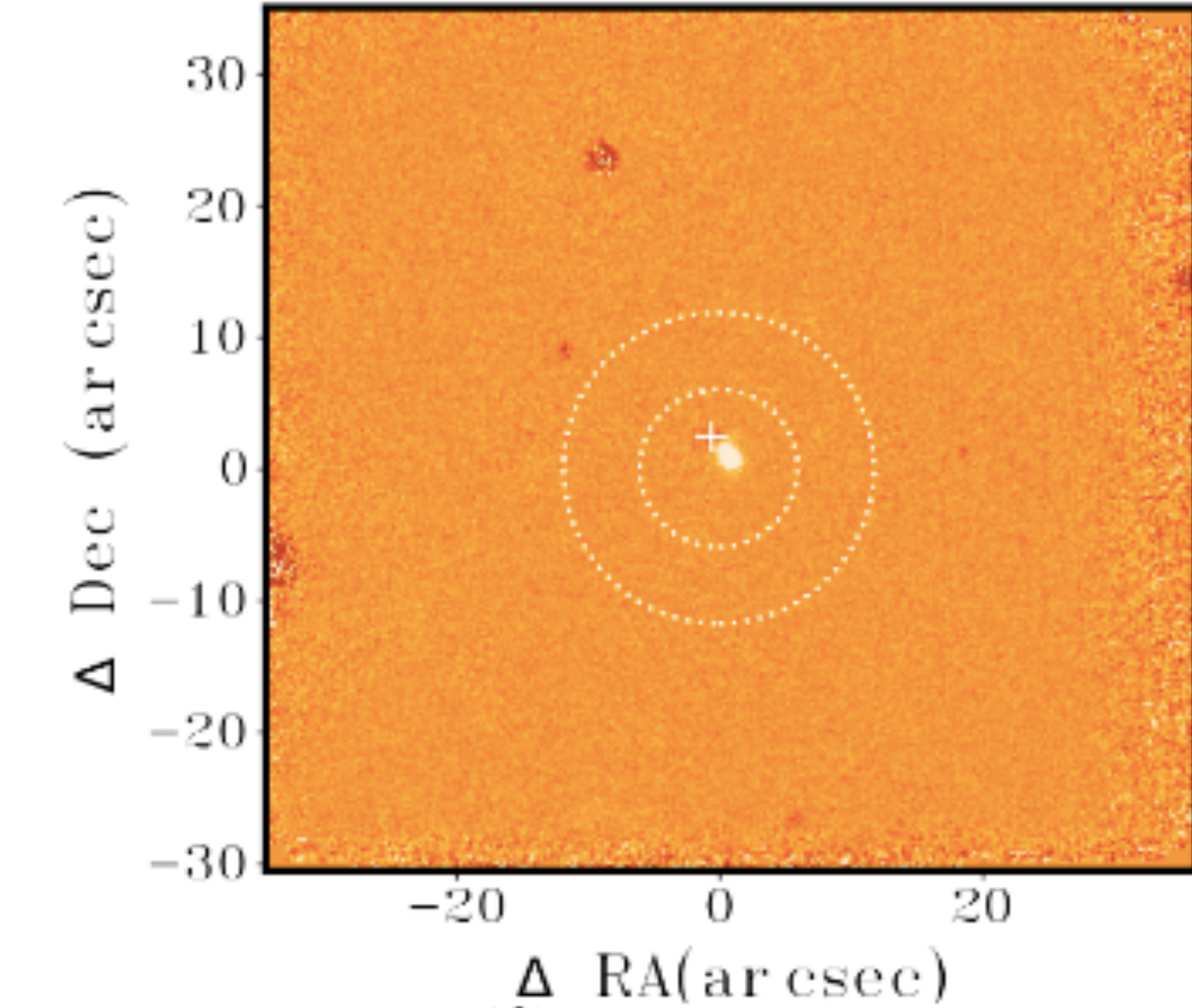
Ultra-Strong Mg II at $z \sim 1.13$ tracing gas accretion from the CGM?

Udhwani et al. in prep



$M_* \approx 5 \times 10^{10} M_\odot$, SFR $\approx 8 M_\odot \text{ yr}^{-1}$

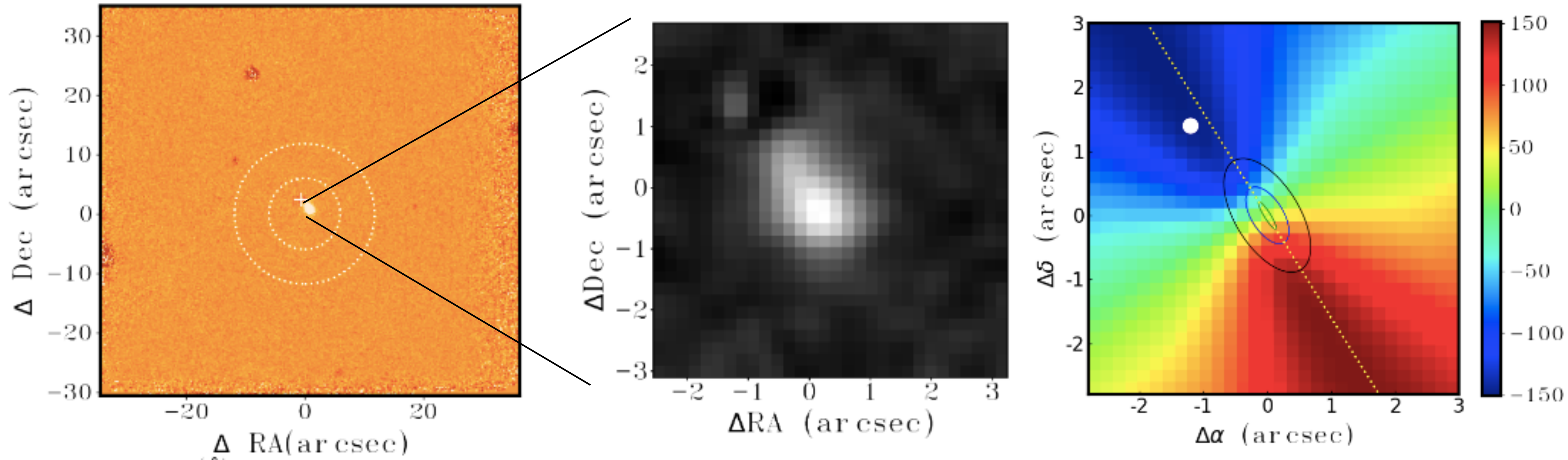
$\rho/R_{vir} \approx 0.12$, $z_{abs} \approx z_{gal}$



no bright companion to the GOTOQ within 500 kpc

Ultra-Strong Mg II at $z \sim 1.13$ tracing gas accretion from the CGM?

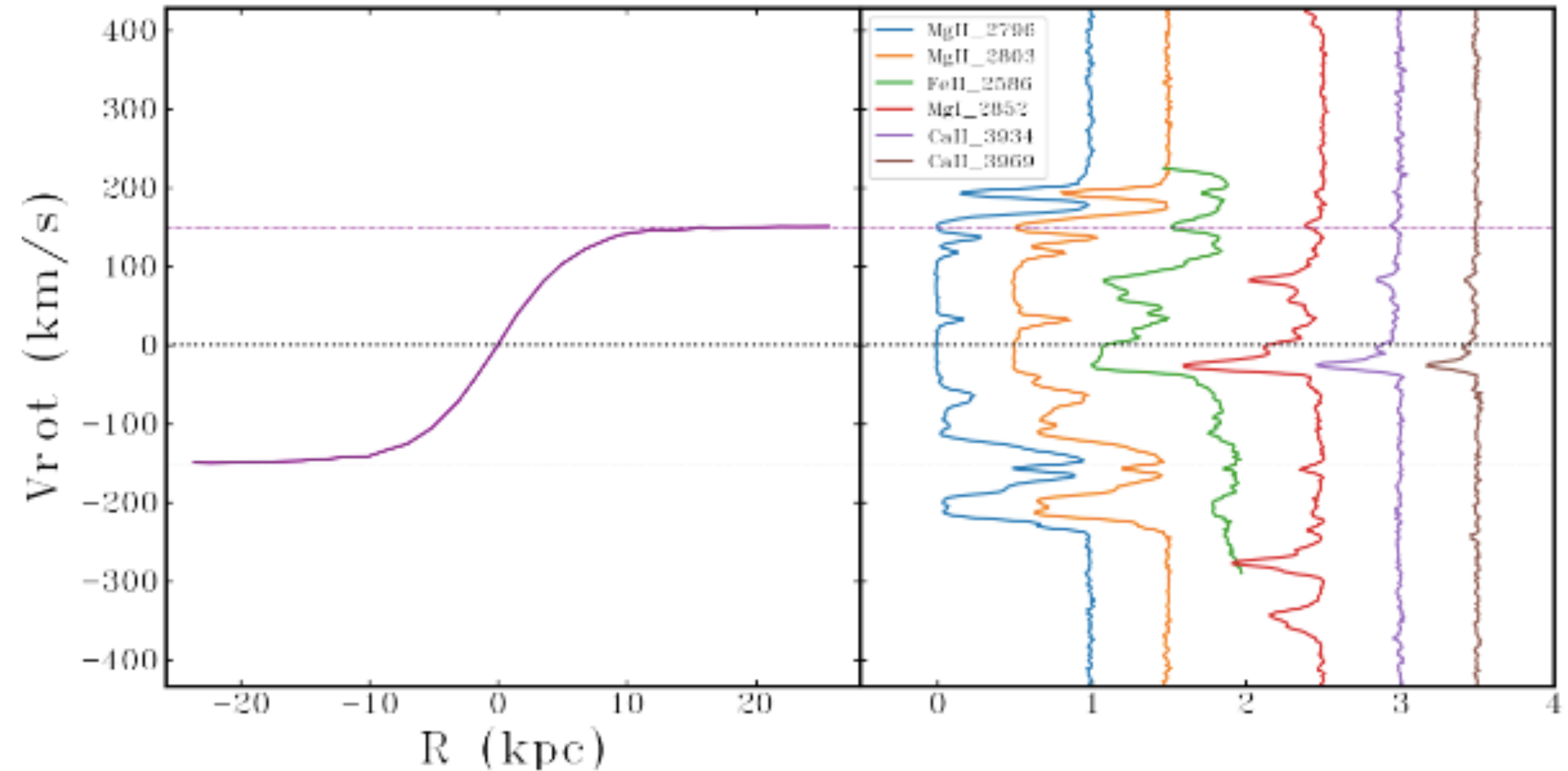
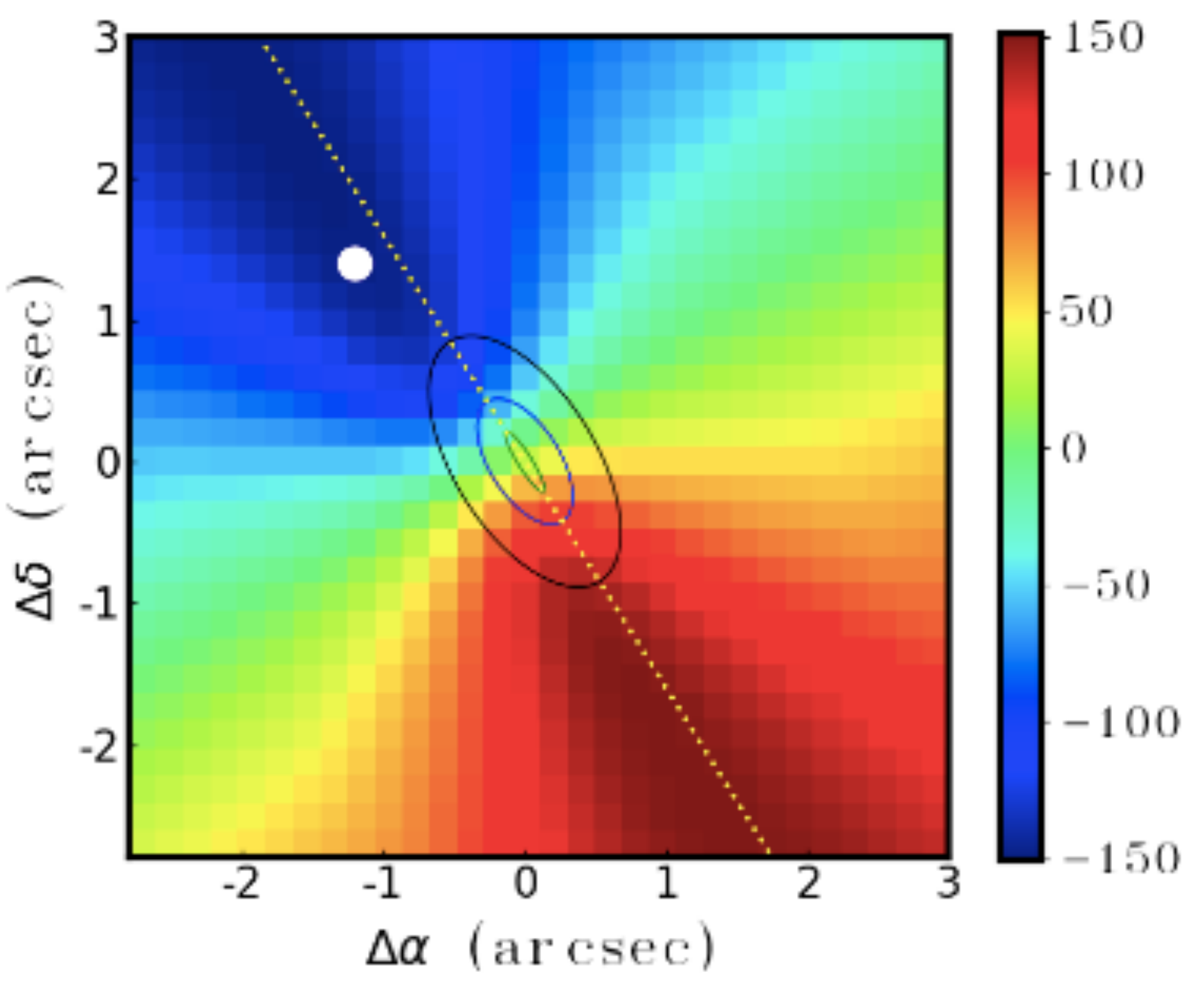
Udhwani et al. in prep



The absorber is nearly co-planar with the projected major axis of the galaxy

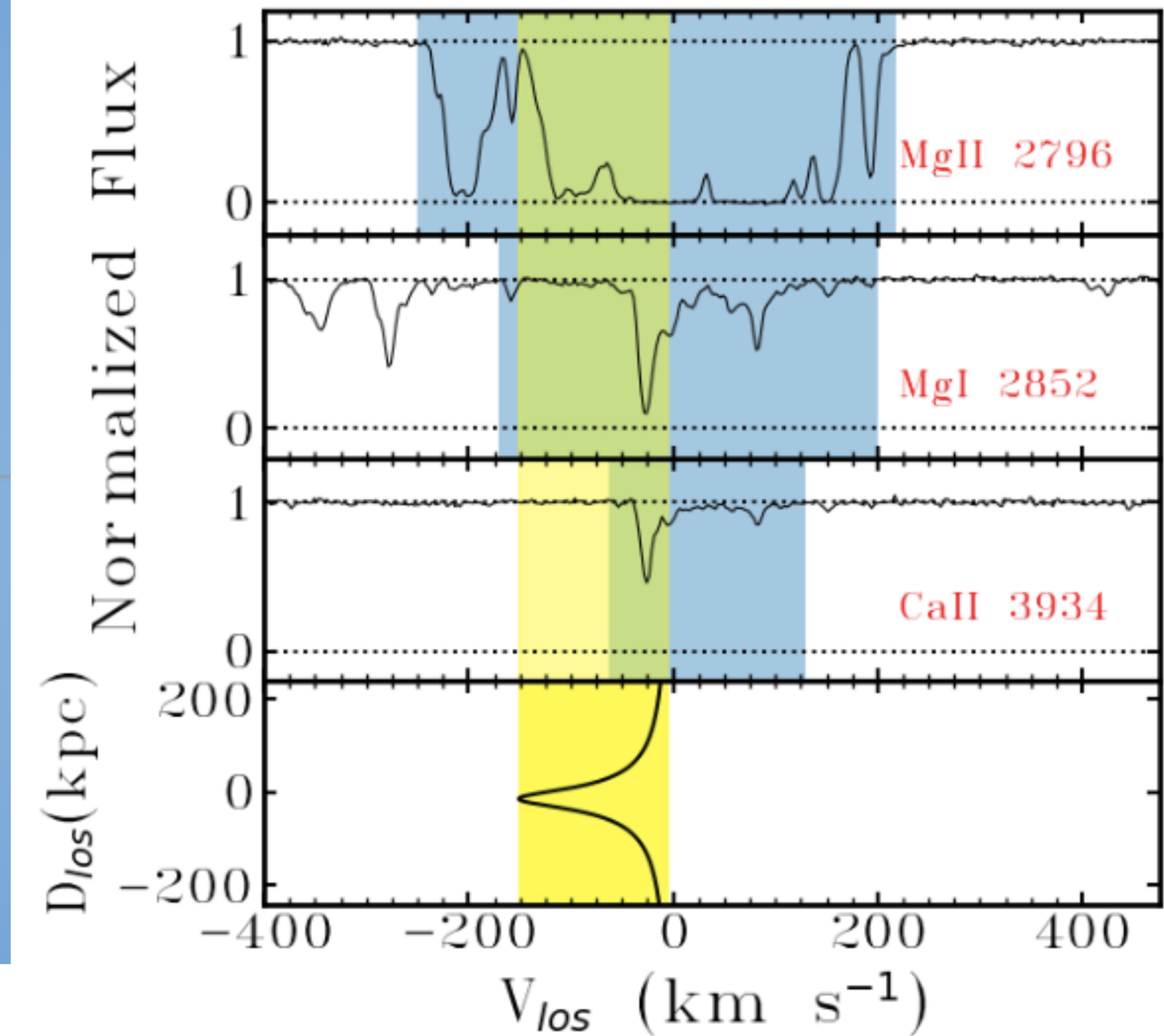
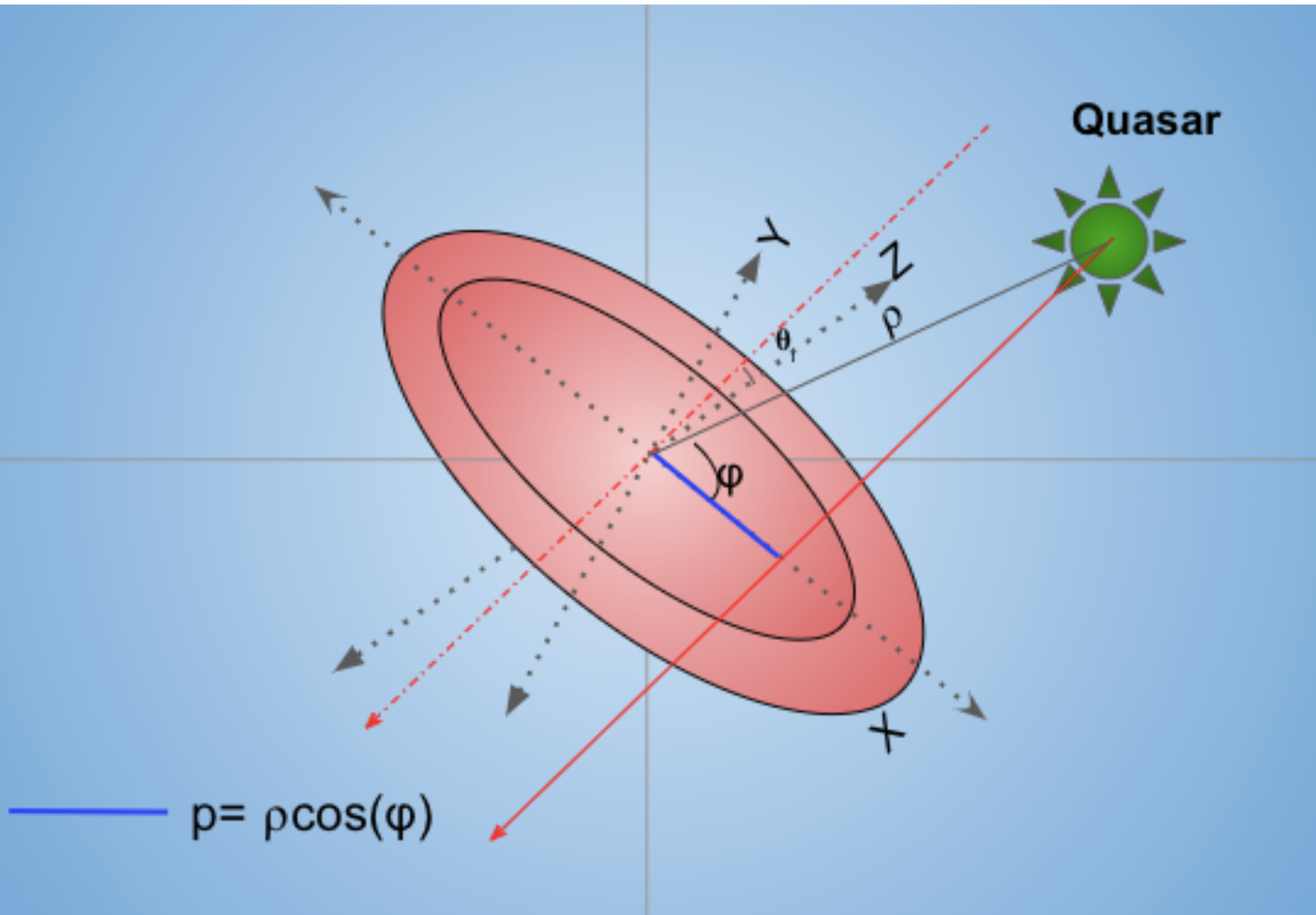
Ultra-Strong Mg II at $z \sim 1.13$ tracing gas accretion from the CGM?

Udhwani et al. in prep



Ultra-Strong Mg II at $z \sim 1.13$ tracing gas accretion from the CGM?

Udhwani et al. in prep



Even very large disk thickness of 100 kpc does not reproduce the full velocity range of absorption

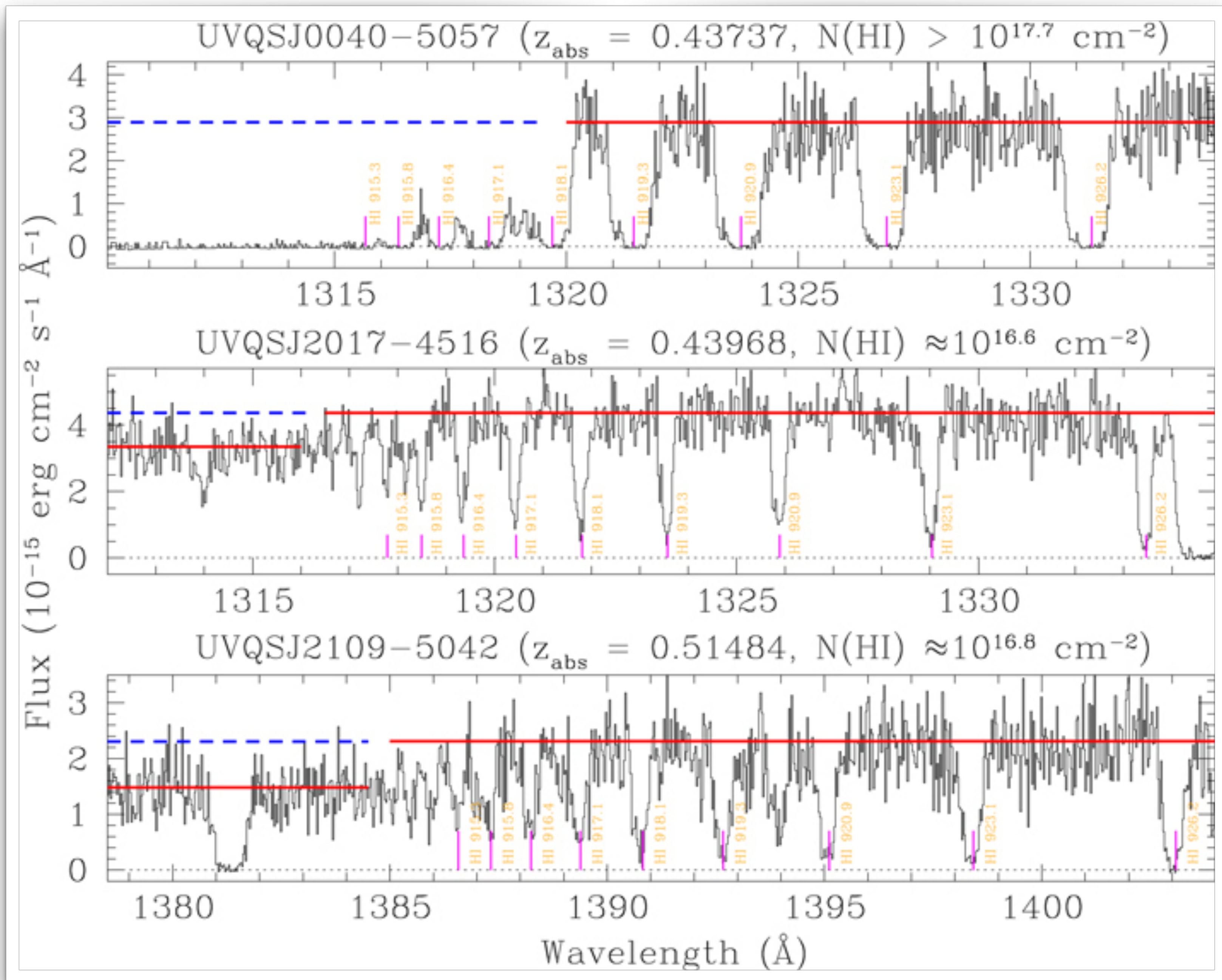
Extrapolanar gas with random velocities have to be contributing to the absorption

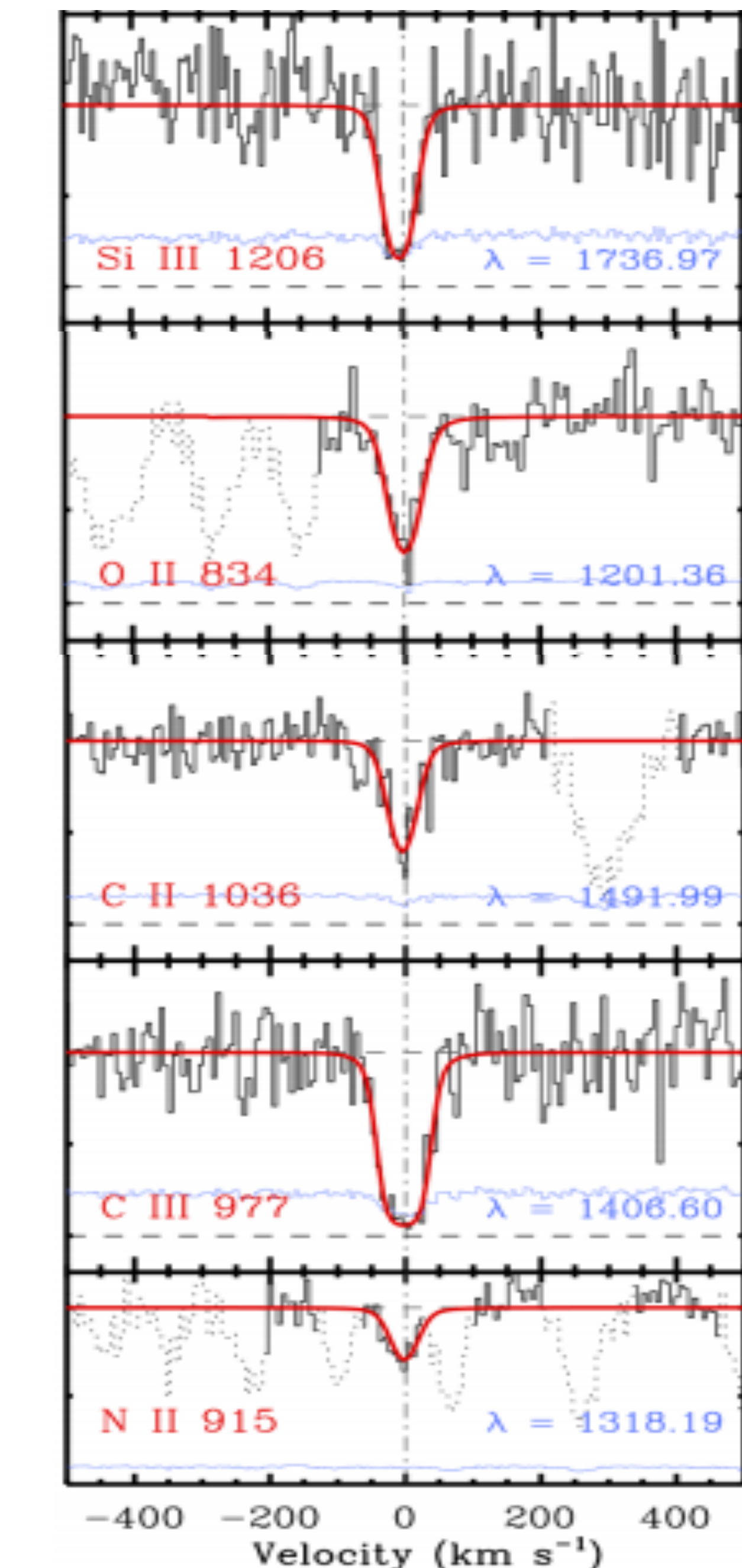
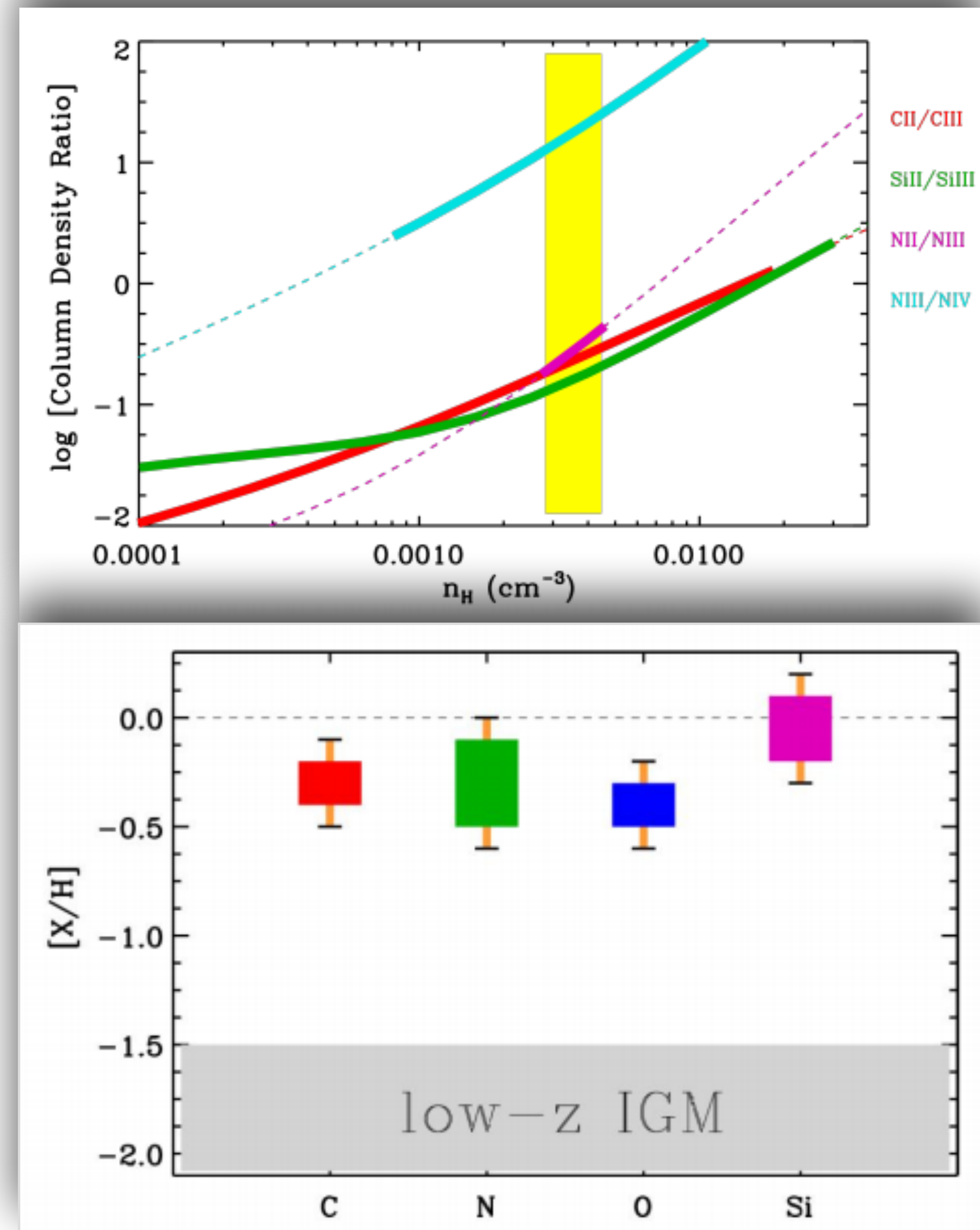
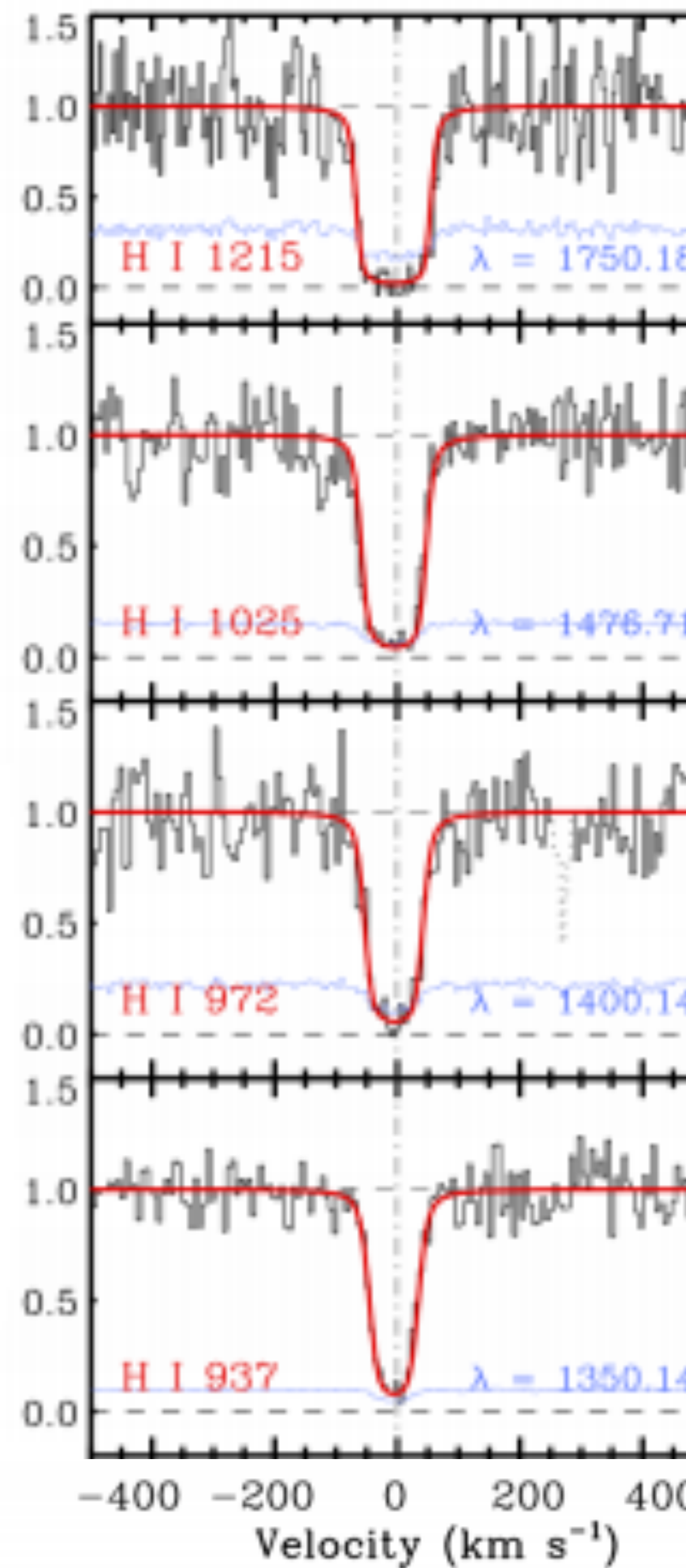
Possibly metal enriched CGM getting accreted : co-rotating + infalling

Metals in Circum-Cluster Medium at $z \sim 0.4$

Cluster	z_{cl}	M_{500} ($10^{14} M_\odot$)	r_{500} Mpc	QSO	z_{QSO}	ρ_{cl}/r_{500}	z_{abs}
(1)	(2)	(3)	(4)	(5)	(6)	(7)	(8)
J0041-5107	0.45 ± 0.04	3.04 ± 0.87	0.87	J0040-5057	0.608	4.4	0.43737
J2016-4517	0.45 ± 0.03	3.19 ± 0.89	0.89	J2017-4516	0.692	4.7	0.43968
J2109-5040	0.47 ± 0.04	3.81 ± 0.87	0.93	J2109-5042	1.262	1.6	0.51484

Table 1. Information about the QSO-cluster pairs. Cluster names (1), photometric redshifts (2), and masses (3) are from Bleem *et al.* (2015). QSO names (5) and redshifts (6) are from Monroe *et al.* (2016). The r_{500} values (4), normalized clustocentric impact parameters of the QSO sightlines (7) and absorber redshifts (8) are from Muzahid *et al.* (2018).





QSO	z_{abs}	$\log N(\text{HI})$	n_{H} (cm^{-3})	$\log N_{\text{H}}$	p/k (K cm^{-3})	T (K)	L (kpc)	[C/H]
UVQS J0040-5057	0.43737	18.63 ± 0.07	$\gtrsim 5 \times 10^{-4}$	$\lesssim 20.9$	$\gtrsim 8.6$	$\lesssim 1.7 \times 10^4$	$\lesssim 492.8$	≥ -0.9
UVQS J2017-4516	0.43968	16.55 ± 0.02	$\sim 3 \times 10^{-3}$	~ 18.8	~ 43.7	$\sim 1.5 \times 10^4$	~ 0.9	-0.35 ± 0.10
UVQS J2109-5042	0.51484	16.72 ± 0.05	$\sim (0.9 - 3.9) \times 10^{-3}$	$\sim [19.0, 19.7]$	$\sim [18.0, 60.9]$	$\sim 1.7 \times 10^4$	$\sim [0.9, 18.4]$	$[-1.0, -0.6]$



High HI column densities in clusters

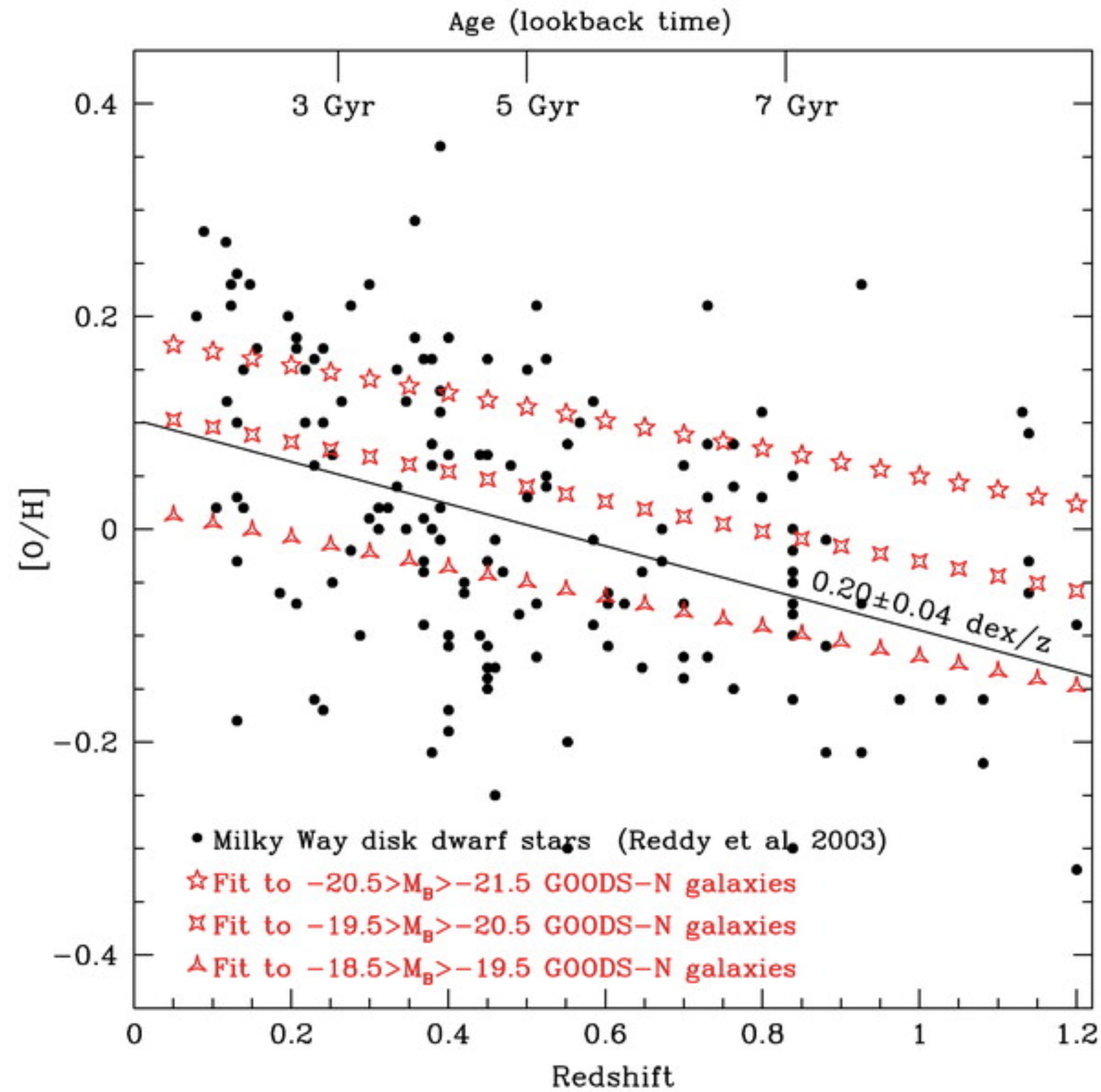


100 times more baryons

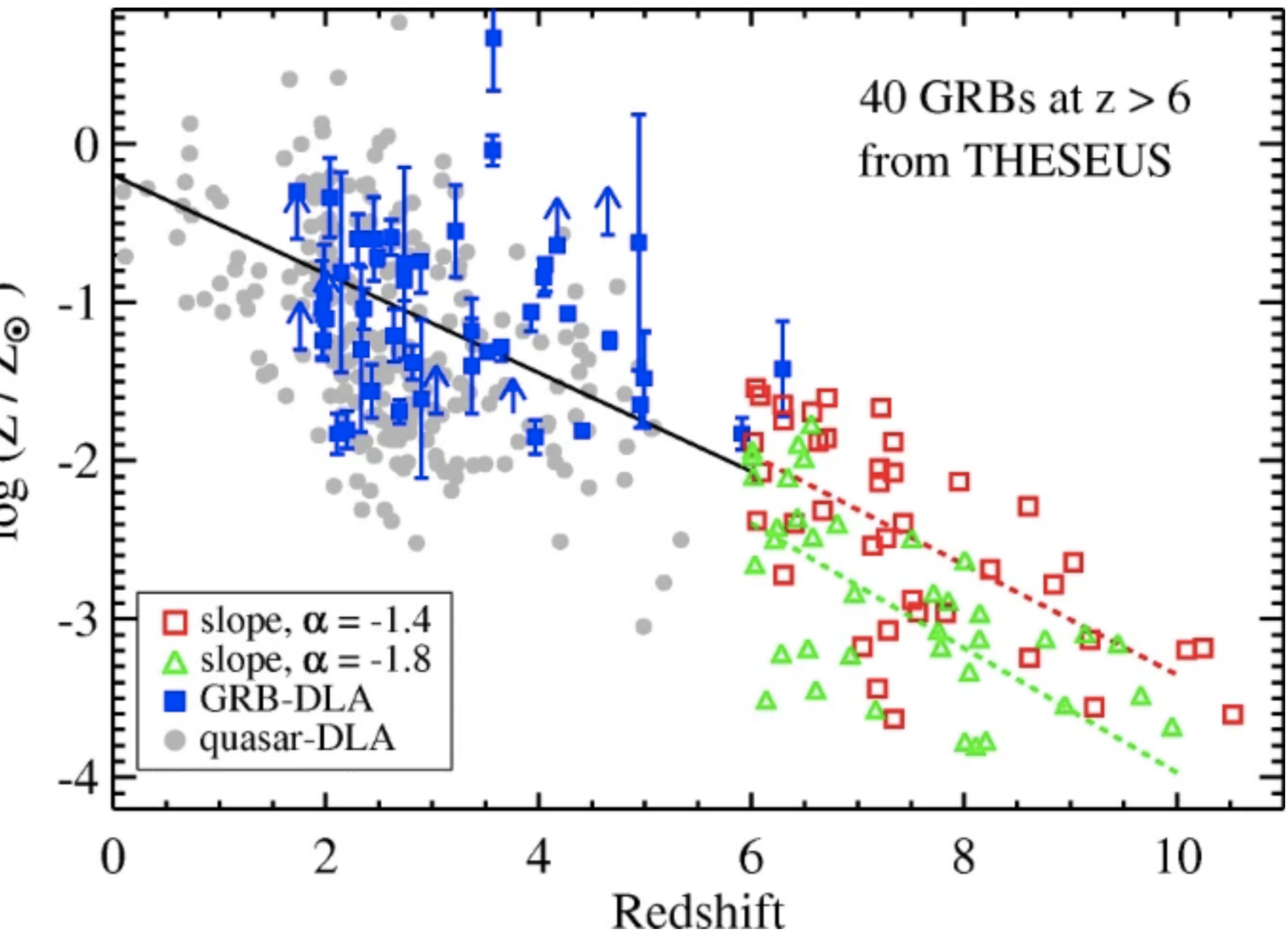


ICM enriched by feedback from star formation, AGN activity and/or ram pressure or tidal stripping

Slow build up of metals



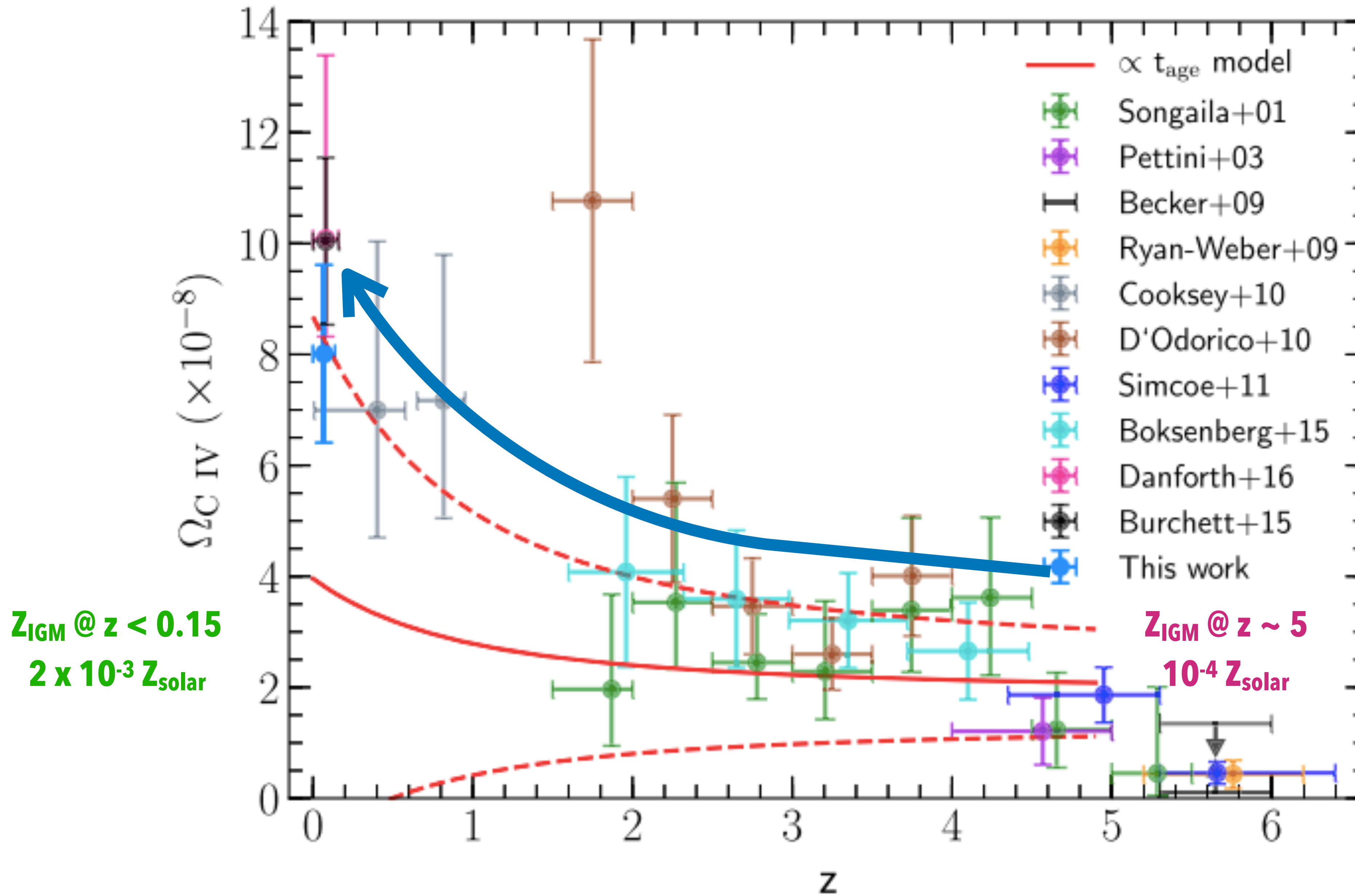
Kobulnicky & Kewley 2004



Tanvir et al. 2021

COS Legacy Survey of C IV

Manuwal et al. (2021)



Mass density of baryons in metals in the CGM / IGM environment show a gradual increase in the last 12 Gyrs

Feedback from SNe and AGN